

SKELETAL EFFECTS OF TERIPARATIDE IN GLUCOCORTICOID-TREATED MICE

By

KATHLEEN S. HOWE

A DISSERTATION PRESENTED TO THE GRADUATE SCHOOL
OF THE UNIVERSITY OF FLORIDA IN PARTIAL FULFILLMENT
OF THE REQUIREMENTS FOR THE DEGREE OF
DOCTOR OF PHILOSOPHY

UNIVERSITY OF FLORIDA

2007

© 2007 Kathleen S. Howe

To my mother and father. My father's recent passing brought great sadness to our family, but I know he would be proud of this accomplishment. My mother has been extremely supportive and her encouragement was instrumental in making this dissertation a reality.

ACKNOWLEDGMENTS

No project of this size occurs without a great deal of support and encouragement. First, and most importantly, I wish to thank the many individuals who directly contributed to this research study. Jodi Long was involved in every aspect of this study. Her enthusiasm, knowledge, and energy contributed immensely to this project. I also owe a debt of gratitude to Dr. Randy Braith for his guidance and support throughout this project and my tenure at this university. His extensive knowledge and support were invaluable to me as I designed and conducted this study. His comments, suggestions, and editorial talents helped bring the study results into sharper focus.

I owe a particular debt of gratitude to Dr. Tom Wronski who helped design this study, allowed me to use equipment in his lab, and helped me to interpret the results. He is the foremost expert on bone biology at the University of Florida and I profited greatly from his knowledge. I would also like to thank Molly Altman and Sally Vanegas who prepared and analyzed bone samples for histomorphometric analysis and Ignacio Aguirre who was always willing to answer my questions. Their knowledge and professionalism helped make this project a success.

I would also like to thank Dr. Russell Turner and Dr. Urszula Iwaniec. They graciously permitted me access to their equipment and expertise. Their enthusiasm for this project and willingness to teach me about bone research has helped my professional development immensely. I have also benefited greatly from my committee's guidance and thank both Dr. Stephan Dodd and Dr. Scott Powers. Their insightful comments and probing questions helped make this a better study. More than that, though, over the past seven years they have provided encouragement and helped shape my professional development. I also owe a debt of gratitude to the wonderful staff at Animal Care Services. They provided outstanding support, training, and

services to this project. Working with them was truly a pleasure. I would also like to thank some of my friends who supported me: Susan Smith who always had a kind word, Vija Purs who grudgingly accepted my research with animals, Ben Webster, who kept me smiling, and, most of all Janet Degner who was always there with a word of encouragement when the going got rough. I also want to thank members of the Applied Physiology and Kinesiology staff. Kim Hatch and Candyce Hudson have provided expert advice and support over the years. Their willingness to help students and their expertise in managing grants greatly eased the way for this project. I would also like to thank James Milford and Susie Weldon. They are the collective memory for the department and seem to always know how to make things happen. Their “can-do” attitude and enthusiastic support was very much appreciated. Finally, I would like to thank my mother who stood behind me unflinching through this arduous journey.

TABLE OF CONTENTS

	<u>page</u>
ACKNOWLEDGMENTS	4
LIST OF TABLES	9
LIST OF FIGURES	11
ABSTRACT	12
CHAPTER	
1 INTRODUCTION	14
Study Purpose	14
Rationale for Study	15
Study Aims	18
Significance of the Study	21
2 MATERIALS AND METHODS	23
Background	23
Animals	23
Animal Housing Conditions	24
Study Group Assignment	25
Pharmacological Agents	25
Study Drugs	25
Prednisolone Succinate	26
Teriparatide	26
Fluorochrome markers	27
Demeclocycline	27
Calcein	27
Anesthesia and Euthanasia	28
Bone Harvesting	28
Study Measures	29
Anthropomorphic Measures	29
Histomorphometry	29
Static bone measurements	30
Dynamic bone measurements	31
MicroCT	32
Femur	32
Vertebrae	33
Statistical Analysis	34

3	LITERATURE REVIEW	36
	Bone Biology	36
	Structure of Bone	36
	Bone Cells	38
	Osteoclasts	38
	Osteoblasts	39
	Osteocytes	39
	Bone Lining Cells	40
	Bone Remodeling	40
	Remodeling Balance – The RANKL/OPG/RANK Axis	43
	Effects of Glucocorticoid Drugs and Teriparatide on Bone	44
	Systemic Effects of Glucocorticoid Drugs	44
	Direct Effects of Glucocorticoids	45
	Indirect Effects of Glucocorticoid Drugs	46
	Decreased intestinal absorption of calcium	46
	Increased renal elimination of calcium	47
	Antagonistic action on gonadal functions	47
	Increased sensitivity to PTH	48
	Bone loss in response to glucocorticoid treatment	48
	Parathyroid Hormone	49
	Dual Nature of PTH: Continuous versus Intermittent Administration	49
	Parathyroid Hormone (PTH 1-84)	49
	Teriparatide (PTH 1-34)	51
	Mechanisms of Action	52
	Studies of Glucocorticoid-Induced Bone Loss in Mice	53
	Validity of the Mouse as a Model of Glucocorticoid-Induced Bone Loss	53
	Glucocorticoid-Induced Bone Loss in Mice	53
	Teriparatide Treatment in Mice	54
	Further Considerations	55
4	RESULTS	56
	Measurement Design	56
	Anthropomorphic Measures	57
	Bone Measures	58
	Measurements of the Lumbar Vertebrae	58
	Bone Volume/Total Volume	59
	Trabecular Number	61
	Trabecular Width/Trabecular Thickness	63
	Trabecular Separation	66
	Measurements of the Distal Femur	67
	Bone Volume	68
	Trabecular Number	71
	Trabecular Thickness/Trabecular Width	72

Trabecular Separation.....	75
Osteoblast Surface and Osteoclast Surface	76
Dynamic Measures of Bone Formation in the Distal Femur.....	79
Mineralizing Surface	79
Mineral Apposition Rate	81
Bone Formation Rate/Bone Surface (BFR/BS).....	82
Mid-Shaft Cortical Bone Data and Significant Changes.....	84
5 DISCUSSION.....	86
Glucocorticoid Drugs Suppressed Bone Formation But Did Not Affect Bone Volume.....	86
Anabolic Effects of PTH Prevented the Inhibitory Changes Associated with Glucocorticoid Drugs.....	89
PTH Increases Bone Mass Quickly	91
Residual Effects of Glucocorticoid Drugs are Apparent During Natural Recovery	92
PTH Treatment After Glucocorticoid Use Was More Effective than Natural Recovery	93
Age-Related Effects on Bone Mass.....	94
Prophylactic Value of Concurrent Treatment with Glucocorticoid Drugs and PTH.....	96
Site Specificity of GC and PTH Treatment.....	97
Conclusions.....	97
Clinical Applications	98
Study Limitations.....	99
Future Directions	100
 APPENDIX	
A SUMMARY OF BONE MEASUREMENTS.....	101
B SUMMARY OF SELECTED STUDIES IN MICE.....	107
LIST OF REFERENCES	111
BIOGRAPHICAL SKETCH	121

LIST OF TABLES

Table	<u>page</u>
3-1 Common Effects of Glucocorticoid Therapy.....	45
4-1 Experimental Groups and Description of Treatments.	56
4-2 Mean Animal Weights by Group.....	57
4-3 Mean Femur Lengths by Group.....	57
4-4 Summary of Histomorphometric Analysis of LV3 by Group.	59
4-5 Summary of MicroCT Analysis of LV2 by Group.....	59
4-6 Significant Changes in Lumbar Vertebra L3 Bone Volume by Group using Histomorphometry.....	60
4-7 Significant Changes in Lumbar Vertebra L2 Bone Volume by Group using MicroCT....	61
4-8 Significant Changes in Lumbar Vertebra L3 Trabecular Width by Group using Histomorphometry.....	64
4-9 Significant Changes in Lumbar Vertebra L2 Trabecular Thickness by Group using MicroCT.....	65
4-11 Summary of MicroCT Analysis of the Distal Femur by Group.	68
4-12 Significant Changes in Distal Femur Bone Volume by Group using Histomorphometry.....	69
4-13 Significant Changes in Distal Femur Bone Volume by Group using MicroCT.....	70
4-15 Significant Changes in Distal Femur Trabecular Number by Group using MicroCT.....	72
4-16 Significant Changes in Distal Femur Trabecular Width by Group using Histomorphometry.....	73
4-17 Significant Changes in Distal Femur Trabecular Thickness by Group using MicroCT....	74
4-18 Significant Changes in Distal Femur Trabecular Separation by Group using Histomorphometry.....	75
4-19 Significant Changes in Distal Femur Trabecular Separation by Group Using MicroCT.....	76
4-20 Significant Changes in Distal Femur Osteoblast Surface and Osteoclast Surface by Group.....	77

4-21	Significant Changes in Distal Femur Mineralizing Surface by Group.....	80
4-22	Significant Changes in Distal Femur Mineral Apposition Rate by Group.....	81
4-23	Significant Changes in Distal Femur Bone Formation Rate by Group using Histomorphometry.....	83
4-24	Summary of Histomorphometric Analysis of Femur Mid-Shaft by Group.....	84
4-25	Summary of Significant Changes in Femur Mid-Shaft Cortical Bone Thickness by Group using MicroCT.....	84
A-1	Summary of Significant Changes in Lumbar Vertebrae L3 based on Histomorphometry.....	101
A-2	Summary of Significant Changes in Lumbar Vertebrae L2 based on MicroCT.....	102
A-3	Summary of Significant Changes in the Distal Femur based on Histomorphometry.....	103
A-4	Summary of Significant Changes in the Distal Femur based on MicroCT.....	104
A-5	Percent Changes in Osteoclast and Osteoblast Surfaces in the Distal Femur.....	105
A-6	Percent Changes in Dynamic Bone Formation Parameters in the Distal Femur.....	106
B-1	Studies Of Glucocorticoid-Induced Bone Loss In Mice.....	108
B-2	Studies using Teriparatide in Mice.....	110

LIST OF FIGURES

Figure	<u>page</u>
2-1 Study Groups, Treatments and Timelines.....	25
4- 1 Lumbar Vertebra L3 Bone Volume/Total Volume by Group using Histomorphometry.....	60
4-2 Lumbar Vertebra L2 Bone Volume/Total Volume by Group using MicroCT.	61
4-3 Lumbar Vertebra L3 Trabecular Number by Group using Histomorphometry.....	62
4-4 Lumbar Vertebra L2 Trabecular Number by Group using MicroCT.	62
4-5 Lumbar Vertebra L3 Trabecular Width by Group using Histomorphometry.	64
4-6 Lumbar Vertebra L2 Trabecular Thickness by Group using MicroCT.	65
4-7 Lumbar Vertebra L3 Trabecular Separation by Group using Histomorphometry.	66
4-8 Lumbar Vertebra L2 Trabecular Separation by Group using MicroCT.	67
4-9 Distal Femur Bone Volume/Total Volume by Group using Histomorphometry.	69
4-10 Distal Femur Bone Volume/Total Volume by Group using MicroCT.....	70
4-11 Distal Femur Trabecular Number by Group using Histomorphometry.....	71
4-12 Distal Femur Trabecular Number by Group using MicroCT.	72
4-13 Distal Femur Trabecular Thickness by Group using Histomorphometry.	73
4-14 Distal Femur Trabecular Thickness by Group using MicroCT.	74
4-15 Distal Femur Trabecular Separation by Group using Histomorphometry.	75
4-16 Distal Femur Trabecular Separation by Group using MicroCT.	76
4-17 Distal Femur Osteoblast Surface by Group using Histomorphometry.	78
4-19 Distal Femur Mineralizing Surface by Group using Histomorphometry.	80
4-20 Distal Femur Mineral Apposition Rate by Group using Histomorphometry.	81
4-21 Distal Femur Bone Formation Rate/Bone Surface by Group using Histomorphometry.....	83
4-22 Mid-Shaft Femur Cortical Thickness by Group using MicroCT.....	85

Abstract of Dissertation Presented to the Graduate School
of the University of Florida in Partial Fulfillment of the
Requirements for the Degree of Doctor of Philosophy

SKELETAL EFFECTS OF TERIPARATIDE IN GLUCOCORTICOID-TREATED MICE

By

Kathleen S. Howe

August 2007

Chair: Randy W. Braith

Major : Health and Human Performance

Synthetic analogs of glucocorticoid (GC) drugs are widely used in treating many inflammatory diseases and conditions and are also used to suppress the immune system in solid organ transplant recipients. However GCs have serious side effects including osteoporosis and bone fractures. We conducted a randomized, prospective investigation of the effects of teriparatide in treating GC-induced osteopenia in mice and examined the extent and character of bone recovery in the distal femur and lumbar spine after exposure to GC when there was

- no subsequent treatment with teriparatide;
- simultaneous GC and teriparatide administration over the entire course of treatment;
- delayed administration of teriparatide

Seven month old male Swiss Webster mice received prednisolone (2.1 mg/kg/d), teriparatide (40ug/kg/d), or vehicle to determine changes in bone structure and turnover after a 4- or 8-week (6 d/wk) treatment regimen. We injected flurochrome markers (declomycin and calcein) before sacrifice and harvested femurs and lumbar vertebrae to assess bone response. Bone samples were analyzed using histomorphometry and microCT and both techniques showed the same trends.

We found GCs suppressed bone turnover but not necessarily bone volume and that teriparatide, a bone anabolic agent, effectively increased bone turnover and inhibited bone changes resulting from GC exposure. The effects of teriparatide were rapid and relative changes were greater in the distal femur than in the lumbar spine. Four and eight weeks of teriparatide significantly increased both the osteoclast surface (Oc.S) and the osteoblast surface (Ob.S), resulting in significant increases in mineralizing surface and mineral apposition rate. Increased Ob.S and Oc.S indicated the increased turnover seen with teriparatide favored bone formation. We also detected a residual effect of GC on bone evidenced by lack of increased bone formation despite increased osteoblastic activity after GC treatment was discontinued. The underlying goal of our study was to demonstrate the efficacy of using PTH to prevent the adverse effects of GCs on bone in mice, as a prelude to studies in humans.

CHAPTER 1 INTRODUCTION

Glucocorticoid-induced bone loss is the leading cause of secondary osteoporosis (1). The negative effects of glucocorticoid (GC) drugs on the skeletal system are well established but there is currently no consensus on the best way to prevent and/or treat the associated bone loss. We hypothesized that teriparatide, currently the only anabolic agent approved for the treatment of established osteoporosis, would be capable of reversing and/or preventing glucocorticoid-induced bone loss. There are a number of patient populations that could benefit from such treatment. Chronic lung disease, rheumatic diseases, and gastrointestinal diseases often involve prophylactic GC use. Patients awaiting solid organ transplants would also benefit, since some transplant centers consider antecedent osteoporosis a contraindication for transplant surgery because immunosuppressant regimens including GC cause rapid bone loss after transplantation. There have been studies examining the effects of GC use in mice (2-5) but no studies have examined the combined use of GC and teriparatide in an animal model. Furthermore, there has only been one study documenting the use of teriparatide in humans exposed to long-term GC therapy (6).

The limited use of teriparatide in humans treated with GC prompted us to select a mouse model for this study. We used the Swiss Webster strain of mice because they have significant levels of cancellous bone in the femur and spine (7), have previously shown loss of bone in response to GC treatment (4,5), and an anabolic response to teriparatide (8). A mouse model allowed us to simulate chronic GC use.

Study Purpose

The purpose of this study was to determine the extent/character of bone recovery following exposure to GC drugs when there was

- No subsequent treatment with teriparatide
- Simultaneous GC and teriparatide administration over the entire course of treatment
- Delayed administration of teriparatide

We used microCT and histomorphometric techniques to evaluate bone mass, bone resorption, bone formation, and microarchitectural endpoints such as trabecular number, thickness, spacing, and connectivity density to determine whether teriparatide improved bone mass and architecture following exposure to GC. This preliminary study, designed to assess the effects of teriparatide on glucocorticoid-induced osteopenia* in mice, was the first step in a research sequence that will help define new treatment options to improve the quality of life for clinical populations exposed to long-term GC therapy and those facing transplant surgeries.

Rationale for Study

Synthetic analogs of GC are a widely used class of drugs that have proven effective in many inflammatory diseases and conditions, including asthma, Chronic Obstructive Pulmonary Disease, rheumatoid arthritis, Crohn's disease and lung diseases such as cystic fibrosis. GC analogs are also a key anti-rejection drug following solid organ transplantation (9,10). However, GC drugs pose serious side effects to the patient. Osteoporosis, with resulting bone fractures, is the most incapacitating sequelae of GC therapy. Bone is a dynamic, living tissue in which there is a normal balance of bone formation and bone resorption. This balance of bone loss and gain helps maintain a healthy skeletal structure capable of withstanding normal loads and stresses. GC drugs disrupt the normal homeostasis of bone and rapidly lead to loss of bone mass and increased fracture risk. GCs have a negative effect on both the hard outer layer of cortical bone and the cancellous bone found next to the marrow. Although GC drugs affect both types of bone, the most profound and rapid effects are seen in cancellous bone.

* Osteoporosis is a term based on T-scores established for human populations. As such, the term osteopenia rather than osteoporosis is used to describe decreased bone mass in animals.

The relationship between long-term GC use and osteoporosis is well established and is often referred to as Glucocorticoid-Induced Osteoporosis (GIO) in humans (11-14). Deleterious effects on the bones are found in dosages often met or exceeded in the treatment of many conditions. Dosages as small as 7.5 mg/day can result in a loss of spinal trabecular bone of 9.5% in 5 months (15) indicating even low doses can cause significant loss of bone. Bone loss occurs most rapidly in the first 6-12 months of treatment and appears to be dose and duration dependent (15-20). Osteoporosis has been reported in 50% of patients exposed to long-term GC treatment and spinal fractures occur at a rate 4-5 times that found in patients not treated with glucocorticoids (12,15). Fracture rates among those taking the drugs for more than five years approach 30% (21).

In solid organ transplant patients, significant loss of bone mass can be detected as early as three months after transplantation (22). Bone mineral density losses average 5-15% during the first year and 1-2% annually subsequently (16,23). The significant morbidity and mortality associated with GIO makes its potential prevention or reversibility an important issue.

Currently there is no established method for preventing GIO. A variety of anti-resorptive treatments have been tried, including calcium supplementation, bisphosphonate agents, estrogenic and androgenic hormones, and calcitonin, but none of these has proven effective in reversing the low bone formation that accompanies long-term GC use (6). We found that calcium/vitamin D supplementation and nasal calcitonin can slow bone loss but is unable to restore lost bone mass (24). Targeted resistance exercise and bisphosphonates have been shown to prevent spinal bone loss in solid organ transplant patients but long-term compliance is problematic (10,25,26). A recent study involving healthy postmenopausal women showed that a combination of a bisphosphonate and a high impact exercise program increased bone mass more

effectively than bisphosphonate treatment alone (27). However, follow-up testing 15 months after cessation of the intervention showed bone gains had not been maintained. If these gains cannot be maintained in otherwise healthy populations, it is unlikely patients taking GC drugs will be able to do so.

Teriparatide proved more efficacious in preventing and/or reversing GIO. Unlike the anti-resorptive drugs such as bisphosphonates, which only slow bone loss, teriparatide has an anabolic effect on bone, which may contribute to increased bone microarchitecture and strength. Studies using teriparatide have shown increases in bone density at the femur neck and particularly the lumbar spine (28-31) and indicate increases are greater with teriparatide than with bisphosphonates (32,33). Fracture reduction has also been associated with the use of teriparatide (29,31,34). A study of postmenopausal women with one to two preexisting non-traumatic vertebral fractures showed that the vertebral fracture risk following teriparatide treatment was reduced by two-thirds and the relative risk of non-vertebral fractures was reduced by one-half (29). To date, there has only been one study examining the efficacy of teriparatide in GIO in humans (6). However, the results of this study were confounded by a simultaneous use of hormone replacement therapy, which acts as an anti-resorptive drug on bone. In that study, the combination of estrogen and teriparatide resulted in significant bone density increases in the axial skeleton but it is unclear whether teriparatide alone can overcome the deleterious effects of GC treatment.

A number of studies have also shown that teriparatide stimulates bone formation, increases cancellous bone volume, architecture, cortical width, and biomechanical properties of bone in both mice (35) and humans (29). Teriparatide has been shown to increase cancellous bone and bone mineral density particularly in the axial skeleton (8,35). Rodents are frequently used as a

model for osteoporosis research because they exhibit bone mass changes similar to humans when exposed to many osteoporosis-inducing stimuli (5). While the ovariectomized rat is the most commonly used animal model for postmenopausal osteoporosis, the mouse may be a better model for glucocorticoid-induced osteopenia (3,5) because researchers have found inconsistent responses to GC exposure suggesting rats may be resistant to the effects of GC exposure (36-38). Studies in mice which have achieved skeletal maturity (4,5) suggest the efficacy of the Swiss Webster strain of mouse in a glucocorticoid-induced model of bone loss (2,5,7). Bone loss patterns in mice exposed to GCs approximate human responses and the response to teriparatide in studies suggests the process is similar in both humans and mice, leading us to choose this animal for the study (3,5,39).

There is also a growing recognition that along with bone mineral density (BMD), bone architecture should be examined to determine the true efficacy of a treatment (40,41). This study was designed to use both histomorphometry and microCT techniques to determine bone responses to GC treatment and whether there was any natural recovery following withdrawal of that treatment. We also, for the first time, determined differing bone response to simultaneous treatment with glucocorticoid and teriparatide (prevention) versus subsequent treatment with teriparatide after bone loss has occurred (reversal).

Study Aims

Research Aim 1. To measure the changes in bone architecture and bone metabolism resulting from teriparatide therapy following, or in conjunction with, GC administration in a skeletally mature animal model.

Hypothesis 1. In a skeletally mature mouse, teriparatide will reverse bone loss caused by 4 or 8 weeks of prednisolone treatment.

Rationale: Mice experience dose-dependent loss of bone in response to GC treatment over a threshold level of 1.4 mg/kg for as little as 27 days although evidence of increased osteoclast numbers appears as early as 10 days of treatment (4,5). This study used a dose of 2.1 mg/kg body weight, consistent with other studies (4,5). Previous studies using mice have shown that chronic GC suppressed bone formation leading to bone loss in both axial and appendicular skeletal sites (2-5). Researchers have noted increased bone resorption (4), osteocyte apoptosis (5), and histomorphometric changes consistent with bone loss (2,3) in response to GC treatment. Subsequent treatment with alendronate resulted in increased osteoclast apoptosis and prevention of osteoblast apoptosis (4). However, although alendronate slowed GC-induced bone loss, it could not prevent it (4).

Research Aim 2. To determine whether there are benefits to treating mice with teriparatide as a prophylactic measure by comparing results when GCs and teriparatide are administered together versus using teriparatide after glucocorticoid-induced bone loss has already occurred.

Hypothesis 2. Starting teriparatide therapy at the same time as GC treatment will result in less bone loss than starting teriparatide after glucocorticoid-induced osteopenia has developed.

Rationale: Numerous studies in humans and animals have shown that GC treatment has negative effects on bones. GCs directly affect bone cells at least in part by increasing osteoclast differentiation and activation levels (4,5), and increasing osteocyte and osteoblast apoptosis (4,5,42,43). Teriparatide's anabolic effects on bone have the potential to slow or reverse these effects. Patients using teriparatide after taking GCs for at least one year showed marked increases in bone density at the spine although these results were less evident at the hip (6). We believed a reversal of bone loss would also be seen in GC-treated mice also treated with

teriparatide. We believed treating animals with teriparatide after GC exposure would likely attenuate bone loss and allow rebuilding of some microarchitectural features. Increased resorption following GC use can cause loss of trabeculae and we did not expect teriparatide to reverse this effect, since teriparatide can only build on existing bone. However, we believed the use of teriparatide after GC exposure would reverse some of the damage and that we would see a greater treatment effect when teriparatide treatment was started at the outset of GC exposure. We believed beginning teriparatide treatment concurrently with GC would result in less overall bone loss since teriparatide would offset the negative effects of the GC drugs.

Research Aim3. To determine the extent of unassisted recovery from GC therapy compared with recovery using teriparatide.

Hypothesis 3. A therapy regimen consisting of 4 weeks of prednisolone use followed by 4 weeks of teriparatide treatment will result in increased bone mass and improved architecture greater than will be seen from natural recovery after withdrawal of GC.

Rationale: We expected GC drugs to decrease bone mass and alter bone architecture. If GC use was halted, we believed bone metabolic processes would return to baseline levels and there would be a gradual restoration of at least some of the lost bone. We expected the natural repair process to be less robust, however, than if teriparatide treatment had been initiated after GC use. Teriparatide is highly anabolic and increases bone turnover and alters metabolism in favor of bone formation. Although teriparatide would be unable to replace lost trabeculae we expected to see increased bone formation on the surface of existing trabeculae.

Research Aim 4. Determine the degree to which skeletal responsiveness to teriparatide would vary by site (femur versus lumbar vertebrae) based on differences in the prevalence of trabecular bone at these sites.

Hypothesis 4. The deleterious effects of GCs and beneficial effects of teriparatide will be seen first and most extensively in the vertebrae.

Rationale: Human studies indicate that the positive effects of teriparatide following GC treatment appear first and to the greatest degree in the lumbar vertebrae (6). In the only study in humans to date examining the effects of teriparatide in GIO, increases in bone density were first detected in the spine (6). Changes in the hip were detected after 12 months of treatment, although these increases in bone density were detected after teriparatide treatment had ended (44). Animal studies have yielded mixed results with some finding the greatest changes in the vertebrae (2,8) and others finding the greatest change in the femur (45). These differences may reflect postural differences in the models, since there is less mechanical loading on the spine in a quadruped. Nevertheless, we believed the most profound changes would be seen in the lumbar vertebrae because this site has more cancellous bone.

Significance of the Study

This study lays the groundwork for future human studies. It is the first step in a research sequence that will help define new treatment options to improve the quality of life for patients exposed to long-term GC therapy and those facing transplant surgeries. This study used microCT and histomorphometry to compare changes in bone quantity and microarchitecture with teriparatide treatment in an animal model of GC exposure. This study also allowed further examination of the specific character of bone loss caused by GC.

Every year nearly 342,000 people in the United States die from lung diseases, which are the 3rd leading cause of death. Many of these patients are given GC drugs to combat the inflammatory conditions of their diseases. Patients suffering from cystic fibrosis, emphysema, and asthma remain on GC treatment for years. A study commissioned by the American Lung Association estimates that in the United States there are 8.6 million patients suffering from

chronic bronchitis and 3.1 million with emphysema. That study also found that 7.7% of adults and 8.8% of children and adolescents under age 18 suffer from asthma (46). With better medical treatments, these patients are surviving longer and it is imperative we find a more effective way to treat the adverse effects of GCs on bone. Additionally, many end stage lung failure patients will be evaluated for possible lung transplant procedures. Some transplant centers view established osteoporosis as a contraindication to lung transplant surgery since patients will need to take a cocktail of immunosuppressant drugs after transplantation and these drugs have deleterious effects on bone. This makes finding an effective treatment for GIO imperative. In the U.S. there have been over 360,000 solid organ transplants since 1988. In 2005, 23,506 solid organ transplants were performed and 90,620 patients remained on waiting lists (47). Solid organ transplantation surgery is increasing over time. Advances in medical science have significantly increased survival times for these patients and preventing or reversing osteoporosis is becoming a more important quality of life issue.

CHAPTER 2 MATERIALS AND METHODS

Background

This study was designed as a randomized, prospective investigation of the effects of teriparatide in treating GC-induced osteopenia in mice. There is strong evidence that glucocorticoids have a deleterious effect on bone. Teriparatide is the only FDA-approved anabolic bone treatment currently available, but it has not been routinely used to reverse GC-induced bone loss. This study uses an animal model to assess the effects of the synthetic glucocorticoid methylprednisolone succinate (prednisolone) and teriparatide at the tissue and cellular level. To evaluate the efficacy of teriparatide to prevent or reverse GIO, 70 mice were randomized among 7 treatment groups receiving a combination of prednisolone, teriparatide, or vehicle to determine changes in bone structure and turnover at the end of a 4-week or 8-week treatment regimen. At the end of the treatment regimen, bone samples were collected to determine changes in bone structure and architecture. This protocol was reviewed and approved by the Institutional Animal Care and Use Committee (IACUC) at the University of Florida.

Animals

The study cohort consisted of 70 male, 7-month old, retired breeder Swiss Webster mice (Harlan Sprague Dawley, Indianapolis, IN). The Swiss Webster, an outbred mouse strain, was selected because they are known to have high levels of trabecular bone (7). Swiss Webster mice achieve peak bone density and cease longitudinal growth in the long bones between 5 and 6 months of age (5) prompting our use of 7-month old mice. Animals had at least seven days to acclimatize to minimize the effects of stress during shipment. Male animals were used to avoid the confounding effects of changes in estrogen levels through the lifecycle of female animals.

We used retired breeders because the costs of feeding and maintaining animals until they reached the age necessary for the study would have been cost prohibitive.

Animal Housing Conditions

Animals were housed in the Special Pathogen-Free (SPF) facility of the Animal Care Services (ACS) department at the University of Florida. Animals were housed one per cage in micro-isolator cages that provided animals with filtered air. Cages were kept in a specially designed rack (American Caging Equipment, Allentown, New Jersey) containing spaces for 70 animals (10 rows with 7 cages per row). Animal cages were moved each week so that animals rotated to different positions within the rack.

Animals were maintained under standard care conditions with 12 hours light/12 hours dark in a climate controlled room with an average temperature of 21 degrees centigrade and humidity of 40%. Animals were fed a standard rodent chow, Teklad Irradiated LM485 mouse/rat chow (Harlan, Indianapolis, IN). This food was irradiated with Cobalt-60 to kill any bacteria or viruses present. The rodent chow had a minimum of 19% crude protein and 5% crude fat and a maximum of 5% fiber. The food contained 0.98% calcium and 0.66% phosphorus. Food intake was not controlled, but food was weighed every three days to determine each animal's consumption. Food debris on the cage floor was not measured and was assumed to be comparable between cages. Water was available ad libitum and was supplied through an automated watering system with the water purified by reverse osmosis. Animals were also provided with a supplemental water bottle. All procedures on animals were conducted under a hood to avoid exposing animals to contaminants. Animals were weighed using a digital balance at the end of their acclimation period, weekly, and prior to sacrifice. Body weights were used to monitor animal health.

Study Group Assignment

Study groups, treatments, and timelines are shown in Figure 2-1.

START	Weeks 1-4	Weeks 5-8	GROUP
(Baseline Sacrifice)			BSL CNTL (n=10)
	VEH	VEH	8 week Vehicle Cntl (n=10)
	GC	SACRIFICE	4 week GC Cntl (n=10)
	GC	GC	8week GC Cntl (n=10)
	GC	VEH	4 week GC/Natural Recovery (n=10)
	GC + PTH	GC + PTH	8 week GC + PTH(n=10)
	GC	GC +PTH	4 week GC/ 4week GC+ PTH (n=10)

Figure 2-1. Study Groups, Treatments and Timelines.

Animals were the same age (7 months) at arrival and were block randomized to groups based on their arrival date at the ACS facility and their body weight. Each week for seven consecutive weeks, 10 animals arrived and were distributed among treatment groups with 1-2 mice/shipment/group.

Pharmacological Agents

Study Drugs

In this study, prednisolone was used to model glucocorticoid treatment. After 4 weeks of exposure to prednisolone, the drug was discontinued in one group of animals to assess natural recovery of the bones. Other animals continued with glucocorticoid treatment alone or were simultaneously treated with teriparatide to see if that drug could prevent or reverse the effects of GC on the bones. Animals receiving teriparatide received subcutaneous injection of 40ug/kg body weight/day, a dose commonly used in studies using mice (8,35). All study drugs and vehicles were formulated so that each animal received a subcutaneous injection volume of approximately 0.1 ml/injection. Animals were restrained by hand and each animal received two

injections per day. Study drugs or vehicle was administered sequentially at approximately the same time of day throughout the study. All study drugs were prepared under sterile conditions.

Prednisolone Succinate

Prednisolone (Webster Veterinary Supply, Sterling MA) or vehicle (sterile saline) was administered at a dose of 2.1 mg/kg/day, 6 days/week. The drug was purchased in liquid form at a concentration of 20 mg/ml and diluted with sterile saline. Prednisolone was prepared fresh 1-2 times per week under sterile conditions in a biochemistry lab in the College of Health and Human Performance.

Teriparatide

Teriparatide (Bachem, Torrence, CA) is a recombinant PTH that consists of the same first 34 amino acids found in endogenous PTH. The anabolic action of the drug has been found to reside in this fragment (48). This drug is currently FDA-approved for use in humans to treat severe osteoporosis.

Teriparatide was purchased in powder form and dissolved in an acidified, 2% heat-inactivated mouse serum stock solution (vehicle) using a formulation used in previous rodent studies (49). Specifically, heat-inactivated mouse serum (obtained from adult, male Swiss Webster mice) was used to make a stock serum solution that was used as vehicle and to dissolve teriparatide. The serum stock solution was prepared by mixing 0.1 ml 0.001N HCL and 97.9 ml sterile saline. The sterile saline and HCL was filtered using a 0.2 micron millipore filter and 2 ml of heat-inactivated serum was then added. The serum stock was divided into 1.5 ml aliquots and stored at -20 degrees C until needed to dilute the PTH stock solution or for use as vehicle.

To prepare the PTH stock, 1 mg of teriparatide was diluted in 1 ml of the serum stock solution. The PTH stock solution was then divided into 10 μ l and 20 μ l aliquots and stored at -80^o C until needed. Storing the PTH stock in small quantities ensured no aliquot was thawed

more than twice. Dissolved teriparatide, was administered at a dose of 40ug/kg/day, 6 days/week subcutaneously in a volume of approximately 0.1 ml/mouse depending on body weight.

Fluorochrome markers

Fluorochrome markers (demeclocycline and calcein) were injected to label actively mineralizing bone. Animals were injected subcutaneously on a pre-determined schedule prior to sacrifice. These fluorochromes bind to calcium and are incorporated into newly forming bone. They provided a means of determining the amount of bone mineralized between fluorochrome treatments. This is a technique commonly used in histomorphometric analysis of bone formation.

Demeclocycline

Animals were injected with demeclocycline (Sigma, St Louis, MO) at a dosage of 15 mg/kg SC 11 and 10 days prior to sacrifice. This drug produces a dull orange fluorescent band on bone that can be seen under ultraviolet light when it binds to calcium in newly formed bone.

Demeclocycline was purchased in powder form and dissolved in sterile saline. The mixture was stirred for at least two hours to insure the demeclocycline completely dissolved. Demeclocycline was prepared fresh the morning of the 11th day prior to sacrifice and used for the -11 and -10 day injections. Any remaining volume was then discarded.

Calcein

Animals were injected with calcein (Sigma, St Louis, MO) SC at a dosage of 15 mg/kg at 4 and 3 days prior to sacrifice. This drug binds to calcium in newly forming bone and appears as a bright green band that can be seen under ultraviolet light. Calcein was purchased in powder form and prepared for injection by dissolving it in sterile saline buffered with sodium bicarbonate. Calcein was prepared fresh the morning of the 4th day prior to sacrifice and used for the 4- and 3-day injections. Remaining calcein was then discarded.

Anesthesia and Euthanasia

Animals were anesthetized using inhaled isoflurane (2-3.5%) with oxygen as the carrier gas using an anesthesia cart with a charcoal filter scavenger attached. Animals were placed one at a time into the anesthesia chamber. The isoflurane gas was started and the animals were observed until unconscious. They were then removed from the chamber and deep anesthesia confirmed by a lack of motor responses to a pinch of the foot. The animals were euthanized by exsanguination from the aorta, followed by cervical dislocation.

Bone Harvesting

Femurs and lumbar vertebrae were harvested to assess (via histomorphometry and microCT) the bone response to treatment in the appendicular and axial skeleton, respectively. Both femurs and vertebrae (13th thoracic through 5th lumbar, T13-L5) were excised from each animal. The femur was disarticulated from the acetabulum and the tibia using a scalpel. A scalpel was also used to shave off the cranial surface of the distal femur to expose the growth plate and metaphysis. The bone was then cut at about the mid-point using a hand-held saw or bone shears.

The lumbar vertebrae were harvested through an incision on the ventral side of the animal. Internal organs were removed and the ventral portion of the vertebral area gently scraped with a scalpel to allow visualization of the vertebrae and intervertebral disks. The lumbar vertebrae were identified by first locating the floating ribs (T11 – T13). A cut was made through the intervertebral disk cranial to the last thoracic vertebrae (T13). The area of the vertebral column to be removed was identified by counting intervertebral disks, which were visible as white bands on the ventral aspect of the spinal column. A second incision was made through the intervertebral disk caudal to the fifth lumbar vertebra. This allowed T13 and lumbar vertebrae L1-L5 to be removed as one section. Removal of T13 with the lumbar vertebrae made it easier

to identify the cranial and caudal ends of the lumbar vertebrae and, therefore, to identify individual vertebrae.

The femurs and lumbar vertebrae were stored in 20-ml glass scintillation vials in phosphate-buffered formalin for 24 hours. After 24 hours, the formalin was poured off and replaced with 70% alcohol. The bones were then kept at 4 degrees C until microCT and histomorphometric assessment.

Study Measures

Anthropomorphic Measures

Animal weights were obtained using a digital scale (Ohaus Scout Pro, Pine Brook, New Jersey). Animals were placed in a weighing bucket to minimize movement and improve weighing accuracy. Animals were weighed after their acclimation period, weekly during the study, and prior to sacrifice. Animal weights were used to determine individual drug dosages and to monitor the health of the animals.

The left femur from each animal was measured using an electronic digital caliper (Little Machine Shop, Pasadena, CA) to confirm lack of longitudinal growth of the femur over time among groups. Each bone was measured twice and the average of these measurements was used. The electronic caliper was zeroed between each measurement.

Histomorphometry

Bone specimen preparation for histomorphometric analysis was carried out at the Wronski Lab, Department of Physiological Sciences, University of Florida using established protocols described elsewhere (50,51). In brief, the right femur and lumbar vertebrae L3 were dehydrated in increasing concentrations of ethanol over a 1-week period and cleared in xylene for 24 hours. The samples were then embedded undecalcified in modified methylmethacrylate to facilitate sectioning. The embedding process involved treating the bones in a series of four

methylmethacrylate solutions (with increasing amounts of a catalyst) that progressively infiltrated the bone over a period of 9 days. The bones were then placed uncapped in a vacuum dessicator for 6-8 hours. Subsequently, the bones were positioned in the center of the vial to optimize the sectioning process and placed in a water bath at 42° C over night. The heat caused the methylmethacrylate to polymerize and harden. Once the methylmethacrylate hardened, the glass vial was broken and removed leaving a plasticized block containing the bone.

The embedded bones were sectioned longitudinally at 4- and 8 μm thickness using Leica/Jung 2050 or 2165 microtomes. Six non-consecutive 4 μm sections and 6 non-consecutive 8 μm sections were cut and mounted on gelatinized glass slides. The two best 4 μm and two best 8 μm sections were selected for analysis. The 4 μm sections were stained for assessment of static (structural and cell) measurements while the 8 μm sections were coverslipped unstained for evaluation of dynamic measurements.

Static bone measurements

The 4 μm thick sections were stained according to the Von Kossa method with a tetrachrome counterstain (Polysciences Inc., Warrington, PA) (50). This stain causes mineralized bone to appear black and bone cells and osteoid to stain blue.

Static structural and cellular endpoints were measured in two 4 μm stained sections using the Trabecular Analysis System (TAS)/Osteomeasure System (Osteometrics Inc., Atlanta, GA) or the Bioquant Elite Bone Morphometry System (R&M Biometrics, Nashville, TN). Endpoints measured or calculated included

- Cancellous bone volume/total volume (BV/TV, %) (percentage of total marrow area occupied by cancellous bone)
- Trabecular width (Tb.Wi, μm) ($1.99 \times \text{B ar}/2/ \text{b Pm}$)
- Trabecular number (Tb.N, #/mm) (BV/TV)/Tb.Th)

- Trabecular separation (Tb.Sp, μm) ($(1/\text{Tb.N}) - \text{Tb.Th}$)
- Osteoblast surface/bone surface (Ob.S/BS, %) (percent of bone surface lined by osteoblasts)
- Osteoclast surface/bone surface (Oc.S/BS, %) (percent of bone surface lined by osteoclasts)

For evaluation of structural endpoints using TAS, the bone section was magnified 2x and a video capture system was used to take an image of the bone. The region of interest (ROI) is 1.5 mm^2 , beginning 0.5mm proximal to the growth plate and extending back toward the diaphysis. The ROI was also 0.25 mm from the cortical bone on either side of the femur. TAS software allowed the user to modify the video image to match the bone section and the software then calculated the amount of bone present within a region of interest. This data was then used to calculate Tb.N, Tb.Th, and Tb.Sp as defined above.

Ob.S and Oc.S were measured using the Bioquant Elite Bone Morphometry System. This system allowed us to manually trace the total perimeter of cancellous bone as well as the portions of cancellous bone surface covered by osteoblasts and osteoclasts to calculate the proportion of the total cancellous bone covered by these cells.

Dynamic bone measurements

Dynamic bone analysis was accomplished using flurochrome-based data collected from unstained 8 μm femur sections using the Osteomeasure System. Two sections from each animal were used and the results averaged. Flurochrome data was used to determine

- Mineralizing surface (MS/BS, %) (percentage of cancellous bone surface with a double flurochrome label; MS/BS is a dynamic index of bone formation).
- Mineral apposition rate (MAR, $\mu\text{m}/\text{day}$) (distance between the two flurochrome labels divided by the number of days between label administration; MAR is an index of osteoblast activity).
- Bone formation rate/bone surface (BFR/BS, $\text{um}^3/\text{um}^2/\text{day}$) ($\text{MS} \times \text{MAR}$; volume of new bone formed per unit of total bone surface per unit time)

The slides were magnified at 200X on the microscope and displayed at 250X on the computer monitor. The area of interest was defined as the area beginning approximately 0.5 mm proximal to the end of the growth plate and consists of a series of fields that, combined, equal a cancellous bone area approximately 1.5 mm X 1.5 mm that is about 375 μm from the cortex. The cancellous bone (with and without fluoro-chrome labels) was outlined using a digitizing tablet. Then, the inner and outer fluoro-chrome labels were outlined where double labeling exists and the distance between these two lines was measured at 4 approximately equidistant points. The software then calculated the MS, MAR, and BFR/BS as defined above.

MicroCT

MicroCT was used for nondestructive three-dimensional evaluation of bone microarchitecture. MicroCT identified subtle changes in three-dimensional bone architecture that cannot be detected by histomorphometry. The bones were scanned using a Scano microCT40 scanner (Scanco Medical AG, Basserdorf, Switzerland). Cancellous bone in the LV and femoral metaphysis was evaluated.

Femur

Prior to placement in the microCT, the femurs were first cleaned of non-skeletal connective tissue and muscle and placed between two thin Styrofoam pads. The Styrofoam pads help kept the samples from moving during the test. The bones and padding were placed in a specially designed tube that was 12.3 mm in diameter. Three femurs were loaded into the tube and scanned sequentially. The tube was then filled with 70% ETOH and covered with parafilm. The samples were scanned at medium resolution at a voxel size of 12.3 x 12.3 x 12.3 μm . Scanning took approximately one hour per bone. Reconstruction of the bones following the scan took an additional hour per bone. The volume of interest in the distal femur consisted of 1.8 mm^2 starting at the growth plate and moving toward the diaphysis. Of the 120 – 180 slices

scanned, 150 were analyzed. Twenty slices (approximately 0.25 mm) of cortical bone were also analyzed in the femoral midshaft. The VOI for cortical bone began at the midpoint of the femur and included 55 slices toward the proximal femur. Of the 55 slices scanned, 20 were analyzed.

Direct cancellous bone measurements in the femur included:

- total tissue volume (combined volume of cancellous bone and bone marrow in the volume of interest (VOI))
- Cancellous bone volume (volume in the VOI occupied by cancellous bone)
- Trabecular thickness
- Trabecular number
- Trabecular separation
- Cortical thickness was measured in a sample from the mid-shaft

Once the bone was scanned and reconstructed, drawing tools provided with the software were used to outline the area of interest (AOI). Every tenth slice was contoured by hand and the software extrapolated the AOI to the remaining slices. A visual inspection of each slice was done to ensure no cortical bone was included in the cancellous ROI. The ROI for the distal femur scanned consisted of the cancellous bone proximal to the growth plate extending to about 1.8 mm toward the diaphysis. The cortical bone analyzed began at approximately the center of the diaphysis to a point 20 uCT slices (250 μm) toward the distal metaphysis.

Vertebrae

The second lumbar vertebrae (L2) was analyzed using uCT. First, L2 was separated from the rest of the vertebrae and non-skeletal connective and muscle tissue was removed. The vertebrae were scanned eight at a time. The spinal canal of each vertebra was threaded onto a slender wooden holder and a small piece of Styrofoam was placed at the bottom of the wooden holder, between each vertebrae, and at the top of the holder. This held the vertebrae upright and

helped controlled movement during the scan. A scout scan was run to identify the area for analysis and then the scan proceeded automatically. The samples were scanned at medium resolution at a voxel size of 12.3 x 12.3 x 12.3 μm . The scan took approximately one hour per bone and required an additional hour per bone reconstruction time prior to analysis. As with the femoral metaphysis, cancellous bone measurements in the vertebrae included

- Total tissue volume
- Cancellous bone volume
- Trabecular thickness
- Trabecular number
- Trabecular separation.

The AOI for the vertebra included all of the secondary cancellous bone between the two growth plates. Once the bone was scanned and reconstructed, the software drawing tools provided were used to contour the AOI at every sixth slice. The software then extrapolated the AOI to the other slices. All slices were reviewed to ensure no cortical bone was included in the AOI.

Statistical Analysis

A power analysis was conducted to determine adequate sample size using data from a study evaluating the effects of treating Swiss Webster mice with the same prednisolone dosage proposed for this study (5). The present study was designed to achieve a power of at least 0.80. Power analysis using SAS version 4.0 (SAS Institute Inc., Cary NC) indicated eight animals per group would result in a 0.87 power. Each group in this study contained 10 animals to insure study power was not compromised if any animals had to be removed from the study prematurely. Data is presented in table format as mean \pm standard deviation (SD) and bar graphs with mean \pm standard error for continuous variables, and as percent change for statistically significant differences between groups. Statistical analysis on data was conducted using SPSS 10.0

statistical software (SPSS Inc, Chicago, IL). Data was analyzed using the nonparametric Kruskal-Wallis test (52). When significant treatment differences were observed, between-group comparisons were performed using the Mann Whitney test of independent samples.

CHAPTER 3 LITERATURE REVIEW

This chapter is divided into two parts. Part A will present a general overview of bone structure and metabolism, including a look at the various types of bone cells that contribute to the remodeling process. The four phases of bone remodeling: activation, resorption, reversal, and formation are also described. In the remodeling process, bone is first resorbed and then new bone is deposited. There is still much we do not understand about this process and how lifestyle, health, and pharmacologic interventions can influence the balance. The second part of this chapter describes the effects of two pharmacological agents, one catabolic (prednisolone) and one anabolic (teriparatide), on bone remodeling. Normal levels of remodeling are altered by both of these drugs, but in different ways, and Part B of this chapter will describe what we know about the influences of these drugs on the mouse model.

Bone Biology

Structure of Bone

There are two basic types: cortical and cancellous. Cortical bone is the hard outer layer of bone and is denser than cancellous bone, which is found closer to the bone marrow. By volume, cortical bone makes up about 80% of the adult human skeleton. The remaining 20% is the more changeable cancellous bone. In contrast to the hard and only slightly porous cortical bone, cancellous bone is a complex three-dimensional network of curved plates and rods in close association with bone marrow and is enclosed by cortical bone. Cancellous bone is made up of a lattice of large plates and rods collectively called trabeculae. The inner or endocortical side of cortical bone within the medullary cavity (53).

Cancellous bone is mainly found in bones of the axial skeleton, in flat and irregular bones, and in the ends of the long bones (53). This type of bone experiences deformation when loaded

and is better able to bear loads without becoming damaged (54). The lattice-like structure of cancellous bone means its surface-to-volume ratio is higher than that of cortical bone. Since remodeling takes place at the surface of bones, the greater relative surface area of cancellous bone means remodeling takes place there at a rate ten times greater than in cortical bone (53,55). Thus, when there is an imbalance leading to more bone resorption than formation, the effects will be most apparent in cancellous bone such as that found in the vertebrae and the ends of long bones.

Bones do not contain cortical and cancellous bone tissue uniformly. A typical long bone has 3 regions that vary in composition. The diaphysis, the shaft of the bone, is comprised mainly of cortical bone. The ends of the long bones, known as the epiphyses, are to a large degree cancellous bone, as are the metaphyses, the conical section of bone connecting the epiphysis and diaphysis. Cancellous bone is made up of plates of bone tissue and loss results in a gradual shift from plate-like to rod-like structures as the dominant elements (56). This contributes to increased fragility of the bone, since spaces within the bone increase as the “struts” connecting one section to another disappear. Electron microscopy of an older person’s bones shows wider spaces and fewer structural connections. This has important implications for bone strength since trabecular struts, once lost, cannot be replaced (56). Trabecular compromise occurs when osteoclasts erode a cavity too deeply or when the osteoblasts are unable to lay down a sufficient amount of replacement bone (56).

The major components of cortical and cancellous bone are type 1 collagen, water, hydroxyapatite mineral, and small amounts of proteoglycans and noncollagenous proteins. Type 1 collagen is a structural protein found mainly in bone and tendons. Hydroxyapatite, $\text{Ca}_{10}(\text{PO}_4)_6(\text{OH})_2$, makes up virtually all of the mineral in bone and represents the major

storehouse for the body's calcium. Calcium is taken in or released based on fluctuating plasma calcium levels and the presence of the major calcium regulating hormones, PTH and calcitonin.

Bone Cells

Bone cells include osteoclasts, osteoblasts, osteocytes, and bone-lining cells. Each cell type is critical to bone remodeling and these cells have complex mechanisms of communication that control their actions and interactions. These cells generally operate in balance with each other, although aging, some disease conditions, and certain drugs can alter that balance. There is ample opportunity for the balance in bone metabolism to shift toward more resorption than deposition since the osteoclast is able to resorb in one day an amount of bone that osteoblasts need several days to replace.

Osteoclasts

Osteoclasts are large, multinucleated cells associated with bone resorption. Osteoclasts originate from hematopoietic stem cells in the bone marrow and travel via the circulatory (or perhaps the lymphatic) system. Mature osteoclasts are responsible for bone resorption, where bone is broken down and the calcium within liberated. Osteoclasts adhere to bone by means of an actin ring that is anchored to the extracellular matrix by integrins. This forms a sealing zone that creates a microenvironment between the osteoclast and the surface of the bone that will be resorbed (57). When osteoclasts attach to bone, the cell is polarized and generates a ruffled border. It is at this ruffled border that vesicles containing cathepsin K and membrane-bound H⁺ ATPase exist. Cathepsin K, an acidic collagenase, degrades the organic component in bone (type 1 collagen) while the H⁺ ATPase secretes hydrochloric acid into the sub-cellular space and dissolves hydroxyapatite (58).

Osteoclasts are found in cavities on the bone surface, which they themselves form, called resorption pits or Howship's lacunae. Interestingly, although associated with resorption,

osteoclasts have no receptors for PTH, the main endogenous mediator of bone breakdown. Instead, osteoclasts have receptors for calcitonin, a hormone that inhibits bone resorption (59).

Osteoblasts

Mature osteoblasts are bone-forming cells that typically reside on the bone surface where they secrete unmineralized matrix, called osteoid, during the bone formation process. They also participate in calcification of bone and regulate the movement of calcium and phosphate into and out of the bone. These cells are normally cuboidal in shape. Osteoblasts themselves produce and secrete a number of substances important to bone metabolism including type 1 collagen, non-collagenous matrix proteins such as osteocalcin and osteonectin, growth factors, prostaglandins E₁ and E₂, Receptor Activator of Nuclear factor kappa B ligand (RANKL) and osteoprotegerin (OPG) and cytokines including interleukin (IL)-1, IL-6, and 11, TNF, and TGF- β (60). Although osteoblasts are most noted for bone formation, they also help control bone resorption since they have receptors for PTH and secrete OPG and RANKL.

In humans, osteoblasts secrete osteoid at the rate of about 1 micrometer per day. This means that either the lifespan of the osteoblast is quite long or that multiple generations of osteoblasts are involved in refilling a given resorption pit since these pits can be quite deep (61,62). When the osteoblast has finished secreting osteoid, it returns to the preosteoblast pool, transforms into a bone-lining cell, gets buried as an osteocyte, or dies (53).

Osteocytes

Osteoblasts which become trapped in the osteoid they secrete are called osteocytes. Each lacuna contains only a single osteocyte. These cells maintain contact with each other and with bone-lining cells via slender processes that reach through the canaliculi of the bone at the gap junctions. There are gap junctions between adjacent bone-lining cells and between bone-lining cells and osteocytes. Osteocytes are thought to be involved in detecting microfractures and the

cell signaling that begins the process of remodeling (53,61,62). They may also be involved in storing mineral ions following a meal rich in calcium and in transporting minerals from deeper skeletal reservoirs to the extracellular fluid compartment after resorption (53).

Bone Lining Cells

The final major bone cell type is the bone-lining cell. These are long, flat cells that cover quiescent (or resting) bone surfaces, where bone is neither being resorbed nor formed. Like osteocytes, bone lining cells originate from osteoblasts. They differ from osteocytes, however, in that they remain on the bone surface rather than being buried in the matrix. As bone formation ends, bone lining cells remain on the newly formed bone surface. They communicate with osteocytes and each other through gap junctions. The bone lining cells assist the osteocytes in moving mineral in and out of the bone and may also play a role in sensing mechanical strain on bone (63).

Bone Remodeling

Bone remodeling is the term used to describe the processes of resorbing old bone and depositing new bone at the same site. Bone remodeling is an on-going “housekeeping” activity of healthy bone. Even in the absence of external stimuli there will be remodeling activity. This process of remodeling is most obvious in its accelerated form when there is a fracture and the body quickly moves to repair the damage. On a more subtle scale, however, the body is constantly replacing old bone and repairing microfractures, the damage caused by daily activity. Repair of this damage helps keep the bones strong by preventing structural weaknesses from accumulating. Continual remodeling helps bone maintain strength and structural integrity, so long as there is a balance between resorption and deposition. In the aggregate, what determines whether more bone is being formed or resorbed is the relative amount of each activity. Hormones such as estrogen, growth hormone, insulin, parathyroid hormone (PTH), testosterone

and agents like fluoride and aluminum directly or indirectly affect the balance to varying degrees (53,61,62,64,65).

Basic Multicellular Units (BMUs) orchestrate bone turnover, removing mechanically unneeded bone and repairing microdamage by laying down new bone. BMUs consist of osteoclasts and osteoblasts that congregate at a specific area of the bone where they have been drawn, possibly by the signaling activity of osteocytes (66). In cortical bone the BMU tunnel in a cone-like pattern through the bone while in the trabecular bone BMUs scallop the surface of the trabeculae to form a trench (39,43). The BMU remodels bone in four distinct phases: activation, resorption, reversal, and formation. When not involved in remodeling, bone is said to be quiescent.

Bone remodeling begins when a quiescent skeletal surface is activated. The activation phase is characterized by a retraction of the bone lining cells at the activation site and formation of new blood vessels that will bring osteoclasts to the resorption site. This exposes mineralized bone surface which may act as a chemoattractant for osteoclast precursor cells (53,61,62). During the activation phase, preosteoclasts fuse to form the characteristic multinucleated mature osteoclasts which will attach themselves to the exposed bone surface (43).

The resorption phase begins when the multinucleated osteoclasts begin to resorb bone at the remodeling site. The osteoclast, with its ruffled border, attaches to the area of the bone to be resorbed; here the osteoclast and the underlying bone form the microenvironment into which the osteoclast secretes acids. When the osteoclast secretes acids into this microenvironment, the collagen matrix breaks down, forming concave pits called resorption pits or Howship's lacunae. In humans, the resorption pits have an average erosion depth of 60 micrometers in trabecular bone and about 100 micrometers in cortical bone. The osteoclasts can erode up to tens of

micrometers per day (61). The whole process of resorption takes 1-3 weeks and culminates with the release of calcium and other compounds from the matrix of the dissolved bone. The end of resorption is marked by osteoclasts migrating from the bone surface to nearby marrow spaces, where they hibernate or die (67).

The third stage of remodeling, reversal, is characterized by preparations to lay down new bone. Phagocytes smooth out ragged edges left by the osteoclasts and a thin layer of collagen and matrix, referred to as a cement line, is laid down. Osteoblasts are drawn to the area through as yet not understood mechanisms. Osteoblasts may be stimulated to mature by signals from compounds such as growth factors released from the bone itself when it breaks down. Some believe these signals occur when the calcium released by resorption activates calcium receptors on osteoblasts. This, theoretically, helps insure bone resorption does not get out of control, since the more resorption there is, the more osteoblasts would be stimulated to form new bone (68). Once at the remodeling site, osteoblasts adhere to the cement line where they begin filling in the resorption cavity with osteoid (43). In the final phase of remodeling, known as formation, new osteoid is secreted by the osteoblasts. Under normal conditions, if there is sufficient calcium available, the new bone is mineralized. Flurochrome labeling is often used to measure this process.

In humans, the entire sequence of resorption and formation at a given remodeling site takes place over a period of several months and it is estimated that the lifespan of a BMU is about 6-9 months (43,64,68). In healthy adults between 3 and 4 million BMUs are activated annually, with about 1 million operating at any given time (43). The remodeling cycle in animals follows the same sequence of events but the time required is significantly less. This accelerated response

in animals makes them an attractive model to predict the effects of conditions and treatments in humans

Remodeling Balance : The RANKL/OPG/RANK Axis

The balance of bone remodeling is controlled by hormones and paracrine influences originating from osteoblasts or stromal cells. The discovery of RANKL and OPG was an important milestone in bone research since this helped explain a seeming paradox of bone remodeling. Namely, that many of the hormones, cytokines, and growth factors that regulate osteoclast activity have receptors on the osteoblast (69). Researchers had also noted that cell cultures of osteoclast precursors physically separated from osteoblasts did not develop into functional osteoclasts (65) and osteoclast apoptosis increased, indicating a close relationship between osteoblasts and the production and differentiation of osteoclasts. RANKL is produced by osteoblasts and binds to RANK receptors on osteoclasts and osteoclast precursors where it stimulates differentiation and greater activity of osteoclasts. OPG is also produced by osteoblasts but is a decoy receptor that competitively binds RANKL. The amount of bone resorption is modulated at least to some extent by the ratio of RANKL to OPG.

It is the ratio of RANKL to OPG, and not just the level of RANKL, that seems to govern whether bone remodeling favors formation or resorption so it is important to see what substances influence the ratio (70). OPG production is stimulated by 1,25 dihydroxy vitamin D₃, BMP-2, TNF- α , IL-1 α and -1 β , and estrogen (1,71). The resulting increase in OPG production removes additional amounts of RANKL, thus decreasing the amount of RANKL available to bind to RANK which results in reduced osteoclast differentiation and activity. Many circumstances lead to increased RANKL production, such as glucocorticoid use, lack of estrogen, and it is often present in diseases like rheumatoid arthritis.

Effects of Glucocorticoid Drugs and Teriparatide on Bone

GCs inhibit the formation of osteoblasts and osteoclasts, increase apoptosis in osteoblasts, and interfere with normal bone remodeling. While the negative effects of GCs on bone have long been recognized, the mechanisms remain to be fully understood (72-75). Glucocorticoids bind to a cytoplasmic glucocorticoid receptor (GR) found on osteoblasts (76). The receptor is a ligand-operated transcription factor. When not bound, the receptor is located in the cytoplasm as a protein complex. When activated, the complex dissociates and the receptor moves into the nucleus and binds to regulatory elements in the promoter regions of certain anti-inflammatory genes (77-79). The GR also inactivates inflammatory genes by binding to transcription factors activator protein-1 (AP-1) and nuclear factor kappaB (NF- κ B) (77,78). With these transcription factors bound there is inhibition of pro-inflammatory cytokines such as IL-1 β , IL-4, IL-5, and IL-8, and TNF- α (77). Genomic effects begin probably no sooner than 30 minutes after GC administration, and are initiated by binding of the steroid to cytosolic receptors. Nongenomic effects occur sooner, often within a few minutes, and are mediated by membrane-bound GC receptors (74). There appears to be general agreement that GCs cause decreased bone formation; the case is not so clear for bone resorption (21,23).

Systemic Effects of Glucocorticoid Drugs

GCs exert a number of effects, both direct and indirect, that influence bone metabolism. (see Table 3-1). The direct effects of glucocorticoid drugs are those that effect the bone cells themselves and includes actions that effect osteoclasts, osteoblasts and osteocytes. Direct effects also include influences on the production of RANKL and OPG and influences on various bone-related growth factors. Indirect effects include influences on organ systems that influence calcium metabolism.

Table 3-1. Common Effects of Glucocorticoid Therapy.

Direct Effects	Indirect Effects
Increased Osteoclast formation	Increased Urinary Calcium Excretion
Increased Osteoblast apoptosis	Increased Intestinal Calcium Absorption
Increased Osteocyte apoptosis	Decreased GH production
Increased RANKL	Hypogonadism
Decreased Osteoblast #s and activity	Impaired renal function
Decreased OPG	Secondary Hyperparathyroidism
Decreased Type I Collagen Production	
Decreased skeletal growth factors (IGF-1, TGF- β)	

RANKL = Receptor activator of nuclear factor (NF)- κ B ligand; OPG = Osteoprotegerin; IGF-1 = Insulin-like Growth Factor; TGF- β = Tumor Growth Factor- β ; GH= Growth Hormone.

Direct Effects of Glucocorticoids

The effects of GCs on osteoblasts are potent, causing pre-osteoblasts to differentiate to adipocytes and decreasing synthesis of type I collagen by mature osteoblasts (80,81). GCs also decrease the ability of osteoblasts to adhere to the extracellular matrix and promotes matrix breakdown by stimulating the activity of interstitial collagenase. Additionally, GCs amplify the response of osteoblasts to endogenous PTH by increasing the number of PTH receptors on the cell (23). The osteoblast lifespan decreases, leaving less time for synthesis of bone matrix and mineralization. Taken together, these effects result in a significant decrease in bone formation as evidenced by sharp reductions in circulating levels of osteocalcin even at low doses (~ 5mg/day in humans) of GC (76,82). GCs also inhibit a number of growth factors such as IGF-1, which increase the synthesis of type I collagen, and decrease collagenase 3 expression (80).

Although there is general agreement that GC use decreases bone formation, it is less clear whether GCs increase bone resorption (23,74,83). Studies of bone cells in vitro have variously shown stimulation and inhibition of osteoclasts in cell cultures (23,83) in response to GC, and decreased apoptosis of mature osteoclasts (75). Some histomorphometric studies have found increased resorption (84) in the presence of GCs but serum and urine markers of bone resorption have shown inconsistent results (84).

GC treatment increases osteoblast production of RANKL and colony-stimulating factor (CSF)-1 (also known as macrophage-colony stimulating factor or M-CSF) (81). The combination of M-CSF and RANKL stimulates osteoclastogenesis. At the same time RANKL is increasing, OPG levels decrease. GC drugs have been shown to inhibit OPG mRNA by 70-90%, increase mRNA levels of RANKL and RANKL/M-CSF-induced TRAP activity by over 50% (1,60,85). This has the potential to shift the bone remodeling balance in favor of resorption by increasing osteoclast formation.

With GC use in humans, there appears to be an early increase in bone loss which moderates over time, creating a biphasic response (76,80,86,87). One explanation for early increases in resorption that subside later is the influence of GCs on induction of IL-6 receptors in bone (87). Since IL-6 is a cytokine important in osteoclast recruitment, any increase in the number of receptors in skeletal tissue could increase bone resorption by recruiting more osteoclasts. At the same time, GCs also inhibit osteoblastogenesis. Declining numbers of osteoblasts eventually will produce less aggregate RANKL, causing reduced osteoclastogenesis as well (88). That may explain observations that the greatest bone losses from GC use are experienced early in treatment and the rate of loss decreases and levels off over time.

Indirect Effects of Glucocorticoid Drugs

In addition to the direct effects of GC on bone metabolism there are also indirect effects that similarly result in bone loss over time. The indirect effects of GCs on bone involve a number of organ systems in the body and are summarized in Table 3-1.

Decreased intestinal absorption of calcium

GC use results in a decrease in calcium absorption in the intestines (80). Although the mechanism is not entirely understood, GCs appear to effect the duodenum by inhibiting active

calcium transport, decreasing the production of calcium-binding proteins and possibly increasing the degradation of 1,25(OH)₂ vitamin D at its binding site (21,74,76,86).

Increased renal elimination of calcium

Increased renal excretion of calcium may be due to a reduction in reabsorption of calcium in the distal tubule of the kidney (74,76). In the presence of GCs, the kidney tubules handle sodium and calcium cations differently (86). GC treatment increases activity of epithelial Na⁺ channels, passive sodium channels on the apical membrane of the distal tubules and conducting duct cells and this increases the activity of Na⁺/Ca²⁺ antiport pumps, resulting in increased calcium extrusion (86). Increased renal calcium excretion coupled with decreased intestinal absorption may lead to secondary hyperparathyroidism (23,74). It is unclear how this affects overall bone remodeling, however. It was once believed that secondary hyperparathyroidism accounted for GC-mediated changes in bone, but research now suggests the situation is much more complex and dynamic (72). Even in cases where secondary hyperparathyroidism occurs, it does not explain the trabecular bone loss seen with GC use (80). In patients with secondary hyperparathyroidism, bone remodeling is increased (80) and the main effects are seen in cortical bone (81) instead of the decreased remodeling that primarily affects cancellous bone as seen in GIO.

Antagonistic action on gonadal functions

Researchers have identified a direct GC-mediated effect on the production of gonadal steroids in men and women (74). It is believed GCs suppress the hypothalamic-pituitary-adrenal axis and inhibit gonadotropin secretion (84). GC treatment has been shown to decrease circulating levels of testosterone in men by about 50% (75). Similar effects on estrogen are believed to occur in women (18,75). Both estrogens and androgens suppress bone resorption by

inhibiting osteoblastic release of local stimulating factors that cause formation of increased numbers of osteoclasts (17,75).

Increased sensitivity to PTH

In vitro studies of isolated bone cells have shown that GCs modulated PTH sensitivity of both osteoblasts and osteocytes such that lower levels of PTH still elicited measurable biochemical changes (18). This may be accomplished by GC-mediated upregulation of osteoblast PTH receptors (74) or increased affinity of the receptor for PTH (23,81). This could explain why changes in bone are seen even when PTH levels remain in the normal range.

Bone loss in response to glucocorticoid treatment

Studies have shown that with GC treatment, there is a loss in trabecular connectivity making this population more susceptible to fracture (23,76,81). This change in bone microarchitecture cannot be detected with densitometry, the most common clinical means of testing for bone loss. Some have suggested that the GC-mediated loss of osteoblasts and osteocytes compromise bone strength independent of bone loss (72). According to this theory, the integrity of bone relies on the network of osteocytes found there. Osteocyte apoptosis may reduce the signaling available to initiate the replacement of damaged bone (73). This may explain why fracture risk increases as early as three months after GC use, even before significant bone loss has occurred (73). In response to this, the Royal College of Physicians of London in recent years suggested using a T score of -1.5 or lower as the treatment threshold for GC users (81). Despite these recommendations, it is estimated that less than 15% of those on long-term steroid treatment also receive preventive medication to prevent osteoporosis (16,22,89) and there still appears to be limited testing for bone loss in GC patients (22). There have been suggestions that preventive treatment should begin at the same time as GC therapy is initiated (89).

Parathyroid Hormone

Dual Nature of PTH* : Continuous versus Intermittent Administration

Parathyroid hormone has a surprising, dual effect in mammals depending on whether delivery is continuous or intermittent. At least since the 1930s researchers have noted that PTH is catabolic when exposure was continuous (as it normally is in the body in response to low plasma calcium levels) but showed anabolic properties when administered intermittently (90-93). The use of PTH in an anabolic role was not seriously pursued, however, until it became possible to manufacture synthetic PTH. In the mid-1970s, recombinant techniques made it possible to sequence the amino acid fragment responsible for the hormone's anabolic effect (90). This anabolic capability resides in the first 34 amino acids on the N-terminal end which is why teriparatide is manufactured as PTH (1-34) (48,92,94).

It has been suggested that at least some of the anabolic effects of intermittent PTH in bone are mediated through an IGF-I-dependent mechanism, while the catabolic effects are mediated through gene expression that causes an increased ratio of RANKL to OPG (95,96). Teriparatide reverses the effects of GC on IGF-I expression in vitro, and this may partially explain its effects in treating GC-induced bone loss (80).

Parathyroid Hormone (PTH 1-84)

Endogenous PTH is an 84-amino acid protein secreted by the chief cells of the parathyroid glands when low serum calcium levels are detected by calcium receptors on the parathyroid glands (97) or there are elevated levels of extracellular phosphate (98). PTH 1-84 is a critical mediator of calcium homeostasis. Calcium-sensing receptors on the surface cells of the parathyroid gland respond to minute-by-minute changes in serum calcium levels (48,94,99) and

* To avoid confusion, PTH produced by the parathyroid glands will be referred to as endogenous PTH or PTH 1-84 and recombinant parathyroid hormone will be referred to as teriparatide or PTH (1-34).

maintain calcium balance through direct actions on bone and kidneys and indirectly through the gastrointestinal tract. When blood levels of calcium are low, PTH stimulates bone resorption to liberate calcium stored in the bone matrix and enhances calcium reabsorption at the distal convoluted tubules of the kidney (94,98). PTH also regulates 1 alpha-hydroxylase activity in the kidney, facilitating the conversion of 25-hydroxyvitamin D to 1,25 dihydroxyvitamin D in the kidney, which then acts on the GI tract to stimulate increased absorption of calcium across the gut (94,99,100).

In humans, the half-life of endogenous PTH in the blood is less than 3 minutes and it is metabolized by both the kidney (20-30%) and liver (60-70%) (90,94). This rapid metabolism means the availability of PTH is determined by the rate of secretion from the parathyroid glands. Endogenous PTH has both rapid and slow effects on bone. The rapid phase occurs within 30-90 minutes after exposure and is characterized by increased osteoclast activity. A second, later phase, is associated with an increase in both the number and activity of osteoclasts (94,101). With continuous PTH exposure there is a decrease in OPG mRNA and an increase in RANKL mRNA.

While the actual mechanisms are not fully understood, PTH may exert its actions by activating a number of enzymes such as collagenase, lysosomal hydroxylases, acid phosphatases, H^+ , K^+ -adenosine triphosphatases, Na^+/Ca^+ exchange systems, cathepsin B, or cysteine proteases. Continuous PTH exposure causes bone lining cells to retract from the bone surface as part of a calpain-dependent modification to the osteocyte cytoskeleton. This allows osteoclasts to attach to the bone surface where they then initiate the process of bone resorption (94). PTH also inhibits osteoclast apoptosis, possibly by stimulating the expression of RANKL and decreasing the expression of OPG by osteoblasts (102).

Teriparatide (PTH 1-34)

Teriparatide, a recombinant parathyroid hormone marketed as FORTEO™ by Eli Lilly pharmaceutical company, is currently the only FDA-approved anabolic drug for osteoporosis. Unlike the anti-resorptive drugs, teriparatide stimulates bone formation, which contributes to increased bone mass, quality, and strength. Teriparatide is administered as a subcutaneous injection typically 20ug/day for 18-24 months in humans. The drug is not recommended for long-duration use since it caused an increased incidence of osteosarcoma in rats after long-term exposure to large doses of the drug (103-105). Teriparatide is manufactured from a strain of *Escherichia coli* modified by recombinant DNA technology (100,106). Teriparatide, which has a bioavailability of around 95% (90,100), reaches peak plasma concentration in about 30 minutes, then drops to virtually undetectable levels in 3-4 hours (90,92,97,100). The systemic clearance of teriparatide is approximately 62 L/hour in women and 94 L/hour in men, which is greater than the rate of normal hepatic plasma flow, indicating both hepatic and kidney clearance similar to PTH (1-84) (100).

Following extensive testing and clinical trials, teriparatide was approved by the FDA in November 2002 (100) for the treatment of postmenopausal women with osteoporosis who are at high risk for fracture and to increase bone mass in men with primary or hypogonadal osteoporosis who are at high risk for fractures (107). Daily injections of teriparatide increase bone mass, microarchitectural structure and bone strength in mice, rats, rabbits, monkeys and humans (97). Studies have shown it provides a statistically significant increase in BMD at clinically important sites such as the lumbar spine (29). The increased bone turnover caused by teriparatide results in additional bone apposition on both periosteal and cancellous bone surfaces (97). The effects of teriparatide are less robust at the femoral neck.

Mechanisms of Action

PTH and teriparatide work through G Proteins and the PTH Receptor 1 (PTH1R) has a similar affinity for both (90). PTH receptors are found predominantly on osteoblasts (but are also found in renal tubular cells) (48,90,94). Binding of PTH to the receptor activates adenylate cyclase and phospholipases A, C, and D and increases intracellular levels of cAMP and calcium (90). Some think it may be the ability of PTH to stimulate both adenylate cyclase and phospholipase C that gives it its dual anabolic and catabolic abilities (48).

The primary effects of teriparatide on osteoclasts are indirect and are mediated by the drug's effects on osteoblasts. Increased bone formation following exposure to teriparatide occurs because of an increase in osteoblast numbers either through enhanced differentiation of pre-osteoblasts or an increase in the number of existing bone lining cells that differentiate into osteoblasts (48,90,108). Teriparatide also has an anti-apoptotic effect on osteoblasts, enabling them to secrete bone matrix for a longer period of time (48,92,100,109). Through these actions, the production of collagen-based bone matrix increases, improving trabecular bone volume and connectivity (90,110). Teriparatide also acts on the cortical surface of cortical bone and increases its thickness without increasing porosity (90,109,111).

Treatment with teriparatide has a variety of effects on osteoblasts, including causing increased secretion of various growth factors, such as transforming growth factor β (TGF- β), IGF I and II, IGF binding proteins, bone morphogenic proteins (BMPs), and cytokines such as IL-1, IL-6 and M-CSF (48,92,95,112). M-CSF, IL-1, RANKL, and TNF β all enhance osteoclast survival (102). The net result is increased bone turnover. However, unlike the increased turnover seen in many disease conditions, the increased turnover associated with teriparatide favors bone formation over resorption. This is what causes teriparatide to have its anabolic effect on bone.

Studies of Glucocorticoid-Induced Bone Loss in Mice

Validity of the Mouse as a Model of Glucocorticoid-Induced Bone Loss

The mouse genome has now been sequenced, making this animal an even more attractive model for scientific research. The mouse has shown its value in studies of bone loss due to aging and sex steroid alterations (3) and some believe it is the preferred rodent model for the study of bone loss due to GC exposure (3-5). This is because some researchers believe the rat may be resistant to the deleterious effects on bone associated with GC exposure and therefore may not represent a good model for this specific condition (36-38). Commonly used mouse strains to assess the effects of GCs include the Swiss Webster (5), the C57B1 (4) and the Balb/C (3) (see table 2). Studies to date have used techniques such as histomorphometry, microCT, serum biochemistry, and DXA to measure bone responses in mice exposed to GCs (2-5). Most studies have reported that GC treatment induces greater axial than appendicular bone loss (5) without significant weight loss or hypogonadism (2,3). A summary of GC-induced bone loss studies using mice listed in Appendix B.

Glucocorticoid-Induced Bone Loss in Mice

Glucocorticoid drugs have been shown to affect mouse bone metabolism during both in vitro and in vivo experiments. In cell culture studies, the number of osteoclast precursors following treatment with prednisolone for 4 or 10 days decreased significantly after just 4 days. Osteoblast precursors also decreased, but only after 10 days of treatment. Despite fewer precursor cells, prednisolone exposure resulted in an 81% increase in osteoclast numbers and a 20-fold increase in the ratio of osteoclasts to osteoblasts perhaps reflecting decreased osteoclast apoptosis (4).

In adult Swiss Webster mice, glucocorticoids affect osteoblasts and osteocytes at a threshold dose of 1.4 mg/kg body weight (5). Some researchers have used this threshold dose (2)

while others have used a dose of 2.1 mg/kg body weight (4,5). At this higher level of treatment, researchers have found increased osteoclast survival in as few as 10 days (4). MicroCT analysis following administration of low levels of GC (1.2 mg/kg) only found significant differences in BV, while there were no significant differences either in Tb.N or Tb.Th (2). Bone changes were generally dose and duration dependent. In one study the greatest changes were detected when 10 mg/kg was administered over a 21-day period (3).

Histomorphometric analysis of the bones has yielded mixed results with some studies finding significant decreases in trabecular thickness while other studies found no significant difference in this measure (2-5). In these studies, histomorphometric analysis of kinetic measures were more consistent and showed significant decreases in mineralizing surface, mineral apposition rate, and bone formation rate (2-5). Studies have also demonstrated a preferential bone loss in the axial skeleton (5) and that spinal BMD decreases in a dose-dependent manner (3-5).

Dynamic measures, such as mineralizing surface (MS), mineral apposition rate (MAR), and bone formation rate (BFR/BS) which are only available using histomorphometry, showed changes in Swiss Webster mice at dosages ≥ 1.2 mg/kg (2,4,5) while it took dosages of 10mg/kg to elicit changes in Balb/C mice (3).

Teriparatide Treatment in Mice

Teriparatide use has resulted in increased bone density and strength when used in mice (2,4,5,7,8). There have been studies treating intact and ovariectomized mice with teriparatide (see table 3-2), though none of these studies examined the effectiveness of teriparatide in preventing or reversing GC-induced bone loss in mice. Studies most commonly used the C57BL/6 (8,35,45), CBA-1 (113), and Swiss Webster strains (7) of mice. In the strains of mice

tested, teriparatide had the greatest anabolic effect in the femur and was dose and duration dependent (7,8,45).

One study found a subcutaneous dose of 40 μ g/kg/day 5 days/week increased BMD within 1-2 weeks in the tibia and within 7 weeks in the vertebrae, suggesting site specific differences occur (45). This finding differs from another study which found the earliest effects in the vertebrae (8). Researchers have reported increased bone mass in cortical as well as cancellous bone, although increases in cortical bone were found primarily in long bones, possibly reflecting a response to mechanical loading patterns (8). Significant effects from teriparatide seem to depend on the presence of existing trabeculae and may be hampered in areas that have suffered severe disruption of trabeculae (8). A summary of studies using PTH in mice is in Appendix B

Further Considerations

We do not fully understand the mechanisms governing GC-induced osteoporosis nor how they effect bone mass and microarchitectural structure. This study seeks to further our understanding of these processes in mice as a prelude to human studies. To date, there has only been one study examining the efficacy of teriparatide in treating glucocorticoid-induced osteoporosis. In this study, postmenopausal women on long-term GC therapy and hormone replacement therapy (HRT) also received teriparatide. The addition of teriparatide resulted in significant bone density increases in the axial skeleton (6). No study of teriparatide alone in glucocorticoid-induced osteoporosis in a human or murine model has been done to date.

CHAPTER 4
RESULTS

Measurement Design

During this experiment, 70 7-month old male Swiss Webster mice were randomized into 7 groups which received prednisolone, teriparatide, or vehicle in an attempt to characterize the effects of teriparatide on bone in glucocorticoid-treated mice. Groups are identified in Table 4-1. At the end of the study, mice were euthanized and both femurs and lumbar vertebrae 2 and 3 (LV 2, LV3) were removed and analyzed using histomorphometry or microCT. Histomorphometric techniques were used on the right femur and L3 to measure the static parameters of BV/TV, Tb.N, Tb.Wi, Tb.Sp and dynamic parameters of MS, MAR, and BFR/BS. MicroCT measures included BV/TV, Tb.N, Tb.Th, and Tb.Sp in the left femur and L2. Cortical BV/TV was also measured in the mid-shaft of the left femurs. Table values are reported as mean \pm standard deviation and figure values are reported as mean \pm standard error.

Table 4-1. Experimental Groups and Description of Treatments.

Group	n =	Treatment (6 days/week)
BSL CNTL	10	Baseline Control
8 WK CNTL	10	8-Week Control. Received GC-vehicle and PTH- vehicle for 8 weeks
GC4/SAC	10	Received GC and PTH-vehicle for 4 weeks and were then sacrificed
GC4/RECV	10	Received GC and PTH-vehicle for 4 weeks and then received GC-Vehicle and PTH-Vehicle for 4 weeks to allow for natural recovery
GC8	10	Received GC and PTH-vehicle for 8 weeks
GC4/GC-PTH4	10	Received GC and PTH-vehicle for 4 weeks and then GC and PTH for 4 weeks
GC-PTH8	10	Received GC and PTH for 8 weeks

GC = prednisolone, 2.1 mg/kg/day; GC-vehicle = sterile saline; PTH = teriparatide 40ug/kg/day; PTH-vehicle = 2% acidified mouse serum.

Anthropomorphic Measures

Animals were weighed at study entry, weekly, and prior to sacrifice. Weight changes were used to monitor animal health and adjust dosages of study drugs. Weight data are presented in Table 4-2. There were no statistical differences in the average weight between the groups either at the start or end of the experiment.

Table 4-2. Mean Animal Weights by Group.

GROUP	Start Wt (g)	End Wt (g)	Diff (g)
BSL CNTL (n =10)		35.8 ± 2.7	n/a
8 WK CNTL (n =10)	35.2 ± 3.4	36.1 ± 2.6	+ 0.9
GC4/SAC (n = 10)	35.3 ± 3.7	34.0 ± 4.2	- 1.3
GC4/RECV (n = 10)	35.7 ± 2.5	36.9 ± 3.5	+ 1.2
GC 8 (n = 10)	35.2 ± 2.3	34.4 ± 3.7	- 0.8
GC4/GC-PTH4 (n = 10)	35.6 ± 1.8	35.1 ± 2.8	- 0.5
GC8/PTH8 (n = 10)	35.1 ± 4.0	35.1 ± 4.2	0.0

Values are expressed as mean ± standard deviation.

Previous studies indicate 7-month old Swiss Webster mice have reached skeletal maturity and have ceased longitudinal bone growth (5). To verify cessation of long bone growth, each animal's left femur was measured and the results are presented in Table 4-3. There were no significant differences in femur length between the groups.

Table 4-3. Mean Femur Lengths by Group.

	BSL CNT (n = 10)	8 WK CNTL (n = 10)	GC4/ SAC (n = 10)	GC4/ RECV (n = 10)	GC 8 (n = 10)	GC4/ GC-PTH4 (n = 10)	GC8/ PTH8 (n= 10)
Femur Length(mm)	15.5 ± 0.4	15.4 ± 0.3	15.3 ± 0.4	15.6 ± 0.3	15.5 ± 0.2	15.6 ± 0.5	15.4 ± 0.4

Results are reported as mean ± standard deviation.

Bone Measures

Histomorphometric analysis was performed on the right femurs of 67 animals and the third lumbar vertebra (L3) of 70 animals. One femur was damaged during tissue harvesting and could not be sectioned and the other two were sectioned but could not be analyzed. Static and dynamic parameters of bone change were measured or derived using methods described in Chapter 3. Measured parameters using histomorphometry included BV/TV, Ob.S Oc.S, MS and MAR. Once BV/TV was determined, values for Tb.N, Tb.Wi*, and Tb.Sp were derived using calculations described elsewhere (51). Once MS and MAR were measured, BFR/BS was calculated as the product of these two. MicroCt was performed on 70 intact femurs and 70 intact second lumbar vertebrae (L2). Static parameters of bone change measured using microCT include BV/TV, Tb.N, Tb.Th*, and Tb.Sp.

Data are presented as the measured or derived values for each parameter. There are also tables showing percent change between groups that reached statistical significance. These tables show the percent change compared to the group in the first column of the table. Percent change is reported for all significant group interactions but only significant differences ($p \leq 0.05$) or trends among comparable groups will be discussed. To simplify data presentation, a separate table is provided within the chapter for each measured or derived parameter. Appendix A, however, contains comprehensive tables for static, dynamic and cellular data by bone for each measurement technique (histomorphometry and microCT).

Measurements of the Lumbar Vertebrae

Histomorphometry data for L3 are summarized in Table 4-4. Lumbar vertebrae L2 was used for microCT and the results are shown in Table 4-5.

* Histomorphometry analyzes a two-dimensional sample so the distance across trabeculae will be reported as Tb.Wi; microCT analyzes samples in three dimensions so the distance across the trabeculae is reported as Tb.Th.

Table 4-4. Summary of Histomorphometric Analysis of LV3 by Group.

	BSL CNTL (n = 10)	8 WKCNTL (n = 10)	GC4/SAC (n = 10)	GC 4/RECV (n = 10)	GC 8 (n = 10)	GC4/PTH4 (n = 10)	GC-PTH8 (n = 10)
BV/TV (%)	12.7 ± 3.3	8.8 ± 3.2	10.9 ± 3.0	9.2 ± 3.4	8.7 ± 2.4	11.0 ± 3.1	12.5 ± 2.1
Tb.N (1/mm)	4.9 ± 0.8	4.1 ± 1.3	4.7 ± 0.8	4.3 ± 0.9	4.5 ± 1.1	4.1 ± 0.7	4.9 ± 0.6
Tb.Wi (µm)	31.0 ± 4.6	25.3 ± 5.0	27.5 ± 3.8	25.1 ± 5.1	23.2 ± 3.0	31.5 ± 4.3	30.9 ± 4.9
Tb.Sp (µm)	185.6 ± 38.4	242.1 ± 82.4	196.7 ± 42.4	223.0 ± 6.4	214.5 ± 6.1	220.7 ± 39.6	182.3 ± 21.0

Results are reported as mean ± standard deviation.

Table 4-5. Summary of MicroCT Analysis of LV2 by Group.

	BSLCNTL (n = 10)	8 WK CNTL (n = 10)	GC4/SAC (n = 10)	GC4/RECV (n = 10)	GC 8 (n = 10)	GC4/PTH4 (n = 10)	GC-PTH8 (n = 10)
BV/TV (%)	19.0 ± 3.6	16.1 ± 3.6	17.4 ± 4.3	15.0 ± 3.8	19.0 ± 4.6	18.8 ± 4.8	22.0 ± 4.4
Tb.N (1/mm)	4.2 ± 0.3	3.9 ± 0.5	3.9 ± 0.5	3.8 ± 0.5	4.4 ± 0.8	3.8 ± 0.5	4.04 ± 0.4
Tb.Th (µm)	48.7 ± 2.8	47.5 ± 3.8	47.1 ± 1.9	45.9 ± 3.0	46.4 ± 2.2	52.1 ± 4.2	54.7 ± 4.9
Tb.Sp (µm)	236 ± 19	259 ± 40	261 ± 33	266 ± 35	232 ± 50	265 ± 35	245 ± 29

Results are reported as mean ± standard deviation.

Bone Volume/Total Volume

Bone volume data based on histomorphometry are presented in Table 4.4, Table 4-6 and Figure 4-1. Bone volume data based on microCT are presented in Table 4-5, Table 4-7, and Figure 4-2. Bone volume was lower in older animals and higher in animals treated with PTH as shown in Figure 4-1 and Figure 4-2. Histomorphometry indicated BV/TV was significantly lower in the 8 WK CNTL (-30.7%, p = 0.03) group compared to BSL CNTL. Significant increases in BV/TV were seen in animals treated with PTH. Animals treated with PTH for 8 weeks had a higher BV/TV than both the 8 WK CNTL (+42%, p = 0.01) and GC8 (+ 43.7%, p = 0.01) groups and a 35.9% (p = 0.03) higher BV/TV than animals in GC4/RECV. Animals in the GC4/GC-PTH4 group had a 26.4% (p = 0.03) higher BV/TV than GC8 animals. MicroCT analysis found significantly higher BV/TV in GC-PTH8 compared to 8 Wk CNTL (+36.6%, p =

0.01), GC4/SAC (+26.4%, p = 0.04), and GC4/RECV (+46.7%, p = 0.00). There was no bone loss in GC8 compared to 8WK CNTL using either histomorphometry (8.7 ± 2.4 vs. 8.8 ± 3.2) or microCT (19.0 ± 4.6 vs. 16.1 ± 3.6). BV/TV did not increase after GC treatment ended.

Table 4-6. Significant Changes in Lumbar Vertebra L3 Bone Volume by Group using Histomorphometry.

GROUP	8WK CNTL	GC4/RECV	GC8	GC4/GC-PTH4	GC-PTH8
BSL CNTL	- 30.7% (p = 0.03)	- 27.7% (p = 0.03)	- 31.5% (p=0.02)		
8 WK CNTL					+ 42.0% (p = 0.01)
GC4/RECV					+ 35.9% (p = 0.03)
GC 8				+ 26.4% (p = 0.03)	+ 43.7% (p = .01)

Results are percent change compared to groups on the left.

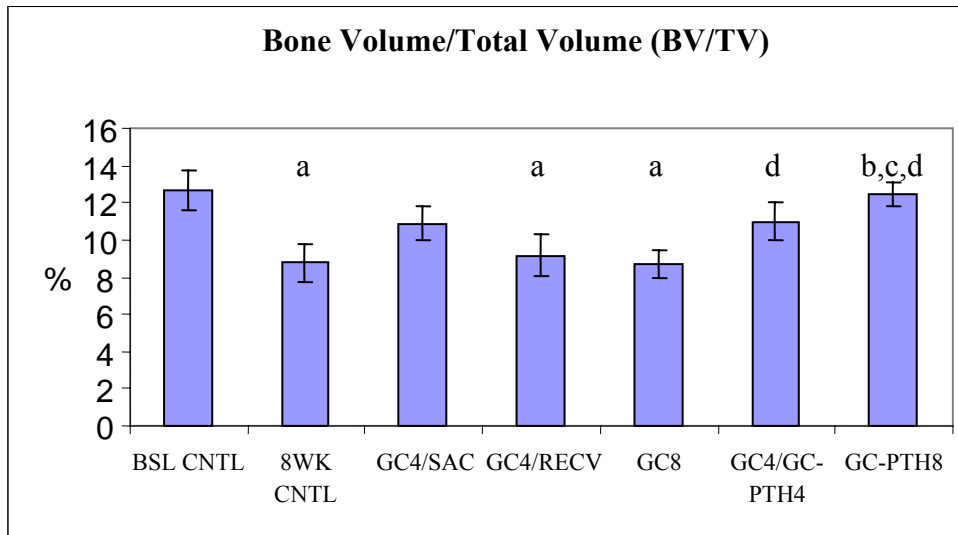


Figure 4- 1. Lumbar Vertebra L3 Bone Volume/Total Volume by Group using Histomorphometry. a = significant compared to BSL CNTL; b = significant compared to 8 WK CNTL; c = significant compared to GC4/RECV; d = significant compared to GC8. Results are percent change compared to groups on the left. Results are reported as mean \pm standard error.

Table 4-7. Significant Changes in Lumbar Vertebra L2 Bone Volume by Group using MicroCT.

Group	GC4/RECV	GC-PTH8
BSL CNTL	- 21.1% (p = 0.03)	
8 WK CNTL		+ 36.6% (p = 0.01)
GC4/SAC		+ 26.4% (p = 0.04)
GC4/RECV		+ 46.7% (p = 0.00)
GC 8	- 21.1% (p = 0.04)	

Results are shown as percent change compared to groups on the left.

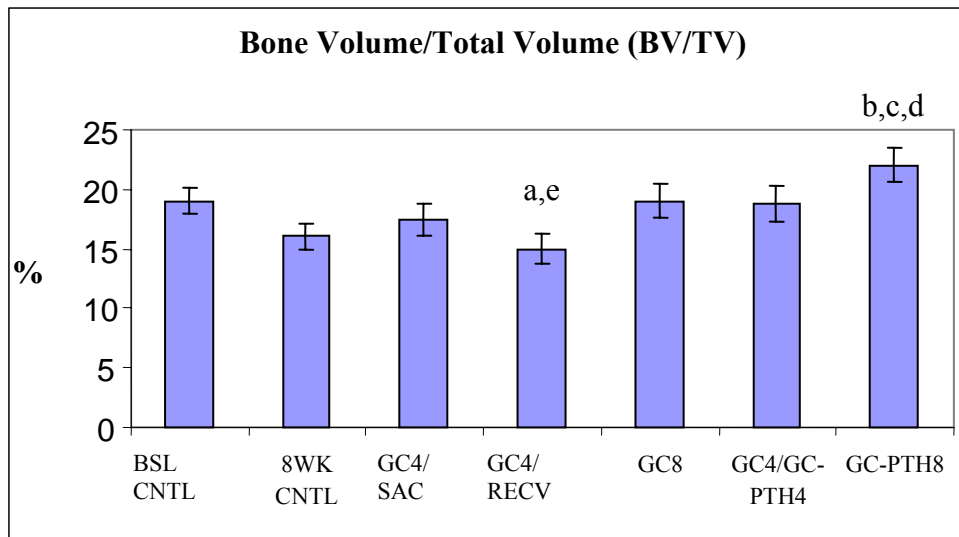


Figure 4-2. Lumbar Vertebra L2 Bone Volume/Total Volume by Group using MicroCT. a = significant compared to BSL CNTL; b = significant compared to 8 WK CNTL; c = significant compared to GC4/SAC; d = significant compared to GC4/RECV; e = significant compared to GC8. Results are reported as mean \pm standard error.

Trabecular Number

Data for trabecular number are presented in Table 4-4, and Figure 4-3 (histomorphometry) and Table 4-5 and Figure 4-4 (microCT). According to histomorphometry, the only significant difference in trabecular number in L3 among treatment groups was between the GC4/GC-PTH4

and GC-PTH8, where the latter group had a higher (19.5%, $p = 0.02$) Tb.N. MicroCT, on the other hand, showed only a non-significant 6.3% difference in these groups (Appendix A). There was, however, a significant difference based on microCT between GC4/RECV (-9.5%, $p = 0.04$) and GC4/GC-PTH4 (-9.5%, $p = 0.02$) compared to BSL CNTL.

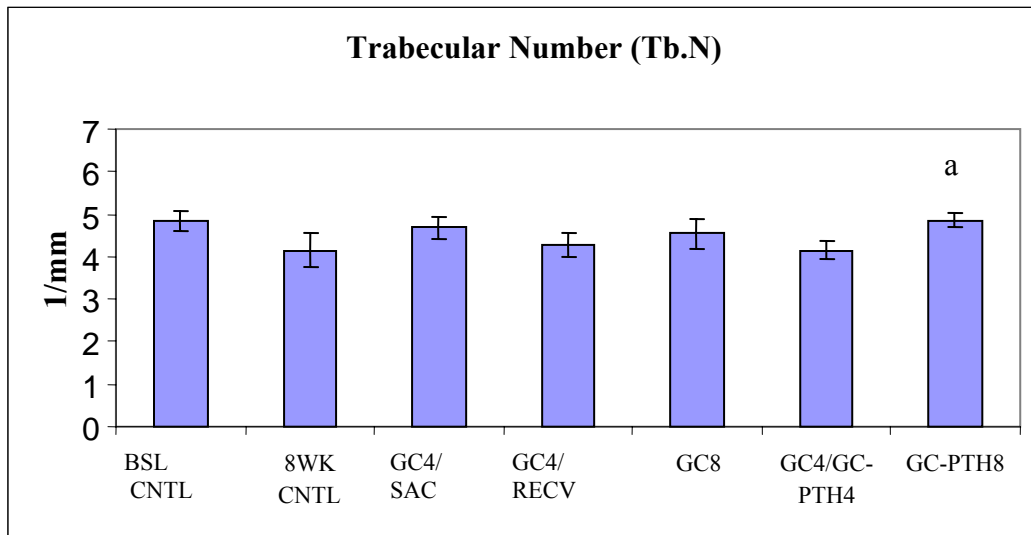


Figure 4-3. Lumbar Vertebra L3 Trabecular Number by Group using Histomorphometry. a = significant compared to GC4/GC-PTH4. Results are reported as mean \pm standard error.

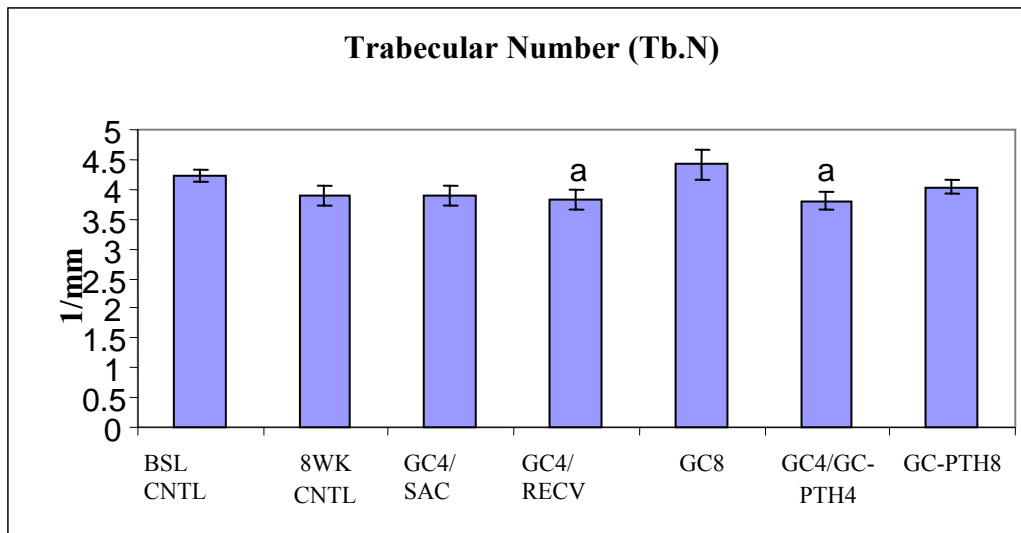


Figure 4-4. Lumbar Vertebra L2 Trabecular Number by Group using MicroCT. a = significant compared to BSL CNTL. Results are reported as mean \pm standard error.

Trabecular Width/Trabecular Thickness

Trabecular Width/Trabecular Thickness was a measure of the mean distance across the trabeculae and changes reflected the effects of prednisolone, teriparatide, or both on this distance. Data for Tb.Wi based on histomorphometry are found in Table 4-4, Table 4-8 and Figure 4-5, while microCT data concerning Tb.Th are presented in Table 4-5, Table 4-9, and Figure 4-6. As shown in Figure 4-5, histomorphometry generally detected higher Tb.Wi in PTH-treated animals and lower Tb.Wi in older animals but no significant difference based on GC treatment in comparably aged animals.

There was a significantly lower Tb.Wi between the BSL CNTL group and animals in the 8 WK CNTL (-18.4%, $p = 0.02$). Histomorphometry and microCT each found significant differences between both of the PTH groups and 8 WK CNTL, GC4/RECV and GC8. There was also a higher Tb.Wi in GC4/GC-PTH4 (24.5%, $p = 0.01$) and GC-PTH8 (22.1%, $p = 0.01$) groups compared with comparably aged animals (8 WK CNTL). Additionally, animals treated with PTH for either four or eight weeks had a 35.8% ($p = 0.00$) and 33.2% ($p = 0.00$) higher Tb.Wi respectively compared to GC8 animals. There was no significant difference in Tb.Th between GC4/GC-PTH4 and GC-PTH8.

Similar to histomorphometric findings, microCT showed significantly higher Tb.Th in animals treated with PTH. Animals in the GC4/GC-PTH4 group had a greater Tb.Th than animals in the 8 WK CNTL (+9.7%, $p = 0.04$), GC4/SAC (+10.6%, $p = 0.01$), GC4/RECV (+13.5%, $p = 0.00$) and GC8 (+12.3%, ($p=0.00$)) groups. Animals treated with PTH for eight weeks showed a higher Tb.Th than 8 WK CNTL (+15.2%, $p = 0.00$), GC4/SAC (+16.1%, $p = 0.00$), GC4/RECV (+19.2%, $p = 0.00$), and GC8 (+17.9%, $p = 0.00$). Again, there was no significant difference in Tb.Th between the GC4/GC-PTH4 and GC-PTH8 groups.

Table 4-8. Significant Changes in Lumbar Vertebra L3 Trabecular Width by Group using Histomorphometry.

Group	8WK CNTL	GC4/SAC	GC4/RECV	GC8	GC4/GC-PTH4	GC-PTH8
BSL CNTL	- 18.4% (p = 0.02)		- 19.0 (p=0.02)	- 25.1 (p= 0.00)		
8 WK CNTL					+ 24.5 % (p =0.01)	+ 22.1 (p = 0.01)
GC4/SAC					+ 14.5% (p = 0.03)	
GC4/RECV					+ 25.5% (p = 0.00)	+ 23.1% (p = 0.01)
GC 8		+ 18.5% (p = 0.02)			+ 35.8% (p = 0.00)	+ 33.2% (p = 0.00)

Results are shown as percent change compared to groups on the left.

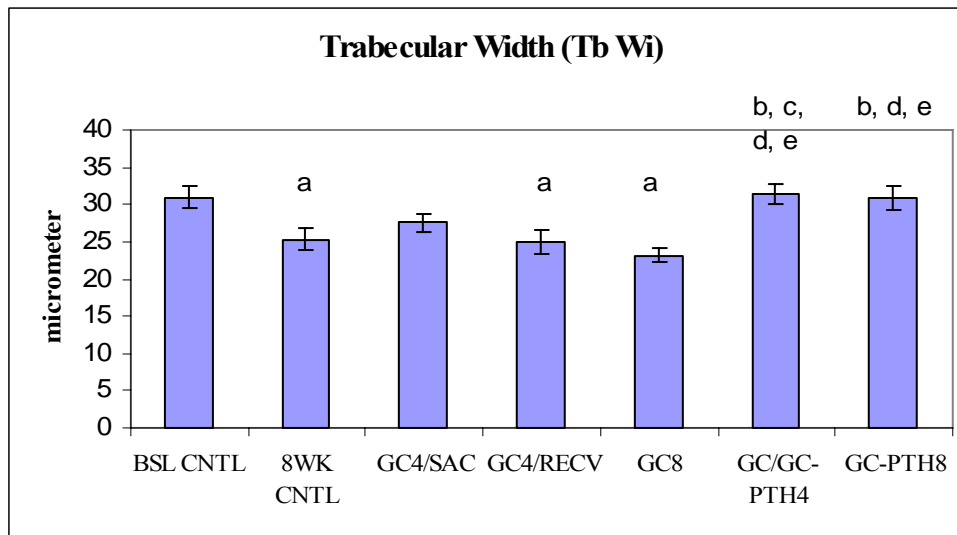


Figure 4-5. Lumbar Vertebra L3 Trabecular Width by Group using Histomorphometry. a = significant compared to BSL CNTL; b = significant compared to 8 WK CNTL; c = significant compared to GC4/SAC; d = significant compared to GC4/RECV; e = significant compared to GC8. Results are reported as mean \pm standard error.

Table 4-9. Significant Changes in Lumbar Vertebra L2 Trabecular Thickness by Group using MicroCT.

Group	GC4/RECV	GC4/GC-PTH4	GC-PTH8
BSL CNTL	- 5.7% (p = 0.02)		+ 12.3% (p = 0.01)
8 WK CNTL		+ 9.7% (p = 0.04)	+ 15.2% (p = 0.00)
GC4/SAC		+ 10.6% (p = 0.01)	+ 16.1% (p = 0.00)
GC4/RECV		+ 13.5% (p = 0.00)	+ 19.2% (p = 0.00)
GC 8		+ 12.3% (p = 0.00)	+ 17.9% (p = 0.00)

Results are shown as percent change compared to groups on the left.

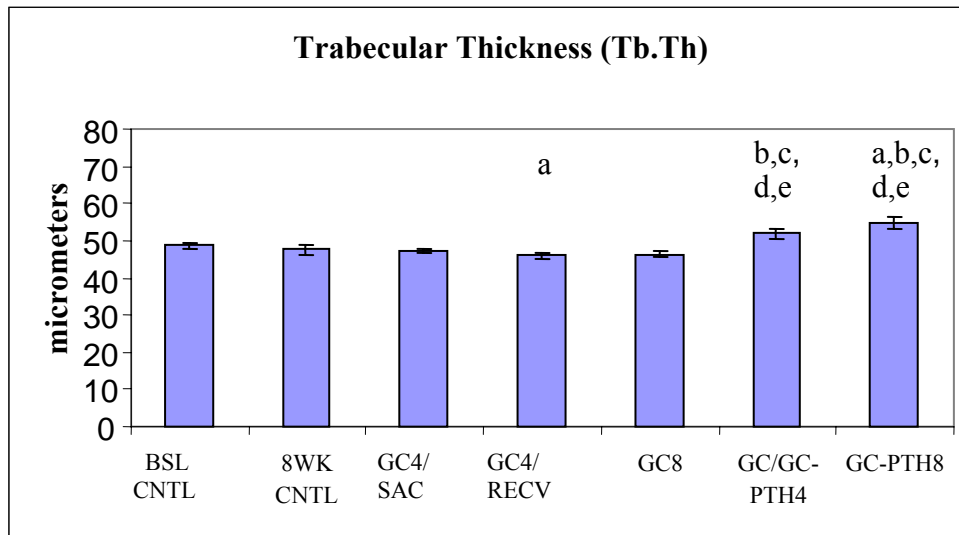


Figure 4-6. Lumbar Vertebra L2 Trabecular Thickness by Group using MicroCT. a = significant compared to BSL CNTL; b = significant compared to 8 WK CNTL; c = significant compared to GC4/SAC; d = significant compared to GC4/RECV; e = significant compared to GC8. Results are reported as mean \pm standard error.

Trabecular Separation

Trabecular separation data are shown in Table 4-4 and Figure 4-7 (histomorphometry) and Table 4-5 and Figure 4-8 (microCT). Trabecular Separation is a reflection of the mean distance between trabeculae within the region of interest. This distance tends to increase when resorption is higher and decrease with increased bone formation. MicroCT results typically showed greater trabecular separation for each group than did histomorphometric analysis, although the differences were not significant. There were no significant differences in Tb.Sp related to age or GC exposure based on microCT or histomorphometry. The only significant differences in trabecular separation in L3 (histomorphometry) were found in PTH-treated animals. The GC-PTH8 group had a significantly lower (-24.7%, $p = 0.03$) Tb.Sp compared with the 8 WK CNTL and GC4/GC-PTH4 (-17.4%, $p = 0.01$) groups (Appendix A). MicroCT indicated significant differences between BSL CNTL and GC4/RECV (+12.7%, $p = 0.03$) and GC-PTH8 (+12.3%, $p = 0.04$).

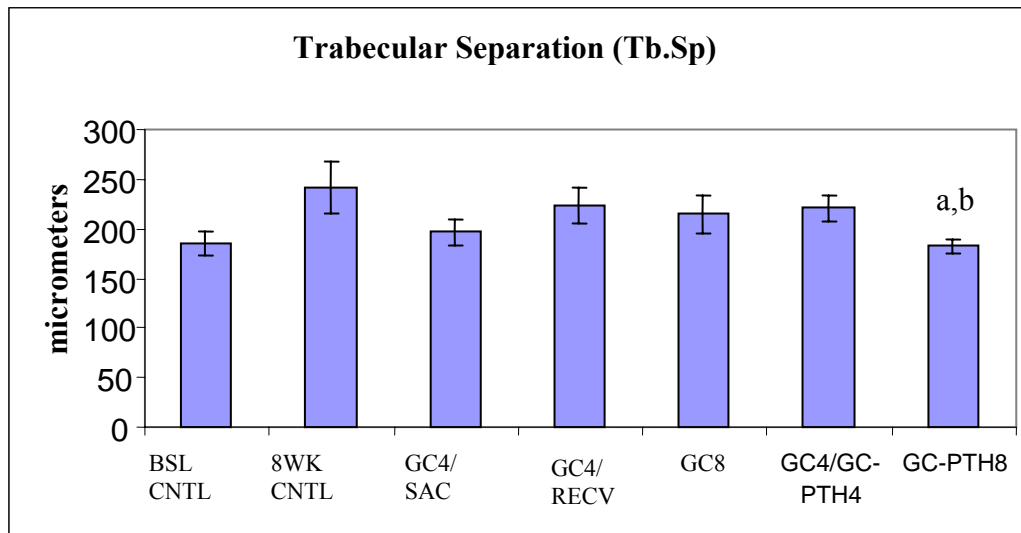


Figure 4-7. Lumbar Vertebra L3 Trabecular Separation by Group using Histomorphometry. a = significant compared to 8 WK CNTL; b = significant compared to GC4/GC-PTH4. Results are reported as mean \pm standard error.

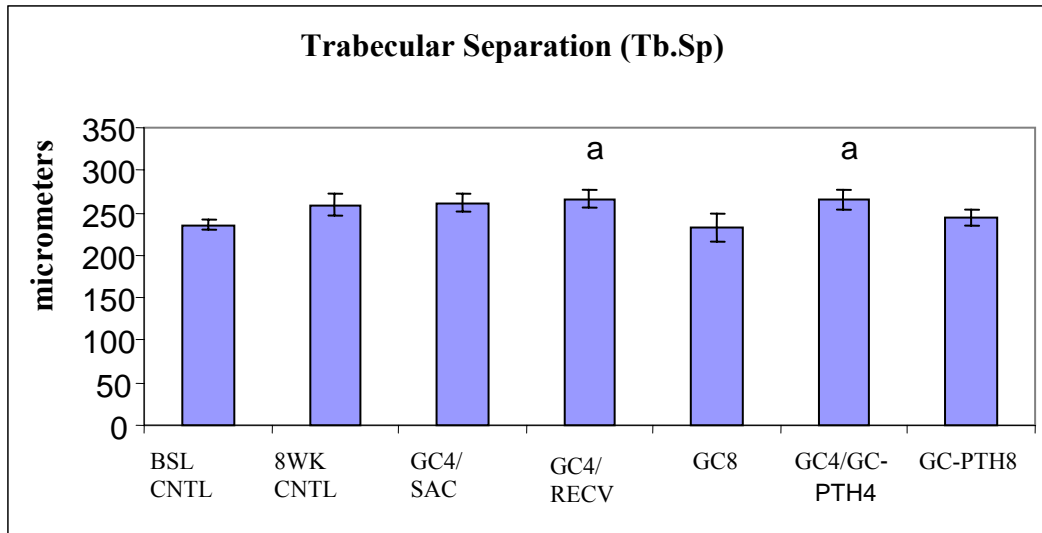


Figure 4-8. Lumbar Vertebra L2 Trabecular Separation by Group using MicroCT. a = significant compared to BSL CNTL. Results are reported as mean \pm standard error.

MicroCT methods showed significant changes in Tb. Sp only in relation to the BSL CNTL group. Histomorphometry did not find changes in any group compared to the BSL CNTL group but did find significant differences in animals treated with PTH, but only after 8 weeks of treatment.

Measurements of the Distal Femur

The right femurs of 67 animals used for this study were harvested for histomorphometric analysis while 70 left femurs from the same animals were analyzed using microCT. Three bones could not be used for histomorphometric analysis for reasons previously described. The femurs were harvested from each animal as described in Chapter 2. From each right femur, two 4 μ m thick sections were stained and used to measure or derive static bone measurements including BV/TV, Tb.N, Tb.Wi, and Tb.Sp. The results of that analysis are summarized in Table 4-10. Femurs used for microCT were scanned intact and the resulting measures of BV/TV, Tb.N, Tb.Th, and Tb.Sp are presented in Table 4-11.

Table 4-10. Summary of Histomorphometric Analysis of the Distal Femur by Group.

	BSL CNTL (n = 10)	8 WK CNTL (n = 9)	GC4/SAC (n = 10)	GC4/RECV (n = 10)	GC 8 (n=9)	GC4/GC-PTH4 (n=9)	GC-PTH8 (n=10)
BV/TV (%)	4.8 ± 2.3	2.6 ± 1.9	4.8 ± 2.3	2.3 ± 2.1	3.1 ± 1.6	4.5 ± 1.7	5.2 ± 2.9
Tb.N(1/mm)	2.0 ± 0.9	1.2 ± 0.8	1.8 ± 0.9	1.2 ± 0.9	1.6 ± 0.8	1.9 ± 0.7	2.2 ± 0.9
Tb.Wi(μm)	28.2 ± 5.9	25.4 ± 7.2	26.1 ± 5.9	21.9 ± 5.5	23.2 ± 6.1	27.9 ± 4.3	28.6 ± 6.1
Tb.Sp (μm)	540 ± 225	1366 ± 1146	694 ± 428	1497 ± 1812	904 ± 916	551.6 ± 195	554 ± 359
Oc.S (%)	0.6 ± 0.2	1.1 ± 1.1	0.4 ± 0.3	1.3 ± 0.8	0.9 ± 0.7	0.8 ± 0.6	1.7 ± 1.2
Ob.S (%)	7.9 ± 13.2	7.2 ± 3.5	1.1 ± 1.2	8.7 ± 8.9	2.1 ± 1.5	13.6 ± 12.0	20.0 ± 7.8
MS (%)	6.7 ± 5.4	3.1 ± 3.2	1.1 ± 1.6	5.9 ± 3.5	1.6 ± 1.8	14.2 ± 5.3	16.8 ± 8.7
MAR (μm/d)	0.9 ± 0.2	0.6 ± 0.2	0.6 ± 0.2	0.7 ± .1	0.6 ± 0.2	0.8 ± 0.1	0.8 ± 0.2
BFR/BS (um ³ /um ² /d)	6.4 ± 6.0	2.2 ± 3.0	0.6 ± 1.0	4.2 ± 2.7	1.0 ± 1.1	10.8 ± 5.7	14.8 ± 12.8

Results are reported as mean ± standard deviation.

Table 4-11. Summary of MicroCT Analysis of the Distal Femur by Group.

	BSL CNTL (n = 10)	8WK CNTL (n = 10)	GC4/SAC (n = 10)	GC4/RECV (n = 10)	GC 8 (n = 10)	GC4/PTH4 (n = 10)	GC-PTH8 (n = 10)
BV/TV (%)	9.9 ± 3.1	6.2 ± 2.1	8.5 ± 3.4	6.0 ± 3.8	8.7 ± 2.6	7.9 ± 2.9	11.5 ± 3.1
Tb.N(1/mm)	2.7 ± 0.63	2.1 ± 0.45	2.5 ± 0.57	2.2 ± 0.78	2.8 ± 0.75	2.5 ± 0.54	2.8 ± 0.47
Tb.Th (μm)	60.7 ± 5.2	64.5 ± 6.3	60.1 ± 2.8	59.9 ± 6.4	56.3 ± 8.5	63.9 ± 5.0	70.6 ± 7.2
Tb.Sp (μm)	383 ± 91	485 ± 113	413 ± 99	500 ± 158	391 ± 154	416 ± 108	361 ± 60

Results are mean ± standard deviation.

Bone Volume

Bone volume data based on histomorphometry are presented in Table 4-10, Table 4-12 and Figure 4-9 while microCT data are presented in Table 4-11, Table 4-13, and Figure 4-10.

Histomorphometry and microCT detected the same trends in BV/TV in the distal femur.

Bone volume tended to be lower with age and higher with exposure to PTH. There was a lower BV/TV in 8Wk CNTL compared to BSL CNTL in histomorphometry and microCT. GC-PTH treatment resulted in higher BV/TV compared to 8 WK CNTL control and GC-treated groups. Compared to GC/RECV, both groups receiving PTH had significantly increased bone volume .

Table 4-12. Significant Changes in Distal Femur Bone Volume by Group using Histomorphometry.

Group	8WK CNTL	GC4/RECV	GC4/GC-PTH4	GC-PTH8
BSL CNTL	- 45.8% (p = 0.03)	- 52.1% (p = 0.01)		
8WK CNTL				+100.0% (p = 0.02)
GC4/RECV			+ 95.6% (p = 0.01)	+ 126.1% (p = 0.01)

Results are shown as percent change compared to groups on the left.

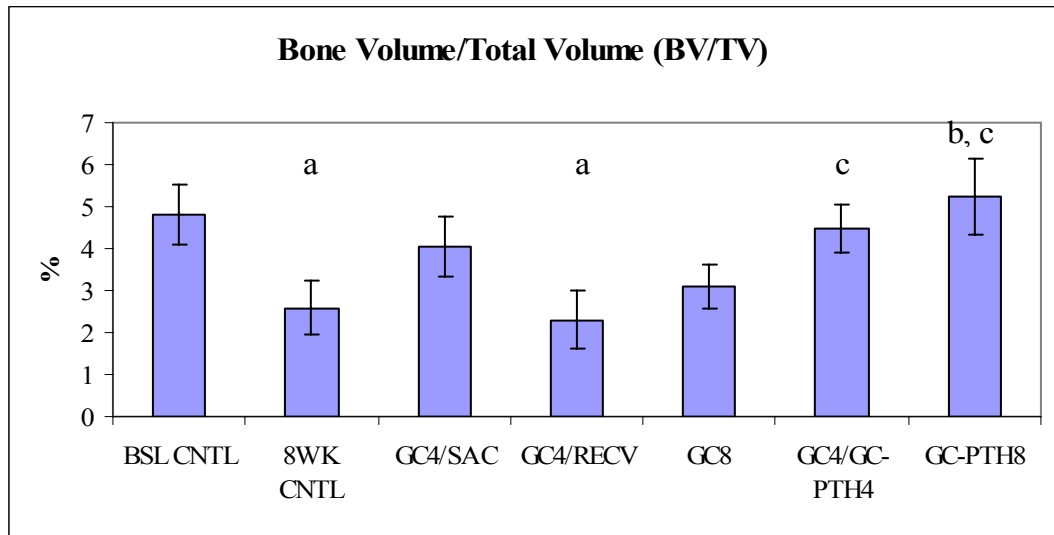


Figure 4-9. Distal Femur Bone Volume/Total Volume by Group using Histomorphometry. a = significant compared to BSL CNTL; b = significant compared to 8 WK CNTL; c = significant compared to GC4/RECV. Results are reported as mean \pm standard error.

There was only a slightly different BV/TV between GC4/SAC animals and the GC4/GC-PTH4 and GC-PTH8 groups and these differences did not reach statistical significance. The GC-PTH8 group had a higher BV/TV than GC4/GC-PTH4 (45.6%, p = 0.02) based on microCT. MicroCT and histomorphometric comparisons of PTH groups with the 8 WK CNTL showed BV/TV was higher in GC4/GC-PTH4 and the GC-PTH8 group, despite the fact these groups also received GC.

Table 4-13. Significant Changes in Distal Femur Bone Volume by Group using MicroCT.

Group	8WK CNTL	GC4/RECV	GC8	GC-PTH8
BSL CNTL	- 37.4% (p = 0.00)	- 39.4% (p = 0.00)		
8 WK CNTL			+ 40.3% (p = 0.03)	+ 85.5% (p = 0.00)
GC4/RECV			+ 45.0% (p = 0.02)	+ 91.7% (p = 0.00)
GC 8				+ 32.3% (p = 0. 004)
GC4/GC-PTH4				+ 45.6% (p = 0.02)

Results are shown as percent change compared to groups on the left.

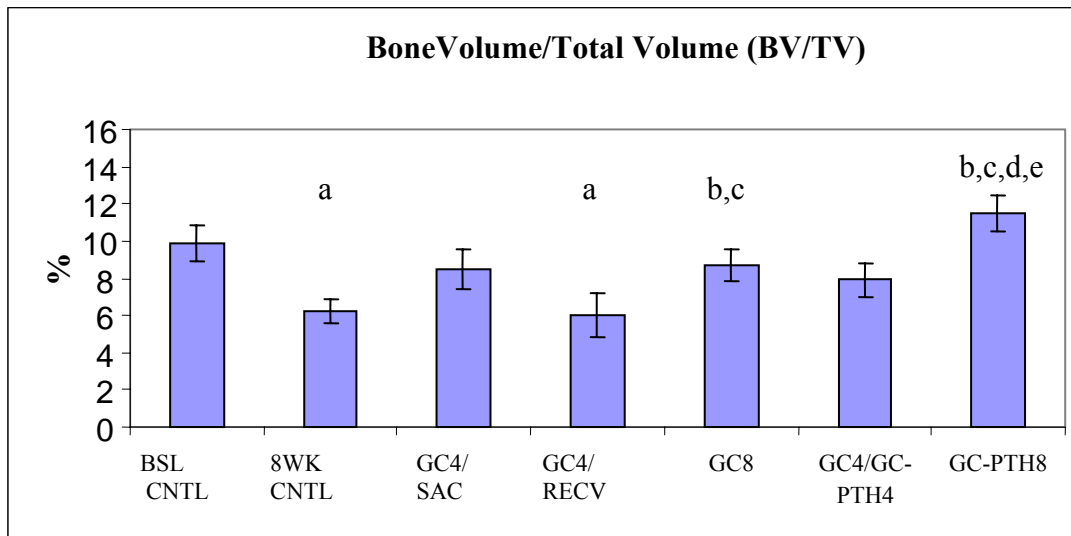


Figure 4-10. Distal Femur Bone Volume/Total Volume by Group using MicroCT. a = significant compared to BSL CNTL; b = significant compared to 8 WK CNTL; c = significant compared to GC4/RECV; d = significant compared to GC8; e = significant compared to GC4/GC-PTH4. Results are reported as mean \pm standard error.

Trabecular Number

Data for trabecular number based on histomorphometry are found in Table 4-10, Table 4-14, and Figure 4-11. MicroCT data on this parameter are found in Table 4-11, Table 4-15, and Figure 4-12. Histomorphometry and microCT detected similar patterns of change; where Tb.N was lower in older animals and higher in animals treated with GC or GC-PTH.

Table 4-14. Significant Changes in Distal Femur Trabecular Number by Group using Histomorphometry.

Group	8WK CNTL	GC4/RECV	GC-PTH8
BSL CNTL	- 40.0% (p = 0.05)	- 40.0% (p = 0.01)	
8 WK CNTL			+ 83.3% (p = 0.03)
GC4/RECV			+ 83.3% (p = 0.03)

Results are shown as percent change compared to groups on the left.

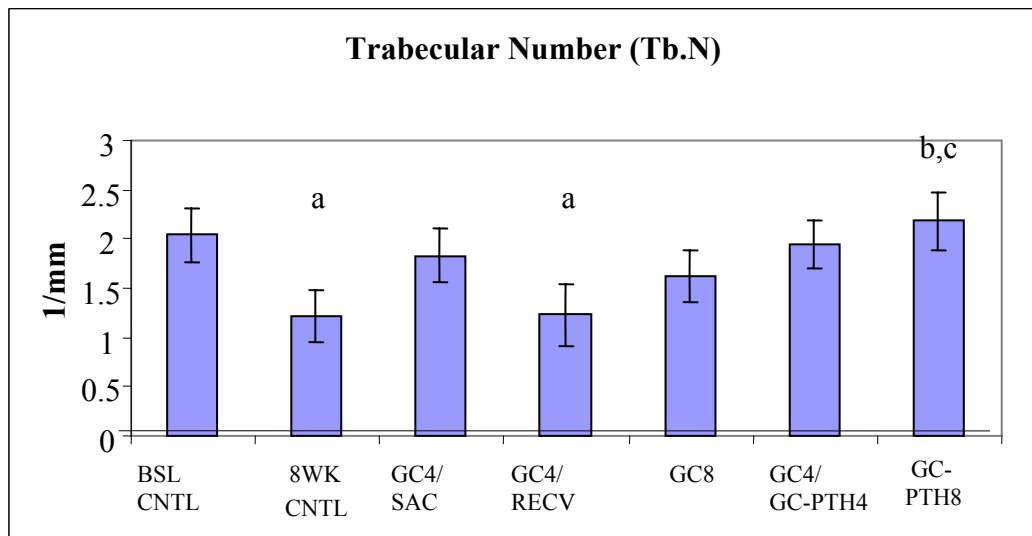


Figure 4-11. Distal Femur Trabecular Number by Group using Histomorphometry. a = significant compared to BSL CNTL; b = significant compared to 8 WK CNTL; c = significant compared to GC4/RECV. Results are reported as mean \pm standard error.

Table 4-15. Significant Changes in Distal Femur Trabecular Number by Group using MicroCT.

Group	8WK CNTL	GC8	GC-PTH8
BSL CNTL	- 22.2% (p=0.05)		
8 WK CNTL		+ 33.3% (p = 0.03)	+ 33.3% (p = 0.00)
GC4/RECV			+ 27.3% (p =0.01)

Results are shown as percent change compared to groups on the left.

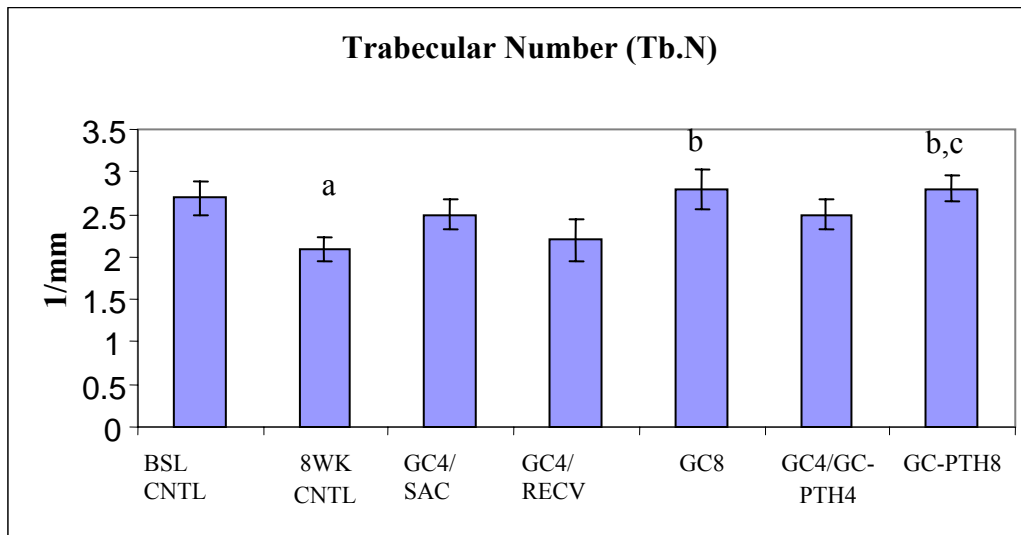


Figure 4-12. Distal Femur Trabecular Number by Group using MicroCT. a = significant compared to BSL CNTL; b = significant compared to 8 WK CNTL; c = significant compared to GC4/RECV. Results are reported as mean \pm standard error.

Trabecular Thickness/Trabecular Width

Data for Tb.Wi in the distal femur based on histomorphometry are found in Table 4-10, Table 4-16, and Figure 4-13. MicroCT data for distal femur Tb.Th are found in Table 4-11, Table 4-17, and Figure 4-14. Histomorphometry and microCT detected the same general patterns in Tb.Th/Tb.Wi in the distal femur. Parameters of Tb.Wi and Tb.Th tended to be lower in response to GC treatment and higher with PTH treatment. There was no significant age effect

apparent in Tb.Wi/Tb.Th as shown in Figure 4-13 and Figure 4-14. Both histomorphometry and microCT found significant differences between PTH-treated animals and the 8 WK CNTL and GC4/RECV groups. Additionally, there was a trend toward decreased Tb.N in GC4/SAC compared to GC4/RECV in both histomorphometry.

Table 4-16. Significant Changes in Distal Femur Trabecular Width by Group using Histomorphometry.

Group	GC4/RECV	GC8	GC4/GC-PTH4	GC-PTH8
BSL CNTL	- 22.3% (p = 0.04)	- 17.7% (p = 0.05)		
GC4/RECV			+ 27.4 (p = 0.05)	+ 30.6% (p = 0.02)
GC 8			+ 20.3% (p = 0.04)	+ 23.3% (p = 0.03)

Results are shown as percent change compared to groups on the left.

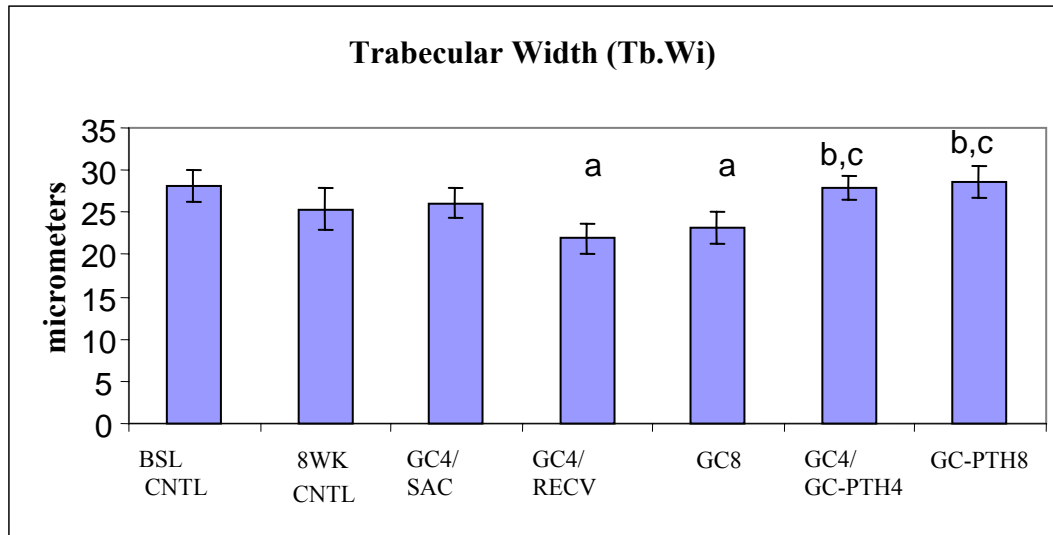


Figure 4-13. Distal Femur Trabecular Thickness by Group using Histomorphometry. a = significant compared to BSL CNTL; b = significant compared to GC4/RECV; c = significant compared to GC8. Results are reported as mean \pm standard error.

Table 4-17. Significant Changes in Distal Femur Trabecular Thickness by Group using MicroCT.

Group	GC8	GC4/GC-PTH4	GC-PTH8
BSL CNTL			+ 16.3% (p = 0.01)
8 WK CNTL	- 12.7% (p = 0.04)		
GC4/SAC		+ 6.3% (p = 0.05)	+ 17.5% (p = 0.00)
GC4/RECV			+ 17.9% (p = 0.00)
GC 8		+ 13.5% (p = 0.05)	+ 25.4% (p = 0.00)
GC4/GC-PTH4			+ 10.5% (p = 0.05)

Results are shown as percent change compared to groups on the left.

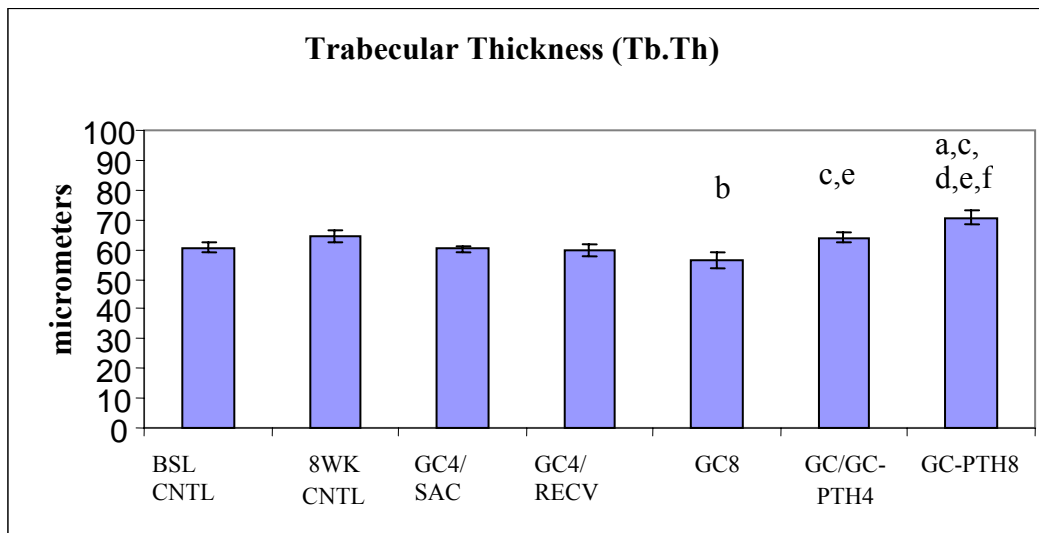


Figure 4-14. Distal Femur Trabecular Thickness by Group using MicroCT. a = significant compared to BSL CNTL; b = significant compared to 8WK CNTL; c = significant compared to GC4/SAC; d = significant compared to GC4/RECV; e = significant compared to GC8; f = significant compared to GC4/GC-PTH4. Results are reported as mean \pm standard error.

Trabecular Separation

Data for trabecular separation based on histomorphometry are found in Table 4-10, Table 4-18, and Figure 4-15. Data from microCT for Tb.Sp are found in Table 4-11, Table 4-19, and Figure 4-16. In general, higher Tb.Sp was seen in older animals and both GC and GC-PTH tended to decrease this parameter as shown in Figure 4-15 and Figure 4-16.

Compared to the BSL CNTL group, Tb.Sp was higher (+153.0%, $p = 0.05$) in the 8WK CNTL group based on histomorphometry.

Table 4-18. Significant Changes in Distal Femur Trabecular Separation by Group using Histomorphometry.

Group	8WK CNTL	GC4/RECV	GC4/GC-PTH4	GC-PTH8
BSL CNTL	+153.0% ($p = 0.05$)	+ 177.2% ($p = 0.01$)		
8 WK CNTL				- 59.4% ($p = 0.03$)
GC4/RECV			- 63.3% ($p = 0.01$)	- 63.0% ($p = 0.03$)

Results are shown as percent change compared to groups on the left.

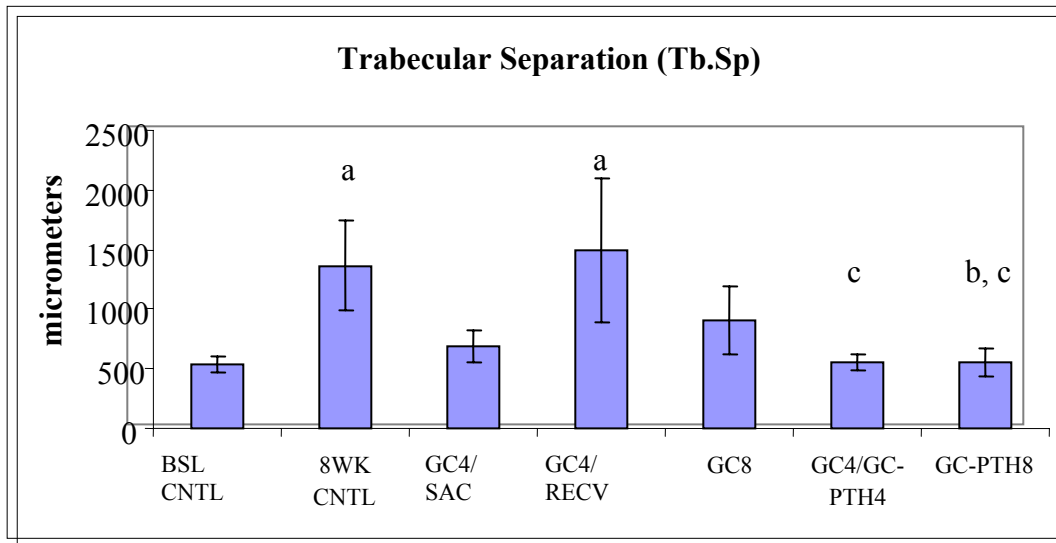


Figure 4-15. Distal Femur Trabecular Separation by Group using Histomorphometry. a = significant compared to BSL CNTL; b = significant compared to 8 WK CNTL; c = significant compared to GC4/RECV. Results are reported as mean \pm standard error.

Table 4-19. Significant Changes in Distal Femur Trabecular Separation by Group Using MicroCT.

Group	GC4/RECV	GC8	GC-PTH8
BSL CNTL	+ 30.5% (p = 0.05)		
8 WK CNTL		- 19.4% (p = 0.03)	- 25.6% (p = 0.00)
GC4/RECV			- 27.8% (p = 0.01)

Results are shown as percent change compared to groups on the left.

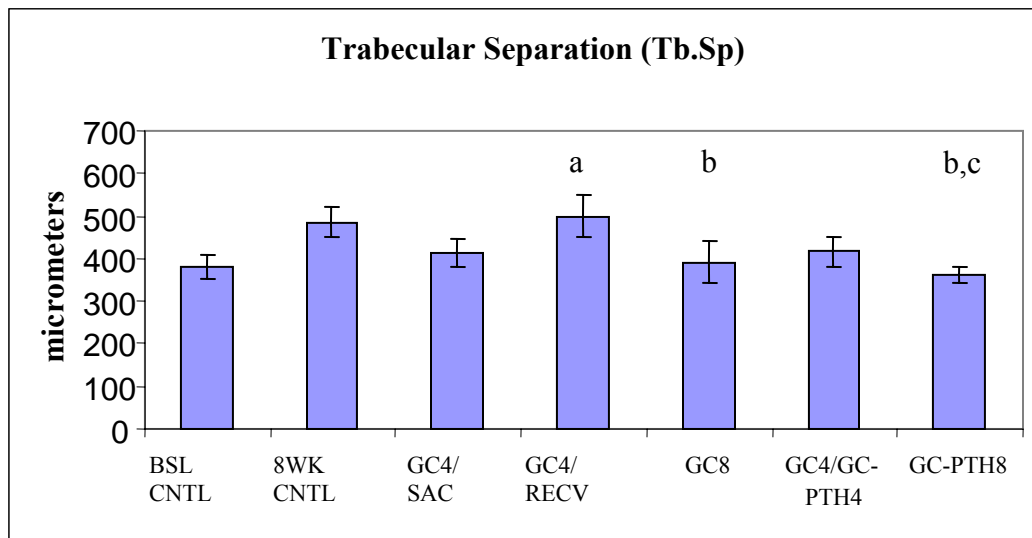


Figure 4-16. Distal Femur Trabecular Separation by Group using MicroCT. a = significant compared to BSL CNTL; b = significant compared to 8 WK CNTL; c = significant compared to GC4/RECV. Results are reported as mean + standard error.

Osteoblast Surface and Osteoclast Surface

Osteoblasts and osteoclasts are the cells involved in resorbing and forming new bone. They act in concert and the balance of numbers and activity levels of these two cell types determines whether there is an overall increase or decrease in bone. Many disease conditions affect the numbers and activity levels of these cells. The ratio in number and activity levels are also influenced by treatments, including PTH. Osteoblast and Osteoclast Surface data are presented in Table 4-10, Table 4-20, and Figures 4-17 and 4-18. There were no significant age-

related changes in Ob.S or Oc.S in the distal femur as shown in Figure 4-17 and Figure 4-18.

Ob.S tended to decrease with GC and increase with GC recovery or PTH. Trends in Oc.S were not as clear cut.

Table 4-20. Significant Changes in Distal Femur Osteoblast Surface and Osteoclast Surface by Group.

Group	GC4/SAC	GC4/RECV	GC8	GC4/GC-PTH4	GC-PTH8
BSL CNTL		Oc.S + 116.7% (p = 0.02)			Oc.S + 183.3% (p = 0.01) Ob.S + 153.2% (p = 0.01)
8 WK CNTL	Oc.S - 63.6% (p = 0.03) Ob.S - 84.7% (P= 0.00)		Ob.S -70.8 (p = 0.00)		Ob.S + 177.8% (p = 0.00)
GC4/SAC		Oc.S + 225% (p = 0.00) Ob.S + 690.9% (p = 0.00)		Ob.S +1,136.4% (p= 0.00)	Oc.S + 325.0% (p = 0.00) Ob.S + 1,718.2% (p = 0.00)
GC4/RECV					Ob.S + 129.9% (p = 0.00)
GC 8		Ob.S + 314.30 % (p = 0.00)		Ob.S + 547.6% (p = 0.00)	Ob.S + 852.4% (p = 0.00)
GC4/GC-PTH4					Oc.S + 112.5% (p = 0.03) Ob.S + 47.1% (p = 0.05)

Results are shown as percent change compared to groups on the left.

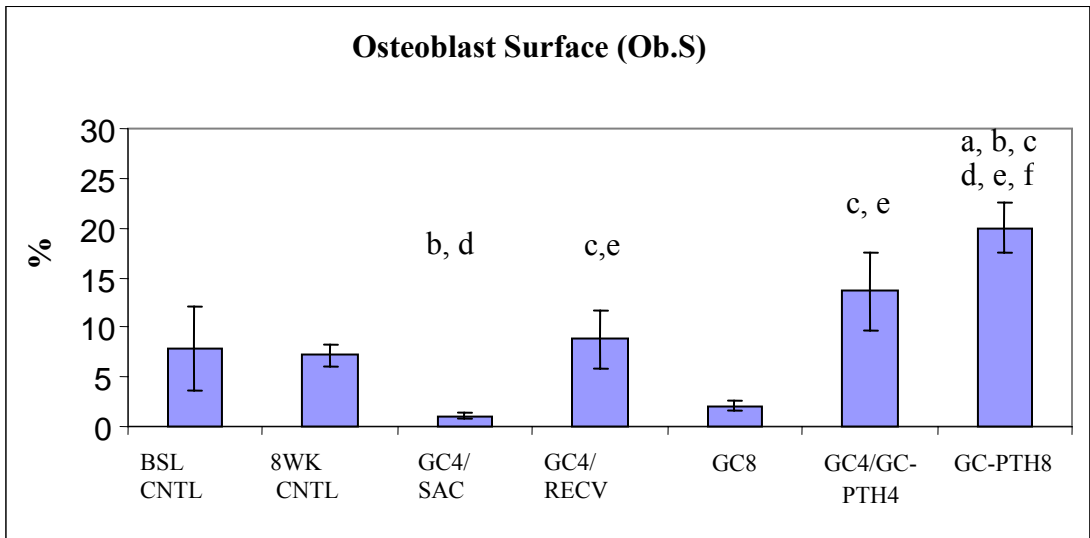


Figure 4-17. Distal Femur Osteoblast Surface by Group using Histomorphometry. a = significant compared to BSL CNTL; b = significant compared to 8 WK CNTL; c = significant compared to GC4/SAC; d = significant compared to GC4/RECV; e = significant to GC8; f = significant compared to GC4/GC-PTH4. Results are reported as mean \pm standard error.

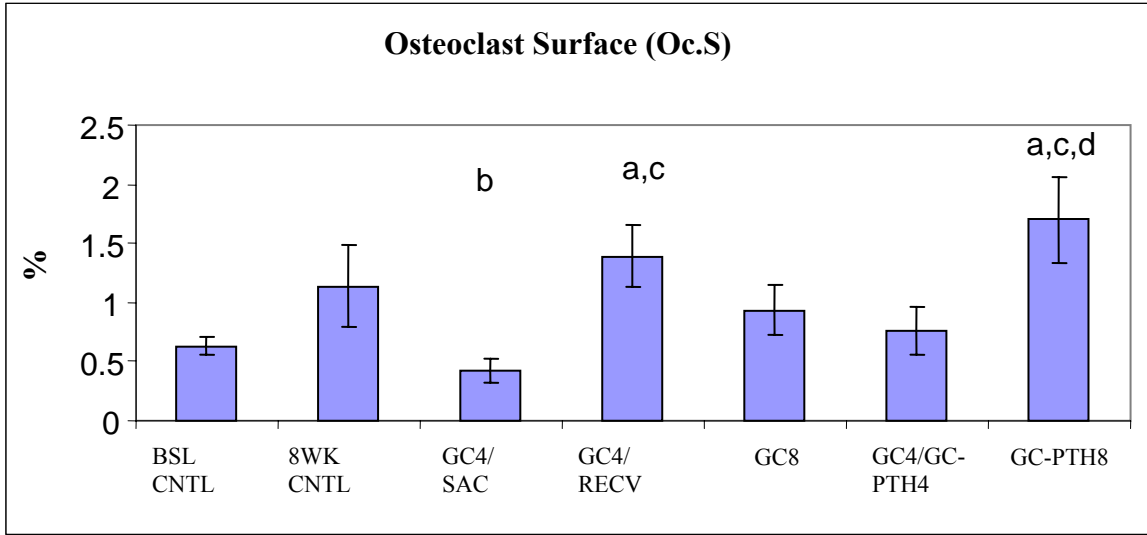


Figure 4-18. Distal Femur Osteoclast Surface by Group using Histomorphometry. a = significant compared to BSL CNTL; b = significant compared to 8 WK CNTL; c = significant compared to GC4/SAC; d = significant compared to GC4/GC-PTH4. Results are reported as mean \pm standard error.

Dynamic Measures of Bone Formation in the Distal Femur

Dynamic measures included mineralizing surface (MS), mineral apposition rate (MAR) and surface referent bone formation rate (BFR/BS). Changes in bone formation were measured or calculated using unstained 8 μm -thick sections. Data for MS, MAR, and BFR/BS are provided in Table 4-10. Differences in MS, MAR, and BFR/BS between groups are shown in Tables 4-22, Table 4-23 and Table 4-24 as well as in Figure 4-19, Figure 4-20 and Figure 4-21, respectively.

Mineralizing Surface

Mineralizing surface was determined by measuring the total perimeter of trabeculae and the percentage of the perimeter with double fluorochrome labeling. Significant changes in MS are shown in Table 4-21.

Mineralizing surface was lower in older animals and those exposed to GC but tended to increase when GC was discontinued and when PTH was used as shown in Figure 4-19. Animals in GC8 had 48.4% ($p = 0.05$) less MS than 8 WK CNTL, while GC4/SAC had 64.5% ($p = 0.02$) less MS than did 8 Wk CNTL. When GC treatment was discontinued, MS increased. Compared to GC4/SAC, GC4/RECV had 436.4% ($p = 0.00$) higher MS and GC4/RECV had a 268.8%, ($p = 0.00$) higher MS than did GC8. GC4/GC-PTH4 also showed a higher MS than 8 WK CNTL (+358.1%, $p = 0.00$), GC4/SAC (1,190.0%, ($p = 0.00$), GC4/RECV (+140.7%, $p = 0.01$), and GC8 (787.5%, $p = 0.00$). Mineralizing surface was even more pronounced in the GC-PTH8 group where it was higher than 8 WK CNTL (441.9%), ($p = 0.00$), GC4/SAC (1,427.3%, $p = 0.00$), GC4/RECV (184.7%, $p = 0.00$), and GC8 (950.0%, $p = 0.00$).

MAR was lower in older animals but was not significantly decreased by GC use. However, MAR tended to increase when GC was discontinued and when PTH was administered

Table 4-21. Significant Changes in Distal Femur Mineralizing Surface by Group.

Group	GC4/SAC	GC4/RECV	GC8	GC4/GC-PTH4	GC-PTH8
BSL CNTL	- 83.8% (p = 0.01)		- 76.8% (p = 0.02)	+111.9% (p = 0.01)	+ 150.7% (p = 0.00)
8 WK CNTL	- 65.4% (p = 0.02)	+ 90.3% (p = 0.05)	- 48.4% (p = 0.05)	+ 358.1% (p = 0.00)	+ 441.9% (p = 0.00)
GC4/SAC		+ 436.4% (p = 0.00)		+ 1,190.0% (p = 0.00)	+1,427.3% (p = 0.00)
GC4/RECV				+ 140.7% (p = 0.01)	+ 184.7% (p = 0.00)
GC 8		+268.8% (P = 0.00)		+ 787.5% (p = 0.00)	+950.0% (p = 0.00)

Results are shown as percent change compared to groups on the left.

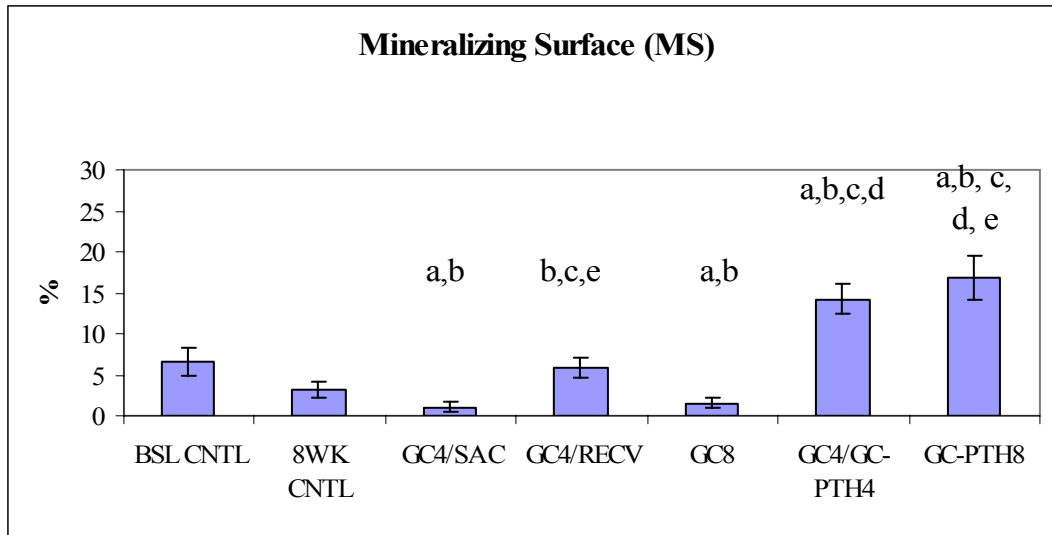


Figure 4-19. Distal Femur Mineralizing Surface by Group using Histomorphometry. a = significant compared to BSL CNTL; b = significant compared to 8 WK CNTL; c = significant compared to GC4/SAC; d = significant compared to GC4/RECV; e = significant compared to GC8. Results are reported as mean \pm standard error.

Mineral Apposition Rate

Significant changes in MAR are shown in Table 4-22 and Figure 4-20.

Table 4-22. Significant Changes in Distal Femur Mineral Apposition Rate by Group.

	8WK CNTL	GC4/SAC	GC4/RECV	GC8	GC4/GC-PTH4	GC-PTH8
BSL CNTL	- 33.3% (p = 0.01)	-33.3% (p = 0.01)		- 33.3% (p = 0.02)		
8 WK CNTL			+ 16.7% (p = 0.03)		+ 33.3% (p = 0.01)	+ 33.3% (p = 0.02)
GC4/SAC			+ 16.7% (p = 0.03)		+ 33.3% (p = 0.01)	+ 33.3% (p = 0.02)
GC4/RECV					+ 14.3% (p = 0.02)	
GC 8					+ 33.3% (p = 0.02)	

Results are shown as percent change compared to groups on the left.

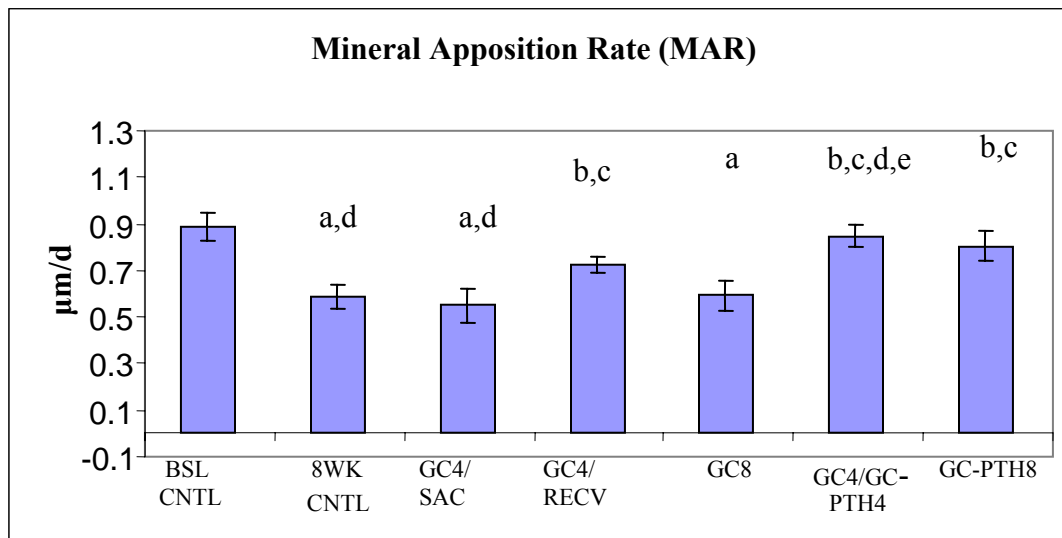


Figure 4-20. Distal Femur Mineral Apposition Rate by Group using Histomorphometry. a = significant compared to BSL CNTL; b = significant compared to 8 WK CNTL; c = significant compared to GC4/SAC; d = significant compared to GC4/RECV; e = significant compared to GC8. Results are reported as mean + standard error.

as shown in Figure 4-20. Mineral Apposition Rate was 33.3% ($p = 0.01$) lower in 8 WK CNTL than in BSL CNTL. Mineral Apposition rate remained the same between GC8 and 8 WK CNTL ($0.6 \mu\text{m}/\text{day}$). However, in animals recovering from GC exposure, GC4/RECV had a 16.7% ($p = 0.03$) higher MAR than 8 WK CNTL and a 16.7% ($p = 0.03$) higher MAR compared with the GC4/SAC group.

Exposure to PTH resulted in the GC-PTH groups having significantly higher MAR than control or GC-treated groups. Compared with comparably aged animals in the 8 WK CNTL group, MAR in the GC4/GC-PTH4 group was 33.3% ($p = 0.01$) greater. The MAR in GC/GC-PTH4 group was also 33.3% ($p = 0.01$) higher than in the GC4/SAC group, 14.3% ($p = 0.02$) higher than in GC4/RECV, and 33.3% ($p = 0.02$) higher than in GC8. MAR was greater in GC-PTH8 than in 8 WK CNTL (+33.3%, $p = 0.02$)

Bone Formation Rate/Bone Surface (BFR/BS)

Both MS and MAR are measured directly, while the third dynamic measure in bone, BFR/BS, was calculated. BFR/BS is derived by multiplying $\text{MS} \times \text{MAR}$ and represents the average amount of bone formed daily ($\mu\text{m}^3/\mu\text{m}^2/\text{day}$). Significant changes in BFR/BS based on treatment groups are found in Table 4-23. There was a non-significant trend toward lower BFR/BS in older animals and a significant decrease in BFR/BS following GC exposure in the GC4/SAC group compared with the 8 Wk CNTL group. However, there was no significant difference in BFR/BS between the GC8 and 8 WK CNTL group. PTH treatment did result in significantly higher BFR/BS. The GC4/PTH4 group had a BFR/BS higher than the 8 WK CNTL (+390.9%, $p = 0.01$), the GC4/SAC (+1,700%, $p = 0.00$), the GC4/RECV (+157.1%, $p = 0.02$), and the GC8 (+980%, $p = 0.00$) groups. This pattern continued with the GC-PTH8 group.

Table 4-23. Significant Changes in Distal Femur Bone Formation Rate by Group using Histomorphometry.

	GC4/SAC	GC4/RECV	GC8	GC4/GC-PTH4	GC-PTH8
BSL CNTL	- 90.6% (p = 0.00)		- 84.4% (p = 0.01)		+ 131.3% (p = 0.02)
8 WK CNTL	- 72.7% (p = 0.02)	+ 90.9% (p = 0.03)		+ 390.9% (p = 0.01)	+ 572.7% (p = 0.00)
GC4/SAC		+ 600.0% (p = 0.00)		+ 1,700% (p = 0.00)	+ 2,366.7% (p = 0.00)
GC4/RECV				+ 157.1% (p = 0.02)	+ 254.4% (p = 0.00)
GC 8		+ 76.2% (p = 0.00)		+ 980.0% (p = 0.00)	+ 1,380.0% (p = 0.00)

Results are shown as percent change compared to groups on the left.

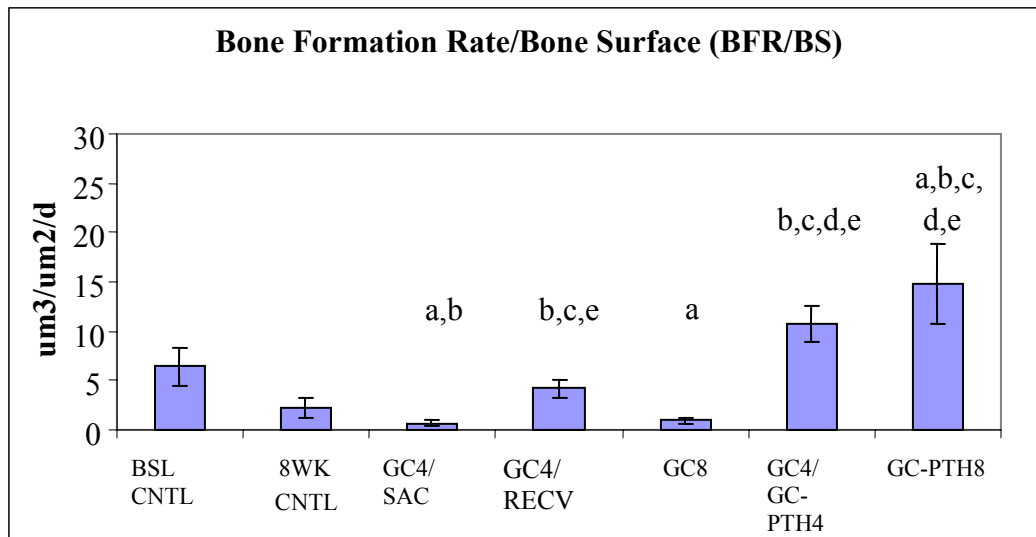


Figure 4-21. Distal Femur Bone Formation Rate/Bone Surface by Group using Histomorphometry. a = significant compared to BSL CNTL; b = significant compared to 8 WK CNTL; c = significant compared to GC4/SAC; d = significant compared to GC4/RECV; e = significant compared to GC8. Results are reported as mean \pm standard error.

Mid-Shaft Cortical Bone Data and Significant Changes

A portion of the mid-shaft of the left femur in 70 mice was also analyzed using microCT. In each animal, 55 slices (1.2 μm each) were scanned and reconstructed. Cortical thickness (Ct.Th) data are presented in Table 4-24, Table 4-25, and Figure 4-22. There was no apparent age-related difference in cortical thickness. While Ct.Th did not change significantly with GC treatment, it did increase significantly with PTH as shown in Figure 4-22. Animals receiving 8 weeks of GC and PTH had significantly higher Ct.Th than BSL CNTL (+8.7%, $p = 0.02$), GC8 (9.5%, $p = 0.02$), or GC4/SAC (+10.7%, $p = 0.00$). The only other significant difference occurred where Ct.Th was 6.7% higher ($p = 0.03$) in the GC4/GC-PTH4 group than in GC4/SAC animals.

Table 4-24. Summary of Histomorphometric Analysis of Femur Mid-Shaft by Group.

	BSL CNTL (n = 10)	8 WK CNTL (n= 10)	GC4/ SAC (n = 10)	GC4/ RECV (n = 10)	GC 8 (n = 10)	GC4/GC- PTH4 (n = 10)	GC- PTH8 (n = 10)
Cortical Thickness	27.5 \pm 1.9	28.3 \pm 2.4	27.0 \pm 1.4	28.2 \pm 1.3	27.3 \pm 1.7	28.8 \pm 1.7	29.9 \pm 2.0

Results are reported as mean \pm standard deviation.

Table 4-25. Summary of Significant Changes in Femur Mid-Shaft Cortical Bone Thickness by Group using MicroCT.

	GC4/GC-PTH4	GC-PTH8
BSL CNTL		+ 8.7% ($p = 0.02$)
GC8		9.5% ($p = 0.02$)
GC4/SAC4	+ 6.7% ($p = 0.03$)	10.7% ($p = 0.00$)

Note: Results are shown as percent change compared to groups on the left.

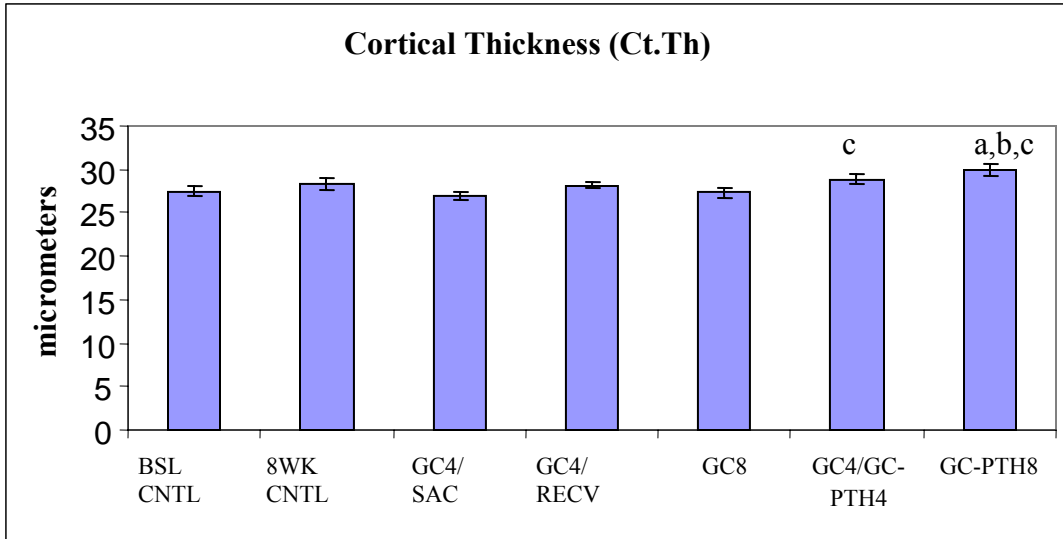


Figure 4-22. Mid-Shaft Femur Cortical Thickness by Group using MicroCT. a = significant compared to BSL CNTL; b= significant with GC8; c = significant with GC4/SAC Results are reported as mean \pm standard error.

CHAPTER 5 DISCUSSION

This was the first prospective study to evaluate the ability of PTH treatment to inhibit the negative skeletal effects of GC in mice. The study examined several aspects of this issue including the cumulative effects of both GC and PTH over time, site specific responses, tissue and cellular changes in response to treatment, and the effectiveness of natural recovery from termination of GCs. The major findings of this investigation are as follows:

- GCs suppress bone formation/turnover but do not necessarily reduce bone volume
- PTH was bone anabolic even in the presence of GCs
- PTH increased bone mass quickly
- There was a residual effect following discontinuation of GC therapy that resulted in no increase in bone mass despite a rebound effect in osteoblast numbers and activity
- Following GC treatment with PTH was more effective in improving bone structural parameters and mineralization than was natural recovery
- The magnitude of response to GC and PTH varied by skeletal site
- There was an age-related decline in bone structural parameters in control animals.

Glucocorticoid Drugs Suppressed Bone Formation But Did Not Affect Bone Volume

A previous study found that bone turnover decreased 67.4% ($p = 0.05$) in Swiss Webster mice treated with GC for 4 weeks (5). Other studies have reported similar findings (2,5,114) and it is generally accepted that exposure to GCs suppresses bone turnover in mice. We also found that turnover decreased but, in contrast to some studies, we observed increased BV/TV, though this only reached the level of statistical significance in the distal femur and only in measurements using microCT.

GCs may have caused an uncoupling of the remodeling process so there was no longer the same amount of bone formed as resorbed. In some previous studies this resulted in a lower

BV/TV in mice, but in the present study we detected a bone specific increase in BV/TV. While we found no significant changes in lumbar spine BV/TV after 8 weeks of GC use, we did detect (by microCT) a significant increase in BV/TV in the distal femur.

At the cellular level, GCs affect osteoblasts, osteocytes, and osteoclasts but typically affect the osteoblast most (39). GCs typically decrease osteoblast and osteoclast numbers and activity levels while also increasing osteocyte apoptosis. The effects on osteoclasts are more variable. Studies invariably find Ob.S declines, but studies have found both increases and decreases in Oc.S (39). Lane found significant increases in Oc.S while Weinstein found increased and decreased Oc.S in different studies (2,5,114). In our study, 4 weeks of GC resulted in an 84.7% ($p = 0.03$) lower Ob.S and a 63.6% ($p = 0.03$) lower Oc.S in the distal femur in GC-treated animals.

In the present study, decreased Ob.S had far-reaching consequences. Mineralizing surface decreased by over 60%, further suggesting an important effect of GCs on osteoblast numbers. Mineralizing surface generally reflects the number of osteoblasts on trabecular surfaces and histomorphometry detected a trend toward decreased Ob.S and Oc.S in the GC8 group compared to 8 WK CNTL although the changes did not reach statistical significance. It is possible that the increased BV/TV seen in this study results from GCs having more of a suppressive effect on osteoclasts than on osteoblasts. If osteoclast activity levels were suppressed more, relative to osteoblast levels, this would result in increased bone volume.

GCs not only affect bone cell numbers, they also influence the activity levels of these cells. In osteoblasts, GCs reduce the time these cells secrete osteoid and actively mineralize bone (72). Although we did not measure osteoid, measurement of dynamic parameters suggest a decrease in bone turnover. In the distal femur, we found MS was 48.4% ($p = 0.05$) lower in GC-treated

animals (GC8) than in 8 WK CNTL animals but found no difference in MAR, an index of osteoblast activity, and only a non-significant, two-fold decrease in BFR/BS. These findings are similar to other studies with respect to MS but differ with studies that found lower MAR and BFR/BS (2,5). Our findings with respect to MAR and BFR/BS are consistent with the differences in BV/TV we detected, however.

It is more difficult to directly assess osteoclast activity levels, but inferences can be made. The typical response to GCs in human disease is decreased bone turnover that disproportionately affects formation rather than resorption. This results in rapid bone loss. Most studies of GC in mice have found that BV/TV declines in a dose-dependent and time-dependent manner. This was the case in several studies, including some using Swiss Webster mice. A previous study found that 6-month old Swiss Webster mice treated for three weeks had a modest 19% ($p = 0.05$) lower BV/TV in the lumbar vertebrae based on histomorphometry and 22% ($p = 0.05$) decrease based on microCT (2). In this same study, Oc.S increased over 100 %, from 0.8 to 1.7% ($p \leq 0.05$), MS decreased by almost one-third, from 42.9 to 29.5% ($p \leq 0.05$) while MAR declined almost 40% from 1.03 to 0.64 μm ($p \leq 0.05$). These changes accompanied a 105% increase in osteocyte apoptosis from 1.9 to 3.9% ($p < 0.05$) (2). Findings such as these have previously been attributed to a decrease in osteoblastogenesis and increased apoptosis of both osteoblasts and osteocytes (2,5,39).

What determines the net balance of formation to resorption is unclear, but our finding of increased BV/TV in mice should not be dismissed without further study since the same phenomenon has been seen in other rodents. In rats, researchers have detected bone loss, bone increase, or no change after exposure to GCs (36-38). There has also been variability reported in mice exposed to GCs. While some studies in mice have reported dose- and time-dependent

losses in BV related to GC use, others have not. Using histomorphometry, one study found no significant decline in BV/TV even though BFR/BS declined significantly (~75%) in the femur. The only significant differences detected by microCT occurred at very high GC dosages, which are known to impact other steroid receptors (3). This suggests that the dose-response to GCs is not linear and that some conditions may cause resorption to be more suppressed than formation. Our findings suggest, that while changes in bone cell numbers were important, changes in activity levels at the cellular level may also be central to the changes we detected in these bones. While both osteoblasts and osteoclasts decreased in number in response to GC treatment, the increased BV/TV found with GC treatment found in our study suggests osteoclast activity levels may have been more severely suppressed relative to osteoblast activity, allowing for increased BV/TV despite decreased numbers of osteoblasts. This requires further examination, however, since there were no measures in this study to detect or quantify osteoclast activity levels.

Anabolic Effects of PTH Prevented the Inhibitory Changes Associated with Glucocorticoid Drugs

Studies evaluating the effects of PTH on mice consistently show it is bone anabolic even under conditions that tend to decrease bone formation and/or bone mass (7,8,45) and our study supports this finding as well. In one study involving ovariectomized mice, PTH treatment resulted in a two-fold increase in MAR and a 3-fold increase in BFR/BS (7).

GCs suppress osteoblast proliferation/ activity levels and PTH, a hormone that stimulates osteoblasts, is able to reverse this trend (6) to overcome the suppressive effects of GCs. PTH and GC together have been tested in rats (115), but the present study is the first to examine the effects of PTH in GC-treated mice. The only human investigation of the combined effects of GC and PTH involved subjects who also took estrogen. In that study, BMD increased linearly during the entire 12 month course of treatment (6). This finding was consistent with other

studies that found that the antiresorptive effects of estrogen did not prevent the bone anabolic response to PTH (116).

The anabolic nature of intermittent PTH on bone is seen in its effects at the cellular level. Following PTH administration to rats and humans, there is typically an increase in both Ob.S and Oc.S, leading to increased bone turnover. Although both Oc.S and Ob.S increase, this change is most dramatic in Ob.S and, therefore, favors bone formation. A study of PTH in intact mice reported a significant increase in Ob.S (45). We found no significant change in Oc.S but a significant increase in Ob.S compared to the GC8 group after 4 weeks (+ 547.6%, $p = 0.00$) and 8 weeks (+ 852.4%, $p = 0.00$) of PTH treatment. This substantial change in osteoblast presence on trabecular surfaces could reflect increased differentiation, decreased apoptosis, or reactivation of bone lining cells. Consistent with the increase in Ob.S, after 4 weeks of treatment with PTH, there was a significant increase in MS (787.5%, $p = 0.00$) MAR (33.3%, $p = 0.02$), and BFR/BS (980.0%, $p = 0.00$) compared to animals receiving eight weeks of GC. The differences in MS and BFR/BS were even more pronounced after 8 weeks of PTH.

In this study, Ob.S was over 1,000% higher in a group of animals treated with PTH for 4 weeks compared to animals treated similarly with GCs (GC4/SAC). The increase in number and activity levels of the osteoblasts resulted in a BFR/BS over ten times the rate seen in GC8 animals in just 4 weeks. Likewise, animals treated with PTH and GC for 8 weeks had over 850% greater Ob.S than did GC8 animals. The magnitude of change in Ob.S makes it unlikely that it could result solely from reactivation of quiescent bone lining cells. The very high increases in Ob.S seen with PTH likely stem from increased osteoblast proliferation as well as increases in osteoblast lifespan (116).

Mineralizing surface is an indirect measure of the osteoblast population and increased numbers of these cells means more bone surface is mineralizing at any given time. Mineralization apposition rate generally reflects the activity level of the osteoblasts, since osteoblasts modulate bone mineralization. The significantly higher MS and MAR detected in the present study are evidence PTH increased both the number and activity levels of osteoblasts. BFR/BS, a function of both MS and MAR, is also significantly higher with PTH, reflecting the shifting balance in bone turnover toward bone formation. There are only a few studies that have examined the effects of PTH following GC therapy on BFR/BS. One of these found that BFR/BS tended to decrease in response to GC alone but increased with PTH alone in rats. That study found that when the two drugs are used simultaneously, there was an intermediate response that increases BFR/BS relative to GC-only treated animals, but kept it lower than with PTH alone (115).

The effects of PTH also appeared to increase over time. Animals in the GC-PTH8 group showed a trend toward even higher bone mass than the GC4/GC-PTH4 animals, according to microCT, but high variability prevented this from reaching statistical significance. MicroCT found a 45.6% ($p = 0.02$) greater BV/TV in distal femur between animals treated with PTH for 8 weeks versus those treated for only 4 weeks. These changes appear driven by additional increases in osteoblast and osteoclast numbers since Ob.S was 47.1% ($p = 0.05$) higher and Oc.S was 112.5% ($p = 0.03$) higher in group receiving 4 additional weeks of PTH. At the end of the 8 weeks of PTH treatment, osteoclasts lined 1.7% of the trabecular surfaces while osteoblasts lined 20% of the trabecular surfaces.

PTH Increases Bone Mass Quickly

Studies have found the effects of PTH are rapid and one study found significant changes in BMD in the tibia of C57BL/J6 mice with just one week of treatment (45), although it took longer

to detect BMD differences in the vertebrae. In the present study, there was also significantly higher Ob.S, MS, MAR, and BFR/BS in the distal femur after 4 weeks of PTH-treatment indicating increases in osteoblast numbers and activity levels quickly influenced both bone formation and mineralization activity. These improvements were evident in increased vertebral BV/TV and Tb.Wi at 4 weeks based on histomorphometry and in Tb.Th based on microCT. Our study mirrors other studies in finding early and significant changes in dynamic indices of bone turnover but a lag of at least 4 or more weeks before structural differences reach statistical significance difference from baseline controls (8,45).

Changes in bone structural parameters were brought about through the ability of PTH to increase bone turnover even though GC was also administered. Animals receiving PTH for 4 weeks showed increases in Ob.S (+547.6%, $p = 0.00$) but a non-significant decrease in Oc.S (-11.1%, $p = ns$) compared to GC8 animals. This helps show why PTH is anabolic since the proportion of the trabecular surfaces covered in osteoblasts increased over 5-fold. PTH also increased the activity levels of osteoblasts as reflected in higher MS, MAR, and BFR/BS. Of interest, animals treated with PTH for 8 weeks while also receiving GCs, showed a further increase in Ob.S (+47.1%, $p = 0.05$) and Oc.S (+112.5%, $p = 0.03$) compared to animals in the GC4/GC-PTH4.

Residual Effects of Glucocorticoid Drugs are Apparent During Natural Recovery

No previous studies have evaluated bone recovery once GC treatment is discontinued. We expected discontinuation of GC treatment would result in natural recovery that would bring the measured parameters closer to control animals. That was not the case since we detected trends toward lower BV/TV, Tb.N and Tb.Th and higher Tb.Sp in the GC4/RECV group than in the GC4/SAC, a group of animals sacrificed immediately following four weeks of GC treatment. This suggests there is a residual effect to GC use that, at least in mice, does not abate in four

weeks. Although there were no statistically significant changes in bone structural parameters, there were significant changes in activity at the cellular level. Four weeks of recovery resulted in significantly higher Oc.S (+225%, $p = 0.00$) and Ob.S (+ 690.9%, $p = 0.00$) compared to GC4/SAC. There was a “rebound” effect in dynamic bone measures, that resulted in MS, MAR, and BFR/BS exceeding even the 8 WK CNTL group. Increases in these parameters, however, did not translate into increased bone mass, suggesting either there was not sufficient time for increased bone mass to be detected or there were GC-induced changes to the bone matrix preventing expected increases. We believe the latter is more likely and that this may represent a change to the bone matrix that inhibits increases in structural bone mass even once GC treatment is discontinued.

The reason for the impaired ability of these bones to increase in mass despite high activity levels in bone cells is unclear, but is not without precedent. Experiments in animals treated with alcohol show similar impaired recovery. When decalcified bone cores from alcohol-treated and control mice were placed subcutaneously in untreated mice, the alcohol-exposed cores showed an impaired ability to re-mineralize (117). It is possible a similar process is at work in glucocorticoid-treated mice. Conversely, it is also possible a longer recovery period would have made a difference. After GCs are discontinued in humans there is a slow reduction in fracture risk over time (23). One study found the relative fracture risk decreased from 2.4 to 1.8 one year after GC is stopped, and continued to move back to pre-treatment baseline risk levels over time (23). These reductions in fracture risk may result from improved structural repairs to the bone over time.

PTH Treatment After Glucocorticoid Use Was More Effective than Natural Recovery

We expected administration of PTH following GC treatment to be more effective in increasing bone structural parameters than natural recovery, and the data support this. In the

vertebrae, Tb.Th was increased by 25.5% ($p = 0.00$) using histomorphometry and by 13.5% ($p = 0.00$) using microCT in GC4/GC-PTH4 compared with GC4/SAC. In the distal femur, BV/TV and Tb.Wi were significantly higher in GC4/GC-PTH4 compared with GC4/SAC while Tb.Sp was significantly lower based on histomorphometry. In the distal femur, BV/TV increased significantly (95.6% ($p = 0.01$)) although there was only a non-significant increase in Ob.S between the GC4/GC-PTH4 and GC4/SAC groups. Histomorphometry did, however, detect significant increases in MS (140.7%, $p = 0.01$), an indication that a greater percentage of the trabeculae were covered in osteoblasts. There was also a 14.3% ($p = 0.02$) increase in MAR, a measure of osteoblast activity levels. The increases in MS and MAR contributed to the significant increase in BFR/BS (+ 157.1, $p = 0.02$) indicating that PTH treatment resulted in increased bone formation. These findings were expected; since PTH is bone anabolic we expected it would have a greater effect on bone parameters than natural recovery after GC-treatment was discontinued. While animals that experienced natural recovery showed a rebound effect in dynamic bone parameters that showed significant increases in MS(90.3%, $p = 0.05$), MAR (16.7%, $p = 0.03$), and BFR/BS (90.9%, $p = 0.03$) compared to 8 WK CNTL, these levels were much more impressive following PTH treatment: MS (441.9%, $p = 0.00$), MAR (33.3%, $p = 0.02$), BFR/BS (572.7%, $p = 0.00$).

Age-Related Effects on Bone Mass

We expected a relatively constant level of bone turnover in these adult male Swiss Webster mice. A previous study, whose goal was specifically to determine when long-bone growth ceased, found that this strain of mice cease longitudinal bone growth in the long bones between five and six months of age (5). Based on this, we expected young adult Swiss Webster mice to have a constant level of bone turnover that would result in stable levels of bone mass throughout the two-month length of the study. Our data suggest, however, this was not the case. Our results

may represent the first reporting that age-related decreases in bone mass occur in Swiss Webster mice begin within a few months of these animals reaching peak bone mass. The effect was seen in histomorphometry of the lumbar spine and both histomorphometry and microCT of the distal femur.

There is evidence of variability between and within in-bred mouse strains with respect to skeletal maturation (118,119) and, this study suggests there may be perhaps also age-related changes to bone in young adult out-bred mice, like the Swiss Webster strain. One study found that the Swiss Webster mouse reaches skeletal maturity between 5 and 6 months of age (5), although no attempt was made to determine the age at which there would be a natural decline in bone mass due to aging. Another study found that the level of osteoblastogenesis decreased three-fold in SAMP6 mice between 3 and 4 months of age and resulted in significant bone loss soon after (120). Data from another study using 10 week old C57BL/J6 mice showed a trend toward decreasing bone volume at about 16 weeks of age (45). Our data also suggest an age-related decrease in bone mass in control animals. The Swiss Webster mice in our study entered at seven months of age and were sacrificed two months later. There was a lower cancellous BV/TV in both the lumbar spine and distal femur, using microCT and histomorphometry, between 7 month old and 9 month old control animals.

In the distal femur, both histomorphometry and microCT found 35-45% less BV/TV and around a 20-40% lower Tb.N in nine month old animals than in their seven month old counterparts. There was also more than double the Tb.Sp according to histomorphometry. Despite these changes there was no significant difference in the Ob.S and Oc.S although Ob.S showed a downward trend while Oc.S showed an upward trend. The downward trend in Ob.S was insufficient to cause a significant difference in MS. However, there was a significant

decline in MAR, suggesting that, while osteoblast numbers may be relatively stable, the osteoblasts were less actively forming bone. The 33.3% ($p = 0.01$) decline in MAR contributed to the almost three-fold decline in BFR/BS in the 8 WK CNTL compared to the BSL CNTL animals.

Prophylactic Value of Concurrent Treatment with Glucocorticoid Drugs and PTH

This study is the first to examine whether there is increased benefit to starting PTH treatment concurrently with GC administration as opposed to using GC first and then later treating with PTH. One group of animals was treated with GC for 4 weeks and then treated for an additional four weeks with both GC and PTH. Another group simultaneously received GC and PTH for 8 weeks. There was a benefit to simultaneous treatment but this may be the result of the additional 4 weeks of PTH. There was a 47.1% ($p = 0.05$) higher Ob.S and a 112.5% ($p = 0.03$) higher Oc.S with 8 weeks of PTH, indicating continued gains in the latter group. In the lumbar vertebrae, the group treated with PTH for 8 weeks also had a significant decrease in Tb.Sp. In the distal femur, significant changes were only seen with microCT, where both BV and Tb.Th were significantly higher. There were no significant differences in MS, MAR, or BFR/BS with additional PTH treatment. These findings suggest that even though 8 weeks of PTH resulted in some additional improvement to bone parameters, 4 weeks of PTH after GC exposure was still highly effective.

Comparing the effects of 4 weeks of PTH use against eight weeks of PTH in animals receiving GC for 8 weeks shows that most of the change occurred in the first 4 weeks of PTH administration. There were continued improvements in the group receiving PTH for 8 weeks, but the magnitude of change was less. 82.9% of the final level of MS seen in the GC-PTH8 group was seen in the GC4/GC-PTH4 group. The same trend was true for MAR which was slightly higher in the 4 week PTH group and BFR/BS where over 70% of the total 8 week

change was seen in the GC4/GC-PTH4 group. These findings suggest PTH was able to reverse the effects of prior GC use sufficiently to make it a valid post-exposure treatment.

Site Specificity of GC and PTH Treatment

In mice, as in humans, BV/TV is higher in the vertebrae than in the femur. In humans however, the effects of both GC and PTH are more prevalent in the vertebrae than in the femur. Humans treated with both GC and PTH increased spinal BMD by 35% while the hip gained only a modest 2% BMD over a one-year period (6). A different relationship has been reported in mice (8) where there is greater change in long bones of the appendicular skeleton than in the axial skeleton. Other studies in rats have reported the same results (39). The difference in results found in rodents may result from biomechanical loading differences between bipeds and quadrupeds (8). In our study, changes with both GC and PTH were also greater in the distal femur than in the lumbar spine. Based on histomorphometry, BV/TV changes were greater in the distal femur than in the lumbar spine (-46% versus -30%) and based on PTH exposure (100% versus 42%). It may be that the biomechanics of weight-bearing activities of the mouse explain the different findings or that there is an additive effect when PTH is acting on a bone already exposed to higher mechanical loading (8,121,122).

Conclusions

This study found that glucocorticoid drugs suppress bone turnover in the Swiss Webster mouse and that these effects can be offset by PTH. The effects of PTH were rapid, with most of the total changes seen over eight weeks occurring in the first 4 weeks. We also found that PTH treatment after GC exposure is more effective at restoring bone mass than natural recovery. We found there are site specific differences in response to PTH and that these caused greater changes to occur in the appendicular rather than in the axial skeleton.

This study also reports some novel findings. We found there was an age-related loss of bone between 7 and 9-month old animals who received only vehicle and no study drugs. We also found that GCs tended to increase bone mass even though there was clearly a suppression of bone turnover. Finally we found a residual effect with GC treatment that inhibited increases in bone mass after GC treatment was discontinued even though osteoblastic activity rebounded after GC removal.

Clinical Applications

The underlying goal for this research was to demonstrate the efficacy of using PTH to mitigate the skeletal effects of GCs in mice, as a prelude to studies in humans. Swiss Webster mice have previously been validated as models of bone loss due to ovariectomy (7) and for GC-induced bone loss (2) and have been described as “a faithful model of the glucocorticoid-induced bone loss in humans”(39). Despite the fact this study found exposure to GC may have increased BV/TV, we believe the results pave the way for follow-on studies using PTH to treat bone loss due to GCs in humans, although our results suggest the response of Swiss Webster mice to GCs may be more variable than previously reported. There has been ample research demonstrating the deleterious effects of GCs and the increased risk of bone fracture that accompanies their use (21,23,73,76,81). This study demonstrated that PTH is effective in reversing the inhibitory effects of GCs on bone formation. Our findings support a clinical application for PTH in patients diseases conditions such as rheumatoid arthritis, COPD and other conditions that result in long-standing GC use. PTH was used in one study with rheumatoid arthritis patients where it increased spinal BMD by 35%, although gains in the hip were a more modest 2% (6). This human study concluded that while anti-resorptive treatments can prevent bone loss, PTH was the only therapy currently available that could reverse the suppressive effects of GCs (6). We believe these findings and our current study show there is potential for successful treatment of

other patients who have experienced long-term glucocorticoid therapy including those that may require solid organ transplants.

Due to the nature of post-transplant immunosuppressant protocols and reports of osteosarcoma in rats exposed to life-time doses of PTH (103-105), we would not recommend the use of PTH after transplant surgery, but this drug may prove efficacious in treating pre-existing, GC-induced osteoporosis in those still awaiting surgery. The rapid effects of the PTH suggest that even if patients could not complete the normal 18-24 month treatment regimen prior to receiving a transplant, even a few months of treatment could be beneficial. Although beneficial effects are more likely to be seen in the spine, one study showed that bone mass in the hip increased six months after PTH was discontinued (44), indicating therapeutic benefits beyond the dosing period.

Study Limitations

As with any study, resource considerations influenced study design and implementation. Animals were housed one to a cage although this was not ideal. Mice are social animals that interact with each other so housing them alone might have affected activity or stress levels. We had to house the mice singly, however, to avoid fighting. These were adult males formerly used for breeding and were highly territorial. We also had to accept delivery of study animals in 7 shipments of 10 mice rather than receiving all animals simultaneously. This was necessary because of the age of the animals involved. The other alternative would have been to buy young animals and age them either at our facility or with the vendor. This would have decreased cohort variation but was cost-prohibitive. We minimized the impact of multiple cohorts by assigning animals from each arriving shipment to each study group.

Future Directions

There were novel findings in this study that warrant further investigation. The finding of negative changes in bone structural parameters in control mice over the two-month course of the study was unexpected. Further studies are needed to verify these differences and establish the significance and mechanisms mediating these changes. If there is a natural loss of bone so quickly after attaining peak bone mass, researchers need to be aware of this so they don't attribute age-related changes to interventional treatments.

The residual effect of GCs on the bone matrix also needs further study. Animals treated with GCs and then allowed to recover showed further declines in bone structural parameters despite increased osteoblastic activity. It is possible bone structural parameters would have returned to normal if more recovery time had been allowed, but it is also possible that the GCs caused a change to the bone matrix that inhibited recovery. If the latter is true, it might partially explain the increased risk of bone fracture after GC therapy.

Finally, we believe the results of this study provide clear evidence of the efficacy of PTH in treating bone changes caused by GC exposure. We believe human clinical populations may also benefit from this treatment as previously discussed.

APPENDIX A
SUMMARY OF BONE MEASUREMENTS

A-1. Summary of Significant Changes in Lumbar Vertebrae L3 based on Histomorphometry.

	BSL CNTL	8WK CNTL	GC4/SAC	GC4/RECV	GC8	GC4/GC-PTH4	GC-PTH8
BSL CNTL		BV/TV -30.7% (p = 0.03)		BV/TV -27.7% (p = 0.03)	BV/TV -31.5 (p = 0.02)		
		Tb.Wi -18.4% (p = 0.02)		Tb.Wi -19.0 (p=0.02)	Tb.Wi -25.1 (p = 0.00)		
8 WK CNTL							BV/TV + 42.0% (p = 0.01)
						Tb.Wi + 24.5 % (p =0.01)	Tb.Wi + 22.1 (p = 0.01)
							Tb.Sp -24.7 % (p = 0.03)
GC4/ SAC						Tb.Wi + 14.5% (p = 0.03)	
GC4/RECV							BV/TV +35.9% (p = 0.03)
						Tb.Wi +25.5% (p = 0.00)	Tb.Wi +23.1% (p = 0.01)
GC 8						BV/TV + 26.4% (p = 0.03)	BV/TV + 43.7% (p = 0.01)
			Tb.Wi + 18.5 (p = 0.02)			Tb.Wi + 35.8% (p = 0.00)	Tb.Wi + 33.2% (p = 0.00)
GC4/GC-PTH4							Tb.N + 19.5% (p =0.02)
							Tb.Sp - 17.4% (p = 0.01)

A-2. Summary of Significant Changes in Lumbar Vertebrae L2 based on MicroCT.

	GC4/RECV	GC4/GC-PTH4	GC-PTH8
BSL CNTL	BV/TV - 21.1% (p = 0.03)	Tb.N -9.5% (p = 0.02)	Tb.Th + 12.3% (p = 0.01)
	Tb.N - 9.5% (p = 0.04)	Tb.Sp + 12.3% (p = 0.04)	
	Tb.Th - 5.7% (p = 0.02)		
	Tb.Sp + 12.7% (p = 0.03)		
8 WK CNTL		Tb.Th + 9.7% (p = 0.04)	BV/TV + 36.6% (p = 0.01)
			Tb.Th + 15.2% (p = 0.00)
GC4/SAC		Tb.Th + 10.6% (p = 0.01)	BV/TV + 26.4% (p = 0.04)
			Tb.Th + 16.1% (p = 0.00)
GC4/RECV		Tb.Th + 13.5% (p = 0.00)	BV/TV + 46.7% (p = 0.00)
			Tb.Th + 19.2% (p = 0.00)
GC 8	BV/TV - 21.1% (p = 0.04)	Tb.Th + 12.3% (p = 0.00)	Tb.Th + 17.9% (p = 0.00)

A-3. Summary of Significant Changes in the Distal Femur based on Histomorphometry.

	8WK CNTL	GC4/RECV	GC8	GC4/GC-PTH4	GC-PTH8
BSL CNTL	BV/TV - 45.8% (p = 0.03)	BV/TV - 52.1% (p = 0.01)			
	Tb.N - 40.0% (p = 0.05)	Tb.N - 40.0% (p = 0.01)			
		Tb.Wi - 22.3% (p = 0.04)	Tb.Wi - 17.7% (p = 0.05)		
	Tb.Sp + 153.0% (p = 0.05)	Tb.Sp + 177.2% (p = 0.01)			
8 WK CNTL					BV/TV + 100.0% (p = 0.02)
					Tb.N + 83.3% (p = 0.03)
					Tb.Sp -59.4% p = 0.03
GC4/RECV				BV/TV + 95.6% (p = 0.01)	BV/TV + 126.1% (p = 0.01)
					Tb.N + 83.3% (p = 0.03)
				Tb.Wi + 27.4% (P=0.05)	Tb.Wi + 30.6% (p = 0.02)
				Tb.Sp - 63.3% (p = 0.01)	Tb.Sp - 63.0% (p = 0.03)
GC 8				Tb.Wi + 20.3% (p=0.04)	Tb.Wi + 23.3% P = 0.03

A-4. Summary of Significant Changes in the Distal Femur based on MicroCT

	8WK CNTL	GC4/RECV	GC8	GC4/GC-PTH4	GC-PTH8
BSL CNTL	BV/TV - 37.4% (p = 0.00)	BV/TV - 39.4% (p = 0.00)			
	Tb.N - 22.2% (p=0.05)	Tb.Sp +30.5% (p = 0.05)			Tb.Th + 16.3% (p = 0.01)
8 WK CNTL			BV/TV + 40.3% (p = 0.03)		BV/TV + 85.5% (p = 0.00)
			Tb.N + 33.3% (p = 0.03)		Tb.N + 33.3% (p = 0.00)
			Tb.Th - 12.7% (p = 0.04)		
			Tb.Sp - 19.4% (p = 0.03)		Tb.Sp - 25.6% (p = 0.00)
GC4/SAC				Tb.Th + 6.3% (p = 0.05)	Tb.Th + 17.5% (p = 0.00)
GC4/RECV			BV/TV + 45.0% (p = 0.02)		BV/TV + 91.7% (p = 0.00)
					Tb.N + 27.3% (p = 0.01)
					Tb.Th + 17.9% (p = 0.00)
					Tb.Sp - 27.8% (p = 0.01)
GC 8					BV/TV + 32.3% p = 0.04
				Tb.Th + 13.5% p = 0.05	Tb.Th +25.4% P = 0.00
GC4/ GC-PTH4					BV/TV + 45.6% (p = 0.02)
					Tb.Th + 10.5% (p = 0.05)

A-5. Percent Changes in Osteoclast and Osteoblast Surfaces in the Distal Femur.

p	GC4/SAC	GC4/RECV	GC8	GC4/GC-PTH4	GC-PTH8
BSL CNTL		Oc.S + 116.7% (p = 0.02)			Oc.S + 183.3% (p = 0.01) Ob.S + 153.2% (p = 0.01)
8 WK CNTL	Oc.S - 63.6% (p = 0.03) Ob.S - 84.7% (P= 0.00)		Ob.S -70.8 (p = 0.00)		Ob.S + 177.8% (p =0.00)
GC4/SAC		Oc.S + 225% (p = 0.00) Ob.S + 690.9% (p = 0.00)		Ob.S +1,136.4% (p= 0.00)	Oc.S + 325.0% (p = 0.00) Ob.S + 1,718.2% (p = 0.00)
GC4/RECV					Ob.S + 129.9% (p = 0.00)
GC 8		Ob.S +314.3% (p = 0.00)		Ob.S + 547.6 (p = 0.00)	Ob.S + 852.4% (p= 0.00)
GC4/GC-PTH4					Oc.S + 112.5% (p = 0.03) Ob.S +47.1% (p = 0.05)

A-6. Percent Changes in Dynamic Bone Formation Parameters in the Distal Femur.

	8WK CNTL	GC4/SAC	GC4/RECV	GC8	GC4/GC-PTH4	GC-PTH8
BSL CNTL		MS - 83.8% (p = 0.01)		MS - 76.8% (p = 0.02)	MS +111.9% (p = 0.01)	MS + 150.7% (p = 0.00)
	MAR - 33.3% (p = 0.01)	MAR - 33.3% (p = 0.01)		MAR - 33.3% (p = 0.02)		
				BFR/BS - 84.4% (p = 0.01)		BFR/BS + 131.3% (p = 0.02)
8 WK CNTL		MS - 64.5% (p = 0.02)	MS + 90.3% (p = 0.05)	MS - 48.4% (p = 0.05)	MS + 358.1% (p = 0.00)	MS + 441.9% (p = 0.00)
			MAR + 16.7% (p = 0.03)		MAR + 33.3% (p = 0.01)	MAR + 33.3% (p = 0.02)
		BFR/BS - 72.7% (p = 0.02))	BFR/BS + 90.9% (p = 0.03)		BFR/BS + 390.9% (p = 0.01)	BFR/BS + 572.7% (p = 0.00)
GC4/SAC			MS + 436.4% (p = 0.00)		MS + 1,190.9% (p = 0.00)	MS + 1,427.3% (p = 0.00)
			MAR + 16.7% (p = 0.03)		MAR +33.3% (p = 0.01)	MAR + 33.3% (p = 0.02)
			BFR/BS + 600.0% (p = 0.00)		BFR/BS + 1,700.0% (p = 0.00)	BFR/BS + 2,366.7% (p = 0.00)
GC4/RECV				MS + 140.7% (p = 0-.01)		MS + 184.7% (p = 0.00)
				MAR + 14.3% (p = 0.02)		
				BFR/BS + 157.1% (p = 0.02)		BFR/BS + 254.4% (p = 0.00)
GC 8			MS +268.8% (p = 0.00)		MS +787.5% (p = 0.00)	MS + 950.0% (p = 0.00)
				MAR + 33.3% (p = 0.02)		
			BFR/BS +76.2% (p = 0.00)		BFR/BS + 980.0% (p = 0.00)	BFR/BS + 1380.0% (p = 0.00)

APPENDIX B
SUMMARY OF SELECTED STUDIES IN MICE

Table B-1. Studies Of Glucocorticoid-Induced Bone Loss In Mice.

Strain	Treatment	Dose (mg/kg)	Age (wk.)	Gender	#/Grp	Time (days)	Results		Type Analysis
SW	Prednisolone (pellet)	2.1	28	M	4-5	27	- Spinal BMD decrease - Preferential loss in axial skeleton - Increased resorption Decreased formation - Increased osteocyte apoptosis	Weinstein (5) 1998	DXA Histomor- phometry
SW	Prednisolone (pellet) Prednisolone + alendronate	2.1	16	M	5-9	4, 10, and 27	- Decreased Osteoclast apoptosis - Increased osteoclast survival - Decreased bone formation rate - Increased osteoblast apoptosis	Weinstein (4) 2002	DXA Histomor- phometry

Table B-1. Continued.

Strain	Treatment	Dose (mg/kg)	Age (wk.)	Gender	#/grp	Time (days)	Results		Type Analysis
Balb/C	Dexa-methasone (IP)	1 and 10	28	F	5	21	- Changes only seen at higher dosages	McLaughlin (3)	Histomor- phometry
							-Decreased BFR/BS and MAR	2002	MicroCT
							- Decreased osteocalcin		Biochemical Assays
SW	Prednisolone (pellets)	1.4	24	M	Unk	21	-Decrease Tr bone volume and strength	Lane (2)	Histomor- phometry
							-Increased size of osteocyte lacunae	2006	MicroCT
							-Increased DPD crosslinks (resorption)		Biochemical Assays
							-Decreased Osteocalcin (formation)		

BFR/BS = bone formation rate/bone surface; BMD = bone mineral density; DPD = deoxypyridinoline; GC = glucocorticoid; Tr = trabecular; MAR = mineral apposition rate; SW = Swiss Webster.

Table B-2. Studies using Teriparatide in Mice.

Strain	Condition	Dose ($\mu\text{g}/\text{kg}$)	Age (wk.)	Gender	N/ grp	Time (Wks)	Results		Type Analysis
C57BL/6	Ovx/sham	40	12	F	4-6	3 or 7	- Increased bone formation rate and BV/TV Increased Oc. S -greater effect in LV than tibia - Little change in cortical bone	Zhou (8)	Histomorphometry
C57BL/6	Intact	40	10	F	9	3 and 7	-greater BMD change in tibia and femur than LV - increased bone turnover	Iida-Klein (45)	Piximus (DXA) Histomorphometry
SW	Ovx	80	11	F	9	4	-Bone loss reversed - Mice lost bone faster than rats - 2-3X increase MAR	Alexander (7)	Histomorphometry MicroCT

BMD = bone mineral density; BV/TV = bone volume/total volume; LV = lumbar vertebrae; MAR = mineral apposition rate; Oc. S = osteoclast surface; Ovx = ovariectomized; SW = Swiss Webster.

LIST OF REFERENCES

1. Hofbauer LC, Gori F, Riggs BL, Lacey DL, Dunstan CR, Spelsberg TC, Khosla S 1999 Stimulation of osteoprotegerin ligand and inhibition of osteoprotegerin production by glucocorticoids in human osteoblastic lineage cells: potential paracrine mechanisms of glucocorticoid-induced osteoporosis. *Endocrinology* **140**(10):4382-9.
2. Lane NE, Yao W, Balooch M, Nalla R, Balooch G, Habelitz S, Kinney J, Bonewald LF 2006 Glucocorticoid-treated mice have localized changes in trabecular bone material properties and osteocyte lacunar size that are not observed in placebo-treated or estrogen-deficient mice. *Journal of Bone and Mineral Research* **21**(14):466-476.
3. McLaughlin F, Mackintosh J, Hayes BP, McLaren A, Uings IJ, Salmon P, Humphreys J, Meldrum E, Farrow SN 2002 Glucocorticoid-induced osteopenia in the mouse as assessed by histomorphometry, microcomputed tomography, and biochemical markers. *Bone* **30**(6):924-30.
4. Weinstein RS, Chen JR, Powers CC, Stewart SA, Landes RD, Bellido T, Jilka RL, Parfitt AM, Manolagas SC 2002 Promotion of osteoclast survival and antagonism of bisphosphonate-induced osteoclast apoptosis by glucocorticoids. *J Clin Invest* **109**(8):1041-8.
5. Weinstein RS, Jilka RL, Parfitt AM, Manolagas SC 1998 Inhibition of osteoblastogenesis and promotion of apoptosis of osteoblasts and osteocytes by glucocorticoids. Potential mechanisms of their deleterious effects on bone. *J Clin Invest* **102**(2):274-82.
6. Lane NE, Sanchez S, Modin GW, Genant HK, Pierini E, Arnaud CD 1998 Parathyroid hormone treatment can reverse corticosteroid-induced osteoporosis. Results of a randomized controlled clinical trial. *J Clin Invest* **102**(8):1627-33.
7. Alexander JM, Bab I, Fish S, Muller R, Uchiyama T, Gronowicz G, Nahounou M, Zhao Q, White DW, Chorev M, Gazit D, Rosenblatt M 2001 Human parathyroid hormone 1-34 reverses bone loss in ovariectomized mice. *J Bone Miner Res* **16**(9):1665-73.
8. Zhou H, Iida-Klein A, Lu SS, Ducayen-Knowles M, Levine LR, Dempster DW, Lindsay R 2003 Anabolic action of parathyroid hormone on cortical and cancellous bone differs between axial and appendicular skeletal sites in mice. *Bone* **32**(5):513-20.
9. Braith RW, Magyari PM, Fulton MN, Aranda J, Walker T, Hill JA 2003 Resistance exercise training and alendronate reverse glucocorticoid-induced osteoporosis in heart transplant recipients. *J Heart Lung Transplant* **22**(10):1082-90.
10. Braith RW, Mills RM, Welsch MA, Keller JW, Pollock ML 1996 Resistance exercise training restores bone mineral density in heart transplant recipients. *J Am Coll Cardiol* **28**(6):1471-7.
11. Boulos P, Ioannidis G, Adachi JD 2000 Glucocorticoid-induced osteoporosis. *Curr Rheumatol Rep* **2**(1):53-61.

12. Clarke B, Leidig-Bruckner G 2005 Fracture Prevalence and Incidence in Solid Organ Transplant Recipients. In: Compston J, Shane E (eds.) Bone Disease of Organ Transplantation. El Sevier Academic Press, Boston.
13. Dennison E, Cooper C 2002 Epidemiology of glucocorticoid-induced osteoporosis. *Front Horm Res* **30**:121-6.
14. Rehman Q, Lane NE 2003 Effect of glucocorticoids on bone density. *Med Pediatr Oncol* **41**(3):212-6.
15. Sambrook P, Lane NE 2001 Corticosteroid osteoporosis. *Best Pract Res Clin Rheumatol* **15**(3):401-13.
16. Boling EP 2004 Secondary osteoporosis: underlying disease and the risk for glucocorticoid-induced osteoporosis. *Clin Ther* **26**(1):1-14.
17. Cohen A, Shane E 2003 Osteoporosis after solid organ and bone marrow transplantation. *Osteoporos Int* **14**(8):617-30.
18. Cohen D, Adachi JD 2004 The treatment of glucocorticoid-induced osteoporosis. *J Steroid Biochem Mol Biol* **88**(4-5):337-49.
19. Rodino MA, Shane E 1998 Osteoporosis after organ transplantation. *Am J Med* **104**(5):459-69.
20. Shane E, Epstein S 2001 Transplantation Osteoporosis. *Transplantation Reviews* **15**(1):11-32.
21. Dalle Carbonare L, Arlot ME, Chavassieux PM, Roux JP, Portero NR, Meunier PJ 2001 Comparison of trabecular bone microarchitecture and remodeling in glucocorticoid-induced and postmenopausal osteoporosis. *J Bone Miner Res* **16**(1):97-103.
22. McIlwain HH 2003 Glucocorticoid-induced osteoporosis: pathogenesis, diagnosis, and management. *Prev Med* **36**(2):243-9.
23. Lafage-Proust MH, Boudignon B, Thomas T 2003 Glucocorticoid-induced osteoporosis: pathophysiological data and recent treatments. *Joint Bone Spine* **70**(2):109-18.
24. Braith RW, Magyari PM, Fulton MN, Lisor CF, Vogel SE, Hill JA, Aranda JM Comparison of calcitonin versus calcitonin + resistance exercise as prophylaxis for osteoporosis in heart transplant recipients. *Transplantation* **In Press**.
25. Braith RW, S.D. G, Musto T, Mitchell MJ, Baz MA 1998 Resistance exercise restored bone mineral density in an osteoporotic patient before lung transplantation. *Journal of Cardiopulmonary Rehabilitation* **36**:18-23.

26. Mitchell M, Fulton M, Lisor C, Baz M, Braith R 2002 Resistance training attenuates glucocorticoid-induced osteoporosis in lung transplant recipients. *Journal of Heart and Lung Transplantation* **in review**.
27. Uusi-Rasi K, Sievanen H, Heinonen A, Kannus P, Vuori I 2004 Effect of discontinuation of alendronate treatment and exercise on bone mass and physical fitness: 15-month follow-up of a randomized, controlled trial. *Bone* **35(3):799-805**.
28. Mitlak BH 2002 Parathyroid hormone as a therapeutic agent. *Curr Opin Pharmacol* **2(6):694-9**.
29. Neer RM, Arnaud CD, Zanchetta JR, Prince R, Gaich GA, Reginster JY, Hodsmann AB, Eriksen EF, Ish-Shalom S, Genant HK, Wang O, Mitlak BH 2001 Effect of parathyroid hormone (1-34) on fractures and bone mineral density in postmenopausal women with osteoporosis. *N Engl J Med* **344(19):1434-41**.
30. Rittmaster RS, Bolognese M, Ettinger MP, Hanley DA, Hodsmann AB, Kendler DL, Rosen CJ 2000 Enhancement of bone mass in osteoporotic women with parathyroid hormone followed by alendronate. *J Clin Endocrinol Metab* **85(6):2129-34**.
31. Kaufman JM, Orwoll E, Goemaere S, San Martin J, Hossain A, Dalsky GP, Lindsay R, Mitlak BH 2005 Teriparatide effects on vertebral fractures and bone mineral density in men with osteoporosis: treatment and discontinuation of therapy. *Osteoporos Int* **16(5):510-6**.
32. Finkelstein JS, Hayes A, Hunzelman JL, Wyland JJ, Lee H, Neer RM 2003 The effects of parathyroid hormone, alendronate, or both in men with osteoporosis. *N Engl J Med* **349(13):1216-26**.
33. Body JJ, Gaich GA, Scheele WH, Kulkarni PM, Miller PD, Peretz A, Dore RK, Correa-Rotter R, Papaioannou A, Cumming DC, Hodsmann AB 2002 A randomized double-blind trial to compare the efficacy of teriparatide [recombinant human parathyroid hormone (1-34)] with alendronate in postmenopausal women with osteoporosis. *J Clin Endocrinol Metab* **87(10):4528-35**.
34. Lindsay R, Nieves J, Formica C, Henneman E, Woelfert L, Shen V, Dempster D, Cosman F 1997 Randomised controlled study of effect of parathyroid hormone on vertebral-bone mass and fracture incidence among postmenopausal women on oestrogen with osteoporosis. *Lancet* **350(9077):550-5**.
35. Pettway GJ, Schneider A, Koh AJ, Widjaja E, Morris MD, Meganck JA, Goldstein SA, McCauley LK 2005 Anabolic actions of PTH (1-34): use of a novel tissue engineering model to investigate temporal effects on bone. *Bone* **36(6):959-70**.
36. Binz K, Schmid C, Bouillon R, Froesch ER, Jurgensen K, Hunziker EB 1994 Interactions of insulin-like growth factor I with dexamethasone on trabecular bone density and mineral metabolism in rats. *Eur J Endocrinol* **130(4):387-93**.

37. King CS, Weir EC, Gundberg CW, Fox J, Insogna KL 1996 Effects of continuous glucocorticoid infusion on bone metabolism in the rat. *Calcif Tissue Int* **59**(3):184-91.
38. Shen V, Birchman R, Liang XG, Wu DD, Lindsay R, Dempster DW 1997 Prednisolone alone, or in combination with estrogen or dietary calcium deficiency or immobilization, inhibits bone formation but does not induce bone loss in mature rats. *Bone* **21**(4):345-51.
39. Manolagas SC, Weinstein RS 1999 New developments in the pathogenesis and treatment of steroid-induced osteoporosis. *J Bone Miner Res* **14**(7):1061-6.
40. Mosekilde L 1995 Assessing bone quality--animal models in preclinical osteoporosis research. *Bone* **17**(4 Suppl):343S-352S.
41. Thompson DD, Simmons HA, Pirie CM, Ke HZ 1995 FDA Guidelines and animal models for osteoporosis. *Bone* **17**(4 Suppl):125S-133S.
42. Weinstein RS 2001 Glucocorticoid-induced osteoporosis. *Rev Endocr Metab Disord* **2**(1):65-73.
43. Weinstein RS, Manolagas SC 2000 Apoptosis and osteoporosis. *Am J Med* **108**(2):153-64.
44. Lane NE, Sanchez S, Modin GW, Genant HK, Pierini E, Arnaud CD 2000 Bone mass continues to increase at the hip after parathyroid hormone treatment is discontinued in glucocorticoid-induced osteoporosis: results of a randomized controlled clinical trial. *J Bone Miner Res* **15**(5):944-51.
45. Iida-Klein A, Zhou H, lu SS, levine LR, Ducayen-Knowles M, Dempster D, Nieves J, lindsay R 2002 Anabolic action of parathyroid hormone is skeletal site specific at the tissue and cellular levels in mice. *Journal of Bone and Mineral Research* **17**(5):808-816.
46. ALA July 2005 Estimated prevalence and incidence of lung disease by lung association territory American Lung Association: Epidemiology and statistical unit research and program services, pp 1-53.
47. 2005 Organ Procurement and Transplantation Network Statistical Database.
48. Swarthout JT, D'Alonzo RC, Selvamurugan N, Partridge NC 2002 Parathyroid hormone-dependent signaling pathways regulating genes in bone cells. *Gene* **282**(1-2):1-17.
49. Wronski TJ, Yen C-F, Qi H, Dann LM 1993 Parathyroid hormone is more effective than estrogen or bisphosphonates for restoration of lost bone mass in ovariectomized rats. *Endocrinology* **132**(2):823-831.
50. Li M, Shen Y, Halloran BP, Baumann BD, Miller K, Wronski TJ 1996 Skeletal response to corticosteroid deficiency and excess in growing male rats. *Bone* **19**(2):81-8.

51. Parfitt AM, Drezner MK, Glorieux FH, Kanis JA, Malluche H, Meunier PJ, Ott SM, Recker RR 1987 Bone histomorphometry: standardization of nomenclature, symbols, and units. Report of the ASBMR Histomorphometry Nomenclature Committee. *J Bone Miner Res* **2**(6):595-610.
52. Conover WJ 1980 *Practical Nonparametric Statistics*. Wiley and Sons, New York, NY, pp 229-237.
53. Bonner F, Worrell RV 1991 *A Basic Science Primer in Orthopaedics*.
54. Reeve J 2000 How do women develop fragile bones? *J Steroid Biochem Mol Biol* **74**(5):375-81.
55. Kanis J 1991 Calcium Requirements for Optimal Skeletal Health in Women. *Calcified Tissue International Supplement* **49**:S33-S41.
56. Parfitt AM 1992 Implications of Architecture for the Pathogenesis and Prevention of Vertebral Fracture. *bone* **13**(Supplement):S41-S47.
57. Vaananen HK, Zhao H, Mulari M, Halleen JM 2000 The Cell Biology of Osteoclast Function. *J Cell Sci* **113**:377-381.
58. Arita S, Ikeda S, Sakai A, Okimoto N, Akahoshi S, Nagashima M, Nishida A, Ito M, Nakamura T 2004 Human parathyroid hormone (1-34) increases mass and structure of the cortical shell, with resultant increase in lumbar bone strength, in ovariectomized rats. *J Bone Miner Metab* **22**(6):530-40.
59. Vaananen HK, Zhao H, Mulari M, Halleen JM 2000 The cell biology of osteoclast function. *J Cell Sci* **113 (Pt 3)**:377-81.
60. Hofbauer LC, Khosla S, Dunstan CR, Lacey DL, Boyle WJ, Riggs BL 2000 The roles of osteoprotegerin and osteoprotegerin ligand in the paracrine regulation of bone resorption. *J Bone Miner Res* **15**(1):2-12.
61. Martin RB 2000 Toward a Unifying Theory of Bone Remodeling. *Bone* **26**(1).
62. Martin RB, Burr DB, Sharkey NA 1998 *Skeletal Tissue Mechanics*. Springer-Verlag, New York.
63. Notelovitz M, Martin D, Tesar R 1991 Estrogen Therapy and Variable-Resistance weight training increase bone mineral in surgically menopausal women. *Journal of Bone and Mineral Research* **6**:583-590.
64. Hazelwood SJ, Bruce Martin R, Rashid MM, Rodrigo JJ 2001 A mechanistic model for internal bone remodeling exhibits different dynamic responses in disuse and overload. *J Biomech* **34**(3):299-308.

65. Takahashi N, Udagawa N, Suda T 1999 A new member of tumor necrosis factor ligand family, ODF/OPGL/TRANCE/RANKL, regulates osteoclast differentiation and function. *Biochem Biophys Res Commun* **256**(3):449-55.
66. Frost H 1997 On Our Age-Related Bone Loss: Insights from a New Paradigm. *Journal of Bone and Mineral Research* **12**(10).
67. Bronner F, Worrell RV 1991 *A Basic Science Primer in Orthopaedics*. Lippincott, Williams, and Wilkins, New York.
68. Hazelwood SJ, Martin RB, Rashid MM, Rodrigo J 2001 A Mechanistic Model for Internal Bone Remodeling Exhibits Different Dynamic Responses in Disuse and Overload. *Journal of Biomechanics* **34**:299-308.
69. Kostenuik PJ 2005 Osteoprotegerin and RANKL regulate bone resorption, density, geometry and strength. *Curr Opin Pharmacol* **5**(6):618-25.
70. Oh ES, Rhee EJ, Oh KW, Lee WY, Baek KH, Yoon KH, Kang MI, Yun EJ, Park CY, Choi MG, Yoo HJ, Park SW 2005 Circulating osteoprotegerin levels are associated with age, waist-to-hip ratio, serum total cholesterol, and low-density lipoprotein cholesterol levels in healthy Korean women. *Metabolism* **54**(1):49-54.
71. Sandy J, Davies M, Prime S, Farndale R 1998 Signal pathways that transduce growth factor-stimulated mitogenesis in bone cells. *Bone* **23**(1):17-26.
72. Dalle Carbonare L, Bertoldo F, Valenti MT, Zenari S, Zanatta M, Sella S, Giannini S, Cascio VL 2005 Histomorphometric analysis of glucocorticoid-induced osteoporosis. *Micron* **36**(7-8):645-52.
73. Dalle Carbonare L, Chavassieux PM, Arlot ME, Meunier PJ 2002 Bone histomorphometry in untreated and treated glucocorticoid-induced osteoporosis. *Front Horm Res* **30**:37-48.
74. Patschan D, Lodenkemper K, Buttgerit F 2001 Molecular mechanisms of glucocorticoid-induced osteoporosis. *Bone* **29**(6):498-505.
75. Reid IR 2000 Glucocorticoid-induced osteoporosis. *Baillieres Best Pract Res Clin Endocrinol Metab* **14**(2):279-98.
76. Manelli F, Giustina A 2000 Glucocorticoid-induced osteoporosis. *Trends Endocrinol Metab* **11**(3):79-85.
77. Adcock IM 2004 Corticosteroids: limitations and future prospects for treatment of severe inflammatory disease. *Drug Discovery Today: Therapeutic Strategies* **1**(3):321-328.
78. Demoly P, Chung KF 1998 Pharmacology of corticosteroids. *Respir Med* **92**(3):385-94.

79. Schacke H, Docke WD, Asadullah K 2002 Mechanisms involved in the side effects of glucocorticoids. *Pharmacol Ther* **96**(1):23-43.
80. Canalis E 2003 Mechanisms of glucocorticoid-induced osteoporosis. *Curr Opin Rheumatol* **15**(4):454-7.
81. Canalis E, Bilezikian JP, Angeli A, Giustina A 2004 Perspectives on glucocorticoid-induced osteoporosis. *Bone* **34**(4):593-8.
82. Ton FN, Gunawardene SC, Lee H, Neer RM 2005 Effects of low-dose prednisone on bone metabolism. *J Bone Miner Res* **20**(3):464-70.
83. Boyde A, Maconnachie E, Reid SA, Delling G, Mundy GR 1986 Scanning electron microscopy in bone pathology: review of methods, potential and applications. *Scan Electron Microsc (Pt 4)*:1537-54.
84. Tamura Y, Okinaga H, Takami H 2004 Glucocorticoid-induced osteoporosis. *Biomed Pharmacother* **58**(9):500-4.
85. Malyszko J, Malyszko JS, Wolczynski S, Mysliwiec M 2003 Osteoprotegerin and its correlations with new markers of bone formation and bone resorption in kidney transplant recipients. *Transplant Proc* **35**(6):2227-9.
86. Ferrari P 2003 Cortisol and the renal handling of electrolytes: role in glucocorticoid-induced hypertension and bone disease. *Best Pract Res Clin Endocrinol Metab* **17**(4):575-89.
87. Canalis E 1996 Clinical review 83: Mechanisms of glucocorticoid action in bone: implications to glucocorticoid-induced osteoporosis. *J Clin Endocrinol Metab* **81**(10):3441-7.
88. Sivagurunathan S, Muir MM, Brennan TC, Seale JP, Mason RS 2005 Influence of glucocorticoids on human osteoclast generation and activity. *J Bone Miner Res* **20**(3):390-8.
89. Reid DM, Harvie J 1997 Secondary osteoporosis. *Baillieres Clin Endocrinol Metab* **11**(1):83-99.
90. Brixen KT, Christensen PM, Ejersted C, Langdahl BL 2004 Teriparatide (biosynthetic human parathyroid hormone 1-34): a new paradigm in the treatment of osteoporosis. *Basic Clin Pharmacol Toxicol* **94**(6):260-70.
91. Fox J 2002 Developments in parathyroid hormone and related peptides as bone-formation agents. *Curr Opin Pharmacol* **2**(3):338-44.
92. Debiais F 2003 Efficacy data on teriparatide (parathyroid hormone) in patients with postmenopausal osteoporosis. *Joint Bone Spine* **70**(6):465-70.

93. Selye H 1932 On the stimulation of new bone formation with parathyroid extract and irradiated ergosterol. *Endocrinology* **16**:547-558.
94. Fitzpatrick LA, Bilezikian JP 1996 Actions of Parathyroid Hormone. In: Bilezikian JP, Raisz LG, Rodan GA (eds.) *Principles of Bone Biology*. Academic Press, San Diego.
95. Locklin RM, Khosla S, Turner RT, Riggs BL 2003 Mediators of the biphasic responses of bone to intermittent and continuously administered parathyroid hormone. *J Cell Biochem* **89**(1):180-90.
96. Canalis E, Centrella M, Burch W, McCarthy TL 1989 Insulin-like growth factor I mediates selective anabolic effects of parathyroid hormone in bone cultures. *J Clin Invest* **83**(1):60-5.
97. Rosen CJ 2004 What's new with PTH in osteoporosis: where are we and where are we headed? *Trends Endocrinol Metab* **15**(5):229-33.
98. Gensure RC, Gardella TJ, Juppner H 2005 Parathyroid hormone and parathyroid hormone-related peptide, and their receptors. *Biochem Biophys Res Commun* **328**(3):666-78.
99. Rosen CJ, Bilezikian JP 2001 Clinical review 123: Anabolic therapy for osteoporosis. *J Clin Endocrinol Metab* **86**(3):957-64.
100. Quattrocchi E, Kourlas H 2004 Teriparatide: a review. *Clin Ther* **26**(6):841-54.
101. Onyia JE, Helvering LM, Gelbert L, Wei T, Huang S, Chen P, Dow ER, Maran A, Zhang M, Lotinun S, Lin X, Halladay DL, Miles RR, Kulkarni NH, Ambrose EM, Ma YL, Frolik CA, Sato M, Bryant HU, Turner RT 2005 Molecular profile of catabolic versus anabolic treatment regimens of parathyroid hormone (PTH) in rat bone: an analysis by DNA microarray. *J Cell Biochem* **95**(2):403-18.
102. Xing L, Boyce BF 2005 Regulation of apoptosis in osteoclasts and osteoblastic cells. *Biochem Biophys Res Commun* **328**(3):709-20.
103. Tashjian AH, Jr., Chabner BA 2002 Commentary on clinical safety of recombinant human parathyroid hormone 1-34 in the treatment of osteoporosis in men and postmenopausal women. *J Bone Miner Res* **17**(7):1151-61.
104. Vahle JL, Long GG, Sandusky G, Westmore M, Ma YL, Sato M 2004 Bone neoplasms in F344 rats given teriparatide [rhPTH(1-34)] are dependent on duration of treatment and dose. *Toxicol Pathol* **32**(4):426-38.
105. Vahle JL, Sato M, Long GG, Young JK, Francis PC, Engelhardt JA, Westmore MS, Linda Y, Nold JB 2002 Skeletal changes in rats given daily subcutaneous injections of recombinant human parathyroid hormone (1-34) for 2 years and relevance to human safety. *Toxicol Pathol* **30**(3):312-21.

106. Berg C, Neumeyer K, Kirkpatrick P 2003 Teriparatide. *Nat Rev Drug Discov* **2**(4):257-8.
107. U.S.Forteo 2004 Prescribing information, Eli Lilly and Company.
108. Qin L, Raggatt LJ, Partridge NC 2004 Parathyroid hormone: a double-edged sword for bone metabolism. *Trends Endocrinol Metab* **15**(2):60-5.
109. Audran M, Insalaco P 2003 Parathyroid hormone therapy for osteoporosis. *Joint Bone Spine* **70**(5):315-7.
110. Jiang Y, Zhao JJ, Mitlak BH, Wang O, Genant HK, Eriksen EF 2003 Recombinant human parathyroid hormone (1-34) [teriparatide] improves both cortical and cancellous bone structure. *J Bone Miner Res* **18**(11):1932-41.
111. Dempster DW, Cosman F, Kurland ES, Zhou H, Nieves J, Woelfert L, Shane E, Plavetic K, Muller R, Bilezikian J, Lindsay R 2001 Effects of daily treatment with parathyroid hormone on bone microarchitecture and turnover in patients with osteoporosis: a paired biopsy study. *J Bone Miner Res* **16**(10):1846-53.
112. Adams AE, Rosenblatt M, Suva LJ 1999 Identification of a novel parathyroid hormone-responsive gene in human osteoblastic cells. *Bone* **24**(4):305-13.
113. Samuels A, Perry MJ, Gibson RL, Colley S, Tobias JH 2001 Role of endothelial nitric oxide synthase in estrogen-induced osteogenesis. *Bone* **29**(1):24-9.
114. Weinstein RS, Jia D, Powers CC, Stewart SA, Jilka RL, Parfitt AM, Manolagas SC 2004 The skeletal effects of glucocorticoid excess override those of orchidectomy in mice. *Endocrinology* **145**(4):1980-7.
115. Oxlund H, Ortoft G, Thomsen JS, Danielsen CC, Ejersted C, Andreassen TT 2006 The anabolic effect of PTH on bone is attenuated by simultaneous glucocorticoid treatment. *Bone* **39**(2):244-52.
116. Samuels A, Perry MJ, Gibson R, Tobias JH 2001 Effects of combination therapy with PTH and 17beta-estradiol on long bones of female mice. *Calcif Tissue Int* **69**(3):164-70.
117. Sibonga JD, Iwaniec UT, Shogren KL, Rosen CJ, Turner RT 2007 Effects of parathyroid hormone (1-34) on tibia in an adult rat model for chronic alcohol abuse. *Bone* **40**(4):1013-20.
118. Knopp E, Troiano N, Bouxsein M, Sun BH, Lostritto K, Gundberg C, Dziura J, Insogna K 2005 The effect of aging on the skeletal response to intermittent treatment with parathyroid hormone. *Endocrinology* **146**(4):1983-90.
119. Halloran BP, Ferguson VL, Simske SJ, Burghardt A, Venton LL, Majumdar S 2002 Changes in bone structure and mass with advancing age in the male C57BL/6J mouse. *J Bone Miner Res* **17**(6):1044-50.

120. Jilka RL, Weinstein RS, Takahashi K, Parfitt AM, Manolagas SC 1996 Linkage of decreased bone mass with impaired osteoblastogenesis in a murine model of accelerated senescence. *J Clin Invest* **97**(7):1732-40.
121. Turner RT, Evans GL, Lotinun S, Lapke PD, Iwaniec UT, Morey-Holton E 2007 Dose-response effects of intermittent PTH on cancellous bone in hindlimb unloaded rats. *J Bone Miner Res* **22**(1):64-71.
122. Turner RT, Lotinun S, Hefferan TE, Morey-Holton E 2006 Disuse in adult male rats attenuates the bone anabolic response to a therapeutic dose of parathyroid hormone. *J Appl Physiol* **101**(3):881-6.

BIOGRAPHICAL SKETCH

Kathleen S. Howe was commissioned as an officer in the United States Air Force after her graduation from the University of Central Florida in 1978. She spent the next 20 years serving in a number of positions in the United States Air Force before retiring as a Lieutenant Colonel in 2000. After her retirement, she returned to the academic world to pursue her interest in bone metabolism. She has spent the past 7 years concentrating on her studies in exercise physiology and bone biology. Her research has centered on interventions to reverse the effects of aging and disease on bone and reversing the effects of secondary osteoporosis. She plans to continue research related to bone metabolism in the future. She has accepted a postdoctoral position in the Department of Nutrition and Exercise Science at Oregon State University where she will examine the effects of alcohol on bone structure and metabolism.